Università degli studi di Napoli Federico II

Dottorato di Ricerca in Scienze Computazionali e Informatiche
XXVIII ciclo

STOCHASTIC METHODS AND MODELS FOR NEURONAL ACTIVITY AND MOTOR PROTEINS

Giuseppe D'Onofrio

Anno Accademico 2015/2016

Contents

Introduction

The main topic of this thesis is to specialize mathematical methods and construct stochastic models for describing and predict biological dynamics such as neuronal firing and acto-myosin sliding.

Neurons are cells of the nervous system that can be of different types depending on their position and task, but all have the main structure: axon, dendrites and cell body. Comparing a neuron with a computer we can say that the dendrites represent the input, the axons and synapses the output and the cell body constitutes the processing unit of the information. Neurons transmit information through electrical and chemical signals that constitute the spike trains. These trains are the object of many studies, because of the generally accepted hypothesis that the information transferred within the nervous system is encoded by the timing and the rate of the spikes.

A powerful tool for neuroscientists is the mathematical theory of stochastic processes. Even if it is rigorous and abstract it allows the description and the computational simulation of many practical phenomena like the olfactory system of a fly, the reaction of a monkey when it looks at a picture of a predator or the answer of the human brain to an acoustic stimulation.

In fact neurons are subject to several sources of noise, so the description of the neuronal activity must be carried out with stochastic models regulated by stochastic differential equations.

At the end of the nineteenth century natural phenomena were modelled by differential equations and it was commonly thought that if all initial data could be collected, one would be able to predict the future almost surely. The advent of quantum mechanics and chaos theory stressed the importance of considering the effects of noise in the environment in which the system we are studing is embedded. This fact does not imply that natural systems are governed by chaos, but there is a limit in the precision of predictions.

The first example of SDE was proposed by Einstein 1905 and then by Langevin in 1908 for the description of the Brownian motion of a small pollen grain suspended in water. Langevin introduced a fluctuating force which represents the incessant impacts of the molecules of the liquid on the

Brownian particle.
An adequate mathematical grounding for the approach of Langevin, however, was not available until more than 40 years later, when Itô formulated his concept of stochastic integration. Before then the solutions of SDEs, obtained using classical methods of resolution, were physically unreasonable. Itô defined the stochastic integral and introduced new rules of derivation using the formula that bears his name: these definitions allowed the development of the stochastic analysis.
Of course these mathematical results on stochastic processes are of general nature and are valid not only in neuroscience. Theory and properties of Gauss-Markov processes and diffusion processes are widely used for modelling the time evolution of dynamical systems in many fields: economics, physics, biology, engineering and medicine. Two examples are taken into consideration in this Thesis: stochastic neuronal activity and motor proteins dynamics.
It should be emphasized that the apparently twofold theme on which we focused the research is part of a strictly unitary context as the methods and tools of investigation adapt naturally to both issues. Models describing the stochastic evolution in the case of neuronal activity or that of the actin-myosin dynamics are governed by stochastic differential equations whose solutions are diffusion processes and Gauss-Markov processes. Of fundamental importance in the study of these phenomena is the determination of the density of the first passage times through one or two time-depending boundaries. For this purpose the development or use of numerical solution algorithms and the comparison of the results with those obtained by simulation algorithms is essential. A particular type of Gauss-Markov process (the time-inhomogeneous Ornstein-Uhlenbeck process) and its first passage time through suitable boundaries are fundamental for modeling phenomena subject to additional (external) time-dependent forces.

We briefly present the structure of this work.

Chapter 1 is dedicated to a quick resume of the basis of stochastic analysis including conditional expectation, the Itô integrals, the definition of SDEs and solution of an SDE focusing on the hypoteses that guarantee the existence and uniqueness of such solution.

In Chapter 2 the analysis of the properties of Gauss-Markov and diffusion processes are presented focusing on their transition probabilities and the related SDEs. Classical results and new contributions on the First Passage Time of these processes through one boundary are reviewed in order to highlight the four possible strategies adopted for the determination of the density

of First Passage Time for specified processes: numerical solution of a second kind Volterra integral equation, analytical evaluation of the moments using the Laplace transform, asymptotic approximations or closed form solutions.

In Chapter 3 these results are applied in the modeling of neuronal activity giving an overview on the models presented in literature marking the difference between renewal and non-renewal processes. The latter processes, despite a more realistic description of the experimental evidences, are more difficult to treat from a mathematical point of view because they involve time-inhomogeneous processes and correlation between spike times. The last part of the Chapter is devoted to the Recurring Passage Time Problem, described by a time-inhomogeneous Ornstein-Uhlenbeck processes and has been the object of study during my visiting at the Laboratory of Mathematical Physics of the Rockefeller University under the supervision of Prof. Marcelo O. Magnasco.

In Chapter 4 a stochastic model for the prediction of the successive spikes that constitute the train of spikes of a neuron is described by means of first passage times of a succession of Gauss-Markov processes each of which is identified by a particular mean function dependent on the first passage time of the previous process An analogous strategy has been carried out to describe the interspike intervals of the same train.

The first part of Chapter 5 contains mathematical results about the random variable First Exit Time, useful in phenomena in which the dynamics is confined in a particular region. Finally the second part deals with the stochastic modeling of the acto-myosin dynamics responsible for the contraction in skeletal muscles.

In order to verify the validity of the proposed models it can not be disregarded the analysis of simulated and/or experimental data. For this reason, in recent years more and more important is the cooperation between the different fields of research, so that the studies of the data obtained through experiments, refining the purely mathematical techniques, lead to new results.

Chapter 1

Preliminaries

In this Chapter we collect a miscellaneous of basic notions about Stochastic Analysis that are essential for the understanding of the results presented in the next chapters. The goal is therefore to recall the basic tools that will be used in the following and not to provide a comprehensive overview on the subject. For this reason, most of the proofs are not presented, which however are classical results and can be found in very interesting and popular textbooks such as [3], [5], [42], [58] and [82].

1.1 Conditional expectation

Let $(\Omega, \mathcal{F}, \mathbb{P})$ be a probability space (see, for instance, [82]).

Definition 1.1.1. Let $A, B \in \mathcal{F}$ be events such that $P(B) > 0$. The conditional probability of A given B is defined as

$$\mathbb{P}(A|B) = \frac{\mathbb{P}(A \cap B)}{\mathbb{P}(B)}. \tag{1.1}$$

If the events A and B are not independent, the information about the occurrence of B improves our "prediction" on A.

Let us now suppose that $\mathcal{G}$ is a sub-σ-algebra of $\mathcal{F}$. Using the Radon-Nikodym theorem it can be shown (see for instance [58] or [82]) that for every integrable real-valued random variable X defined on Ω there exists a $\mathcal{G}$-measurable random variable Z (i.e. $Z : (\Omega, \mathcal{G}) \to \mathbb{R}$ is measurable) such that:

$$\int_B X d\mathbb{P} = \int_B Z d\mathbb{P}_{\mathcal{G}}, \quad \forall B \in \mathcal{G}. \tag{1.2}$$

We note that by $\mathbb{P}_{\mathcal{G}}$ in the second integral of (1.2) we indicate the measure $\mathbb{P}$ restricted to the σ-algebra $\mathcal{G}$.

Definition 1.1.2. The $\mathcal{G}$-measurable random variable Z is $(\mathbb{P}_{\mathcal{G}})$-almost surely unique, is indicated by $\mathbb{E}(X|\mathcal{G})$ and is called *conditional expectation of X given $\mathcal{G}$*.

The expression (1.2) can be written in the following form:

$$\mathbb{E}(X1_B) = \mathbb{E}(Z1_B), \quad \forall B \in \mathcal{G}$$

where $1_{(\cdot)}$ is the the indicator of the event $(\cdot)$.
The conditional expectation enables us to define the conditional probability with respect to a σ-algebra.

Definition 1.1.3. Let $\mathcal{G}$ be a sub-σ-algebra of $\mathcal{F}$ and let $E \in \mathcal{F}$ be an event. We say that the random variable $\mathbb{P}(E|\mathcal{G})$ is the *conditional probability of E with respect to the sigma-algebra $\mathcal{G}$* if:

- $\mathbb{P}(E|\mathcal{G})$ is $\mathcal{G}$-measurable,
- $\mathbb{E}[1_H \mathbb{P}(E|\mathcal{G})] = \mathbb{P}(E \cap H)$ for any $H \in \mathcal{G}$.

1.2 Stochastic Processes and Stopping Times

In the following we recall from [42] some definitions concerning stochastic processes.

Definition 1.2.1. A *stochastic process* is a collection of random variables $X(t) = \{X(t), t \geq 0\}$ on $(\Omega, \mathcal{F})$ which take values in a measurable space $(E, \mathcal{E})$, called *state space*.

If we fix the sample point $\omega \in \Omega$, the function $t \mapsto X(t, \omega)$ is the trajectory (or sample path) of the process $X(t)$ associated to ω. It can be viewed as the mathematical abstraction of the results of a random experiment that can be observed continuously in time. If we fix t, we obtain a random variable $\omega \in \Omega \mapsto X_t(\omega)$.

The index t is commonly interpreted as time. When $E \equiv \mathbb{R}$ the stochastic process is real and in this case it is usually equipped with the Borel σ-algebra $\mathcal{E} = \mathcal{B}(\mathbb{R})$, i.e. the smallest σ-algebra containing all the open sets of $\mathbb{R}$.

Definition 1.2.2. The joint distributions of the vectors $(X(t_1), \ldots, X(t_k))$ on E^k, for $k \in \mathbb{N}$ and $t_1, \ldots, t_k \in [0, +\infty)$ are the *finite dimensional distributions of the process $X(t)$*.

The last definition is important because the Kolmogorov Consistency Theorem ensures that a stochastic process is identified by the family of its finite-dimensional distributions.

The temporal feature of a stochastic process suggests a flow of time, so it makes sense at time t to talk about past, present and future of the process. For this reason it is important to consider sequences of σ-algebras, i.e. filtrations.

Definition 1.2.3. A *filtration* on the measurable space $(\Omega, \mathcal{F})$ is a non-decreasing family $\{\mathcal{F}_t, t \geq 0\}$ of σ-algebras such that:

i) $\mathcal{F}_t \subseteq \mathcal{F}, \quad \forall t \in [0, +\infty)$,

ii) $\mathcal{F}_s \subseteq \mathcal{F}_t, \quad \forall s \leq t < +\infty$.

We set $\mathcal{F}_\infty := \sigma\left(\cup_{t\geq 0}\mathcal{F}_t\right)$, where $\sigma\left(\cup_{t\geq 0}\mathcal{F}_t\right)$ is the σ-algebra generated by $\cup_{t\geq 0}\mathcal{F}_t$, i.e. the smallest σ-algebra containing every set in $\cup_{t\geq 0}\mathcal{F}_t$.

Definition 1.2.4. The stochastic process $\{X(t), t \geq 0\}$ is *adapted* to the filtration $\{\mathcal{F}_t, t \geq 0\}$ if, for each $t \geq 0$, $X(t)$ is a $\mathcal{F}_t$-measurable random variable.

This notion gives a physical interpretation: it describes non-anticipating processes. These processes may depend only on past events and not on future ones.

Since the random process $\{X(t), t \geq 0\}$ is a family of random variables $X(t)$ we say that it is measurable if each $X(t)$ is $\mathcal{F}/\mathcal{B}(\mathbb{R})$-measurable. However for a rigorous definition we have to consider the product spaces.

Definition 1.2.5. The stochastic process $X(t)$ is called *measurable* if, for every $A \in \mathcal{B}(\mathbb{R})$, the set $\{(t, \omega), X(t, \omega) \in A\}$ belongs to the product σ-algebra $\mathcal{B}([0, +\infty)) \otimes \mathcal{F}$.

Definition 1.2.6. The stochastic process $X(t)$ is called *progressively measurable* with respect to the filtration $\{\mathcal{F}_t, t \geq 0\}$ if, for each $t \geq 0$ and $A \in \mathcal{B}(\mathbb{R})$, the set $\{(s, \omega), 0 \leq s \leq t, \omega \in \Omega, X(s, \omega) \in A\}$ belongs to the product σ-algebra $\mathcal{B}([0, t)) \otimes \mathcal{F}_t$.

A progressively measurable process is adapted and measurable.

A stochastic process that is adapted and is the most important and used in literature and applications is the Wiener process.

Definition 1.2.7. The *standard Wiener process* $\{W(t), t \geq 0\}$ is a continuous one-dimensional stochastic process adapted to the filtration $\{\mathcal{F}_t, t \geq 0\}$ that have the properties:

i) $\mathbb{P}(W(0) = 0) = 1$;

ii) $W(t) - W(s)$ is independent of $\mathcal{F}_s$ for $t > s$;

iii) the random variable $W(t) - W(s)$ is normally distributed with mean zero and variance $\mid t - s \mid$.

$W(t)$ is often called also the standard Brownian motion. It is a gaussian process with independent and stationary increments, is markovian, is a martingale and has almost everywhere continuous but non-differentiable trajectories.

Finally we give the definition of σ-algebra at a Stopping Time (see [42],[58]) that plays an important role in the definition of the strong Markov property, presented in the next chapter.

Definition 1.2.8. A random time $\mathcal{T}$ is a *stopping time* of the filtration $\{\mathcal{F}_t, t \geq 0\}$ if the event $\{\mathcal{T} \leq t\}$ belongs to the σ-algebra $\mathcal{F}_t$ $\forall t \geq 0$. A random time $\mathcal{T}$ is an *optional time* of the filtration $\{\mathcal{F}_t, t \geq 0\}$ if $\{\mathcal{T} < t\} \in \mathcal{F}_t$ $\forall t \geq 0$.

Definition 1.2.9. Let $\mathcal{T}$ be a stopping time of the filtration $\{\mathcal{F}_t, t \geq 0\}$. We define the *$\sigma$-algebra at $\mathcal{T}$* as:

$$\mathcal{F}_{\mathcal{T}} = \{A \in \mathcal{F}_\infty : A \cap \{\mathcal{T} \leq t\} \in \mathcal{F}_t, \forall t \geq 0\}.$$

1.3 Stochastic integral

Let consider the stochastic basis $(\Omega, \mathcal{F}, (\mathcal{F}_t), \mathbb{P})$. Let $\{W(t), t \geq 0\}$ be a Wiener process adapted to the filtration and $\{X(t), t \geq 0\}$ a stochastic process. The idea of Itô was to define the stochastic integral $\int_{t_0}^{t} X(s)\, dW(s)$ as a suitable limit of simple processes [41].

Definition 1.3.1. A process $X(t)$ is *simple* if there exists a strictly increasing sequence of real numbers $0 = t_0 \leq t_1 < t_2 < \ldots$, as well as a sequence of random variables ξ_i, $(i = 0, 1, 2...)$ such that $\forall i$ ξ_i is $\mathcal{F}_{t_i}$-measurable and there exists a constant C such that $\sup_{n \geq 0} |\xi_n(\omega)| \leq C$ for every $\omega \in \Omega$, and

$$X(t, \omega) = \xi_0(\omega) 1_{\{0\}}(t) + \sum_{i=1}^{\infty} \xi_i(\omega) 1_{[t_i, t_{i+1})}(t), \quad t \geq 0, \omega \in \Omega.$$

We call $M_2[t_0, t]$ the class of processes for which the stochastic integral can be defined.

Definition 1.3.2. $M_2[t_0, t]$ is the class of real-valued processes $\{X(t),\ t \geq 0\}$, progressively measurable with respect to the filtration $\{\mathcal{F}_t, t \geq 0\}$ and such that

$$\mathbb{E}\left[\int_{t_0}^{t} \mid X_s \mid^2 ds\right] < \infty.$$

The progressive measurability guarantees that the process is non anticipating and so $X(t)$ is independent of the increments $W(s) - W(t)$, $\forall s > t$. This assumption is not very restrictive, in fact most of the real phenomena described by stochastic processes have this property.

The simple processes belong to the class $M_2[t_0, t]$ and for them the stochastic integral is defined as stated in the following definition. Let us consider the partition

$$t_0 < t_1 < t_2 \cdots < t_{n-1} < t_n = t$$

of the interval $[t_0, t]$. We define the points τ_i such that $t_{i-1} < \tau_i < t_i$ for $i = 1, \ldots, n$.

Definition 1.3.3. The stochastic integral of the simple process $X(t)$ with respect to the Wiener process $W(t)$ is the random variable

$$I_t = \int_{t_0}^{t} X(s, \omega)\ dW(s, \omega) = \sum_{i=0}^{n-1} X(\tau_i, \omega)[W(t_{i+1}, \omega) - W(t_i, \omega)].$$

It is clear that the definition depends on the particular choice of the points τ_i. If we take $\tau_i = t_i$, we obtain the Itô integral, if we take $\tau_i = \frac{t_{i+1}+t_i}{2}$ we obtain the Stratonovich integral. We note that in the case of the Stratonovich integral even if $X(t)$ is non-anticipating, there is no independence of the increments $W(s) - W(t)$.

It is possible to extend the definition of stochastic integral to the entire class $M_2[t_0, t]$, because the class of simple processes is dense in $M_2[t_0, t]$.

Theorem 1.3.4. *For every process $X(t) \in M_2[t_0, t]$ there exists a sequence of simple processes $X_n(t) \in M_2[t_0, t]$ such that*

$$\lim_{n\to\infty} \mathbb{E}\left\{\int_{t_0}^{t} \mid X_n(s, \omega) - X(s, \omega) \mid^2\ ds\right\} = 0.$$

Definition 1.3.5. The sequence $X_n(t)$ *converges in mean square* to $X(t)$ if

$$\lim_{n\to\infty} \mathbb{E}\left(\mid X_n - X \mid^2\right) = 0.$$

and we write $X = \text{m.s.}\lim_n X_n$ (mean square limit).

Theorem 1.3.6. *If $X_n(t) \in M_2[t_0, t]$ is a sequence of simple processes then there exists a process $X(t) \in M_2[t_0, t]$ such that*

$$\int_{t_0}^{t} X(s,\omega)\ dW(s,\omega) = m.s.\lim_{n\to\infty} \int_{t_0}^{t} X_n(s,\omega)\ dW(s,\omega).$$

Theorems 1.3.4 and 1.3.6 enable us to define the stochastic integral for a process $X(t) \in M_2[t_0, t]$ in the following way:

$$\int_{t_0}^{t} X\ dW = \text{m.s.}\lim_n \int_{t_0}^{t} X_n\ dW,$$

where $\{X_n(t)\}$ converges to $X(t)$ in $M_2[t_0, T]$.

For the properties, the proofs and some examples of stochastic integrals see [34], [42], [57], [58] and references therein.

1.4 Stochastic Differential Equations

In the stochastic basis $(\Omega, \mathcal{F}, (\mathcal{F}_t), \mathbb{P})$ we consider the following Stochastic Differential Equation (SDE)

$$dX(t) = b[t, X(t)]dt + \sigma[t, X(t)]dW(t) \tag{1.3}$$

with initial condition $X(0) = \xi$, where $b[t, X(t)]$ and $\sigma[t, X(t)]$ are the drift and diffusion coefficients, respectively. $\{W(t), t \geq 0\}$ is a standard Wiener process and $\{X(t), t \geq 0\}$ is a suitable real-valued stochastic process with continuous sample paths.
The equation (1.3) has to be read as a different representation of the integral equation:

$$X(t) = X(0) + \int_0^t b[s, X(s)]ds + \int_0^t \sigma[s, X(s)]dW(s). \tag{1.4}$$

Following [42] we recall some important definitions.

Definition 1.4.1. A *strong solution* of the SDE (1.3) on the given space $(\Omega, \mathcal{F}, \mathbb{P})$ and with respect to the fixed standard Brownian motion $W(t)$ and initial condition ξ, is a process $X(t)$ with continuous sample paths and with the following properties:

i) $X(t)$ is adapted to the filtration $\{\mathcal{F}_t, t \geq 0\}$,

ii) $\mathbb{P}[X(0) = \xi] = 1$,

iii) $\mathbb{P}\left[\int_0^t \{|b[s, X(s)]| + \sigma^2[s, X(s)]\} ds < \infty\right] = 1$,

iv) $X(t) = X(0) + \int_0^t b[s, X(s)]ds + \int_0^t \sigma[s, X(s)]dW(s)$ holds almost surely.

Definition 1.4.2. A solution $X(t)$ of SDE (1.3) is *pathwise unique* if for every other process $Y(t)$ solution of (1.3), $X(t)$ and $Y(t)$ are indistinguishable.

Definition 1.4.3. $X(t)$ and $Y(t)$ are *indistinguishable* if almost all their sample paths agree

$$\mathbb{P}[X(t) = Y(t), \forall t \geq 0] = 1.$$

Let us recall the conditions that guarantee the existence and uniqueness of a strong solution of SDE (1.3).

Theorem 1.4.4 ([42]). *Suppose that the coefficients $b[t, X(t)]$ and $\sigma[t, X(t)]$ satisfy the global Lipschitz condition*

$$||b(t, x) - b(t, y)|| + ||\sigma(t, x) - \sigma(t, y)|| \leq K||x - y||, \tag{1.5}$$

and linear growth condition

$$||b(t, x)||^2 + ||\sigma(t, x)||^2 \leq K^2(1 + ||x||^2), \tag{1.6}$$

for every $0 \leq t < \infty$, $x, y \in \mathbb{R}$, where K is a positive constant. On some probability space $(\Omega, \mathcal{F}, \mathbb{P})$ let ξ be a real-valued random variable independent of the Wiener process $W(t)$ and with finite second moment: $\mathbb{E}||\xi||^2 < \infty$. Let $\{\mathcal{F}_t, t \geq 0\}$ be a filtration. Then there exists a pathwise unique continuous process $\{X(t), t \geq 0\}$ adapted to $\{\mathcal{F}_t, t \geq 0\}$ which is a strong solution of SDE (1.3) with initial condition ξ. Moreover the process $\in M_2[0, T]$: for every $T > 0$ there exists a constant C, depending only on K and T such that

$$\mathbb{E}||X(t)||^2 \leq C(1 + \mathbb{E}||\xi||^2)e^{Ct}; \quad 0 \leq t \leq T.$$

The condition on the independence of ξ with respect to W ensures that ξ is non-anticipating, whereas the condition (1.8) excludes the case in which the solution goes to infinity in finite time.

So a strong solution is considered on a given probability space, with respect to a given filtration and a given Wiener process. When the probability space, the filtration and the driving Wiener process are not imposed, but are themselves part of the problem we talk about weak solutions.

Definition 1.4.5. A *weak solution* of the SDE (1.3) is a triple

$$(X, W), (\Omega, \mathcal{F}, \mathbb{P}), (\mathcal{F}_t)$$

where:

i) $(\Omega, \mathcal{F}, \mathbb{P})$ is a probability space and $(\mathcal{F}_t)$ is a filtration satisfying the usual condition (i.e. $\mathcal{F}_0$ contains all $\mathbb{P}$-null sets) ,

ii) $X = \{X(t), t \geq 0\}$ is a continuous real-valued process adapted to $(\mathcal{F}_t)$ and $W = \{W(t), t \geq 0\}$ is a Wiener process,

iii) $\mathbb{P}\left[\int_0^t \{|b[s, X(s)]| + \sigma^2[s, X(s)]\} ds < \infty\right] = 1$,

iv) $X(t) = X(0) + \int_0^t b[s, X(s)]ds + \int_0^t \sigma[s, X(s)]dW(s)$ almost surely.

Again following [42] we state, now, the theorem of existence of a weak solution for SDE (1.3) in the case of $\sigma(t, X) = 1$.

Theorem 1.4.6. *Consider the SDE*

$$dX(t) = b[t, X(t)]dt + dW(t), \quad 0 \leq t \leq T, \tag{1.7}$$

where T is a fixed positive number, $W(t)$ is a Wiener process and $b(t, x)$ is a Borel-measurable, real-valued function on $[0, T] \times \mathbb{R}$ which satisfies

$$||b(t, x)|| \leq K(1 + ||x||), \qquad 0 \leq t \leq T, \ x \in \mathbb{R} \tag{1.8}$$

for some positive constant K.
Then for any probability measure μ on $(\mathbb{R}, \mathcal{B}(\mathbb{R}))$, equation (1.7) has a weak solution with initial distribution μ.

Moreover Theorem 1.4.6 ensures that the solution is unique in the sense of probability law.

Definition 1.4.7. We say that *uniqueness in the sense of probability law* holds if, for any two solutions of equation (1.7), $(X, W), (\Omega, \mathcal{F}, \mathbb{P}), (\mathcal{F}_t)$ and $(\tilde{X}, \tilde{W}), \left(\tilde{\Omega}, \tilde{\mathcal{F}}, \tilde{\mathbb{P}}\right), (\tilde{\mathcal{F}}_t)$ with the same initial distribution, the two processes $X, \tilde{X}$ have the same law.

Chapter 2

Gauss-Markov and Diffusion processes

This Chapter is devoted to the collection of the main definitions and properties about the Gauss-Markov and Diffusion processes and their associated First Passage Time random variables. Next section is devoted to the Markov property and to the role these markovian processes play in the theory of SDEs.

2.1 The Markov property

Let $(\Omega, \mathcal{F}, \mathbb{P})$ be a probability space with a filtration $\{\mathcal{F}_t, t \in T\}$, where T is a continuous parameter set.

Definition 2.1.1. A stochastic process $\{X(t), t \in T\}$, is *Gaussian* if the finite collection of random variables $X(t_1), \ldots, X(t_n)$ has a multivariate normal distribution for every n and $t_1, \ldots, t_n \in T$.

Along the lines of [42] we give the following definitions.

Definition 2.1.2. Let μ be a probability measure on $(\mathbb{R}, \mathcal{B}(\mathbb{R}))$. A real-valued stochastic process $\{X(t), t \in T\}$ adapted to the filtration $\{\mathcal{F}_t, t \in T\}$, is said to be a *Markov process* with initial distribution μ if

(i) $\mathbb{P}(X(0) \in \Gamma) = \mu(\Gamma), \ \forall \Gamma \in \mathcal{B}(\mathbb{R})$

(ii) for $s, t \geq 0$ and $\Gamma \in \mathcal{B}(\mathbb{R})$,

$$\mathbb{P}[X(t+s) \in \Gamma | \mathcal{F}_s] = \mathbb{P}[X(t+s) \in \Gamma | X(s)], \quad \mathbb{P}\text{-almost surely.}$$

The probability appearing on the right-hand side of (ii) is conditioned on the $\sigma-$algebra generated by $X(s)$ (see Definition 1.1.3). The property (ii) is known as the memoryless of the process and roughly speaking it means that the conditional probability is determined entirely by the knowledge of the most recent state of the process. If it holds also for any random times we talk about strong Markov property.

Definition 2.1.3. Let μ be a probability measure on $(\mathbb{R}, \mathcal{B}(\mathbb{R}))$. A real-valued stochastic process $\{X(t), t \in T\}$, progressively measurable on $(\Omega, \mathcal{F}, (\mathcal{F}_t), \mathbb{P})$, is said to be a *strong Markov process* with initial distribution μ if

(i) $\mathbb{P}(X(0) \in \Gamma) = \mu(\Gamma), \ \forall \Gamma \in \mathcal{B}(\mathbb{R})$

(ii) for any optional time S of $\{\mathcal{F}_t, t \in T\}$ and $\Gamma \in \mathcal{B}(\mathbb{R})$

$$\mathbb{P}[X(S+t) \in \Gamma | \mathcal{F}_S] = \mathbb{P}[X(S+t) \in \Gamma | X(S)], \quad \mathbb{P}\text{-almost surely.}$$

The probability appearing on the right-hand side of (ii) is conditioned on the $\sigma-$algebra generated by $X(S)$, i.e. the collection of all sets of the form $\{X(S) \in A\}$ and $\{X(S) \in A\} \cup \{S = \infty\}$ with $A \in \mathcal{B}(\mathbb{R})$. Finally, we note that every strong Markov process is a Markov process.

We consider the following SDE

$$dX(t) = A_1(X(t), t)dt + \sqrt{A_2(t)}dW(t), \text{ with } X(t_0) = x_0 \tag{2.1}$$

for $t \geq t_0$, where $W(t)$ is the Wiener process and $A_1(x,t)$ and $A_2(t)$ are respectively the drift and the infinitesimal variance of the process $X(t)$:

$$\begin{aligned} A_n(x,t) &= \lim_{\Delta t \to 0} \frac{1}{\Delta t} E\{[X(t+\Delta t) - X(t)]^n | X(t) = x\} \\ &= \lim_{\Delta t \to 0} \frac{1}{\Delta t} \int_{\mathbb{R}} (z-x)^n f(z, t+\Delta t | x, t) dz \quad (n = 1, 2). \end{aligned} \tag{2.2}$$

In the last equation, $f(z, t+\Delta t|x,t)$ represents the transition probability density function of the process $X(t)$, i.e.

$$f(x,t|y,\tau) = \frac{\partial}{\partial x} \mathbb{P}(X(t) < x | X(\tau) = y) \tag{2.3}$$

and since $X(t)$ is Markov $f(x,t|y,\tau)$ satisfies the following Chapman-Kolmogorov integral equation

$$f(x,t|y,\tau) = \int_{\mathbb{R}} f(x,t|z,u) f(z,u|y,\tau) dz, \quad x, y \in \mathbb{R}; \tau, u, t \in T, \tau < u < t. \tag{2.4}$$

In Section 1.4 we recalled that under the hypotheses of measurability, global Lipschitz condition (1.5) and restriction on the growth (1.8) of the involved infinitesimal moments $A_1(x,t)$ and $A_2(t)$, Equation (2.1) admits a solution.

Determined that the solution exists, there remains the problem of finding it. The classical "diffusion equations approach" is to evaluate the transition probability functions $f(x,t|\cdot,\cdot)$ of the solution process using the techniques of resolution of the partial differential equations. In fact, each $f(x,t|y,\tau)$ of the solution process satisfies the following Fokker-Planck equation and the associated initial condition:

$$\begin{aligned} \frac{\partial f(x,t|y,\tau)}{\partial t} &= -\frac{\partial}{\partial x}[A_1(x,t)f(x,t|y,\tau)] + \frac{1}{2}\frac{\partial^2}{\partial x^2}[A_2(t)f(x,t|y,\tau)] \\ \lim_{t\to\tau} f(x,t|y,\tau) &= \delta(x-y). \end{aligned} \tag{2.5}$$

The Kolmogorov consistency theorem [57] guarantees that a stochastic process is determined by the family of its finite-dimensional distributions. Thanks to the Markov property these distributions can be obtained knowing the initial distribution and the transition probabilities. Next theorem goes in this direction:

Theorem 2.1.4 ([3]). *If the SDE (2.1) satisfies the conditions of existence and uniqueness of Theorem 1.4.4, the solution $X(t)$ of the equation for arbitrary initial values is a Markov process whose initial probability distribution at the instant t_0 is the distribution of $X(t_0)$ and whose transition probabilities are given by*

$$\mathbb{P}[X(t) \in E | X(s) = x]$$

where $X(t)$ is the solution of the associated integral equation

$$X(t) = x + \int_s^t A_1(X(u),u)du + \int_s^t \sqrt{A_2(u)}dW(u), \quad t_0 \le s \le t. \tag{2.6}$$

In particular if the coefficients $A_1(X,t) \equiv A_1(X)$ and $A_2(t) \equiv A_2$ are independent of t, the solution of (2.1) is an homogeneous Markov process with stationary transition probabilities.

Theorem 2.1.4 ensures that the solutions of SDEs of the type of (2.1) are Markov processes, the next theorem shows when those solutions are also diffusion processes:

Theorem 2.1.5 ([3]). *If the SDE (2.1) satisfies the condition of existence and uniqueness of Theorem 1.4.4 and if the coefficients $A_1(X,t)$ and $A_2(t)$ are continuous functions with respect to t, the solution $X(t)$ of the equation is a Diffusion process.*

In the next section we show a different approach that is helpful in the case of Gauss-Markov processes and in particular in the context of the first passage time problem.

2.1.1 Basics on Gauss-Markov Processes

In the rest of the section we will assume that the process $\{X(t), t \in T\}$, where $T = [0, +\infty)$, is a real continuous Gaussian process with the following properties:

1. $m(t) := E[X(t)]$ is continuous in T;
2. the covariance $c(s,t) := E\{[X(s) - m(s)][X(t) - m(t)]\}$ is continuous in $T \times T$;
3. $X(t)$ is non-singular except possibly at the end points of T, i.e. $X(t)$ has a non-singular normal distribution except possibly at $t = 0$, where $X(0)$ could be equal to $m(0)$ with probability 1.

We recall an important characterization of the Gauss-Markov (GM) processes:

Theorem 2.1.6. *A Gaussian process is Markov if and only if its covariance satisfies*

$$c(s,u) = \frac{c(s,t)c(t,u)}{c(t,t)} \tag{2.7}$$

for all $s \leq t \leq u$, with s, t, u belonging to the interior of T.

In particular well-behaved solutions of (2.7) can be written as product of two functions $h_1(t)$, $h_2(t)$, i.e.

$$c(s,t) = h_1(s)h_2(t), \quad s \leq t \tag{2.8}$$

where

$$r(t) = \frac{h_1(t)}{h_2(t)} \tag{2.9}$$

is a monotonically increasing function and $h_1(t)h_2(t) > 0$ because of the assumed non-singularity of the process on the interior of T. The transition probability density function $f(x,t|y,\tau)$ of a GM process is a normal-type density characterized respectively by conditional mean and variance:

$$\begin{aligned} E[X(t)|X(\tau) = y] &= m(t) + \frac{h_2(t)}{h_2(\tau)}[y - m(\tau)] \\ D^2[X(t)|X(\tau)] &= h_2(t)\left[h_1(t) - \frac{h_2(t)}{h_2(\tau)}h_1(\tau)\right] \end{aligned} \tag{2.10}$$

for $t, \tau \in T$, $\tau < t$, i.e.

$$f(x,t|y,\tau) = \frac{1}{\sqrt{2\pi D^2[X(t)|X(\tau)]}} \exp\left\{-\frac{\{x - E[X(t)|X(\tau)=y]\}^2}{2D^2[X(t)|X(\tau)]}\right\} \quad (2.11)$$

If $m(t), h_1(t), h_2(t) \in \mathcal{C}^1(T)$, $f(x,t|y,\tau)$ satisfies the Fokker-Planck equation (2.5) with $A_1(x,t)$ and $A_2(t)$ given by

$$A_1(x,t) = m'(t) + [x - m(t)]\frac{h_2'(t)}{h_2(t)}, \quad A_2(t) = h_2^2(t)r'(t), \quad (2.12)$$

where the prime denotes the derivative with respect to the argument. In this case we can call the GM processes also Gauss-Diffusion (GD) processes. Equations (2.12) show that for GD processes the drift is in general time-dependent and dependent on x at most linearly and the infinitesimal variance depends at most on t. In fact, setting

$$a(t) = \frac{h_2'(t)}{h_2(t)}, \quad b(t) = m'(t) - m(t)\,\frac{h_2'(t)}{h_2(t)}, \quad \sigma^2(t) = h_2^2(t)\,r'(t), \quad (2.13)$$

the infinitesimal moments (2.12) for the GD process $\{X(t), t \in T\}$, alternatively, can be rewritten as space-linear functions as follows:

$$A_1(x,t) = a(t)x + b(t), \qquad A_2(t) = \sigma^2(t) \quad \text{for} \quad t \geq 0. \quad (2.14)$$

The Gauss-Markov process $X(t)$, with mean $m(t)$ and covariance factors $h_1(t)$, $h_2(t)$, satisfies the following Doob's representation formula (see, for instance, [23])

$$X(t) = m(t) + h_2(t)W[r(t)], \quad (2.15)$$

where $W(t)$ is a standard Wiener process.

Proposition 2.1.7 ([7]). *The GD process $X(t)$ solution of equation (2.1) is characterized , alternatively, by the following infinitesimal moments:*

$$A_1(X,t) = m'(t) + h_2'(t)W[r(t)], \quad A_2(t) = h_1'(t)h_2(t) - h_1(t)h_2'(t). \quad (2.16)$$

In particular, $A_1(X,t) \equiv \mathbb{E}[dX(t)]$.

Proof. Note that applying the Itô differentiation rule on both sides of (2.15),

$$\begin{aligned} dX(t) &= m'(t)dt + h_2'(t)W[r(t)]dt + h_2(t)\sqrt{r'(t)}dW(t) \\ &= \{m'(t) + h_2'(t)W[r(t)]\}\,dt + h_2(t)\sqrt{r'(t)}dW(t). \end{aligned} \quad (2.17)$$

From (2.15), $W[r(t)] = [X(t) - m(t)]/h_2(t)$; recalling (2.12) and (2.1), one has

$$m'(t) + h_2'(t)W[r(t)] = m'(t) + h_2'(t)\frac{[X(t) - m(t)]}{h_2(t)} = A_1(X,t)$$
$$h_2(t)\ \sqrt{r'(t)} = \sqrt{A_2(t)}.$$

and so equations (2.16) hold. □

We stress that we can derive the coefficient functions $a(t), b(t)$ and $\sigma^2(t)$ of equations (2.13) when we specify the mean and the autocovariance function of the corresponding GM process as shown in the following theorem.
Using (2.14) the SDE (2.1) becomes

$$dX(t) = [a(t)X(t) + b(t)]dt + \sigma(t)dW(t), \quad X(0) = x_0 = m(0). \tag{2.18}$$

In Proposition 5 of [13] the authors provide a way to find the process solution of (2.18). Since it is Gaussian its probability law is completely specified by the mean and covariance functions.

Theorem 2.1.8. *The solution of SDE (2.18) is the GD process having the mean and covariance functions*

$$m(t) = \left[x_0 + \int_0^t b(\tau)e^{-\int_0^\tau a(s)ds}d\tau\right] e^{\int_0^t a(s)ds} \qquad (t \in T)$$
$$c(\tau,t) = \left[\int_0^t \sigma^2(\xi)e^{-2\int_0^\xi a(s)ds}d\xi\right] e^{\int_0^t a(s)ds} e^{\int_0^\tau a(s)ds} \qquad (0 \le \tau \le t). \tag{2.19}$$

We note that we can determine the covariance factors:

$$h_1(t) = \frac{1}{\sigma(0)}\left[\int_0^t \sigma^2(\xi)e^{-2\int_0^\xi a(s)ds}d\xi\right] e^{\int_0^t a(s)ds}$$
$$h_2(t) = e^{\int_0^t a(s)ds}\sigma(0), \qquad (t \ge 0). \tag{2.20}$$

2.1.2 Examples

The GM process class includes several processes widely studied in the theory of stochastic processes. Among all we recall:

- The **Wiener process** $\{W(t), t \geq 0\}$ with the following infinitesimal moments

$$A_{1_W}(x,t) = b_W, \qquad A_{2_W}(t) = \sigma_W^2, \quad \text{for} \quad t \geq 0, \tag{2.21}$$

has the mean $m(t)$ and covariance factors $h_1(t)$, $h_2(t)$ as follows

$$\begin{aligned} &m_W(t) = b_W t + c_W, \\ &h_{1_W}(t) = \sigma_W t, \quad h_{2_W} = \sigma_W, \quad (b_W, c_W \in \mathbb{R}, \sigma_W \in \mathbb{R}^+). \end{aligned} \tag{2.22}$$

Its coefficient functions $a(t), b(t), \sigma^2(t)$, for $t \geq 0$ can be derived from (2.13) using (2.22), they are such that

$$a(t) \equiv 0, \quad b(t) \equiv b_W \quad \text{and} \quad \sigma^2(t) \equiv \sigma_W^2. \tag{2.23}$$

Moreover, from (2.10), for $0 \leq \tau < t$

$$\begin{aligned} E_W(t|y,\tau) &= E[W(t)|W(\tau) = y] = y + b_W(t-\tau) \\ D_W^2(t|\tau) &= D^2[W(t)|W(\tau)] = \sigma_W^2 \cdot (t-\tau). \end{aligned} \tag{2.24}$$

- The well-known **Ornstein-Uhlenbeck (OU) process** $\{U(t), t \geq 0\}$ has the infinitesimal moments for $t \geq 0$

$$A_{1_U}(x,t) = -a_U x + b_U, \qquad A_{2_U}(t) = \sigma_U^2, \tag{2.25}$$

and mean and covariance factors:

$$\begin{aligned} &m_U(t) = \frac{b_U}{a_U} + \left(c_U - \frac{b_U}{a_U}\right) e^{-a_U t}, \\ &h_{1_U}(t) = \frac{\sigma_U}{2a_U}(e^{a_U t} - e^{-a_U t}), \quad h_{2_U}(t) = \sigma_U e^{-a_U t}, \end{aligned} \tag{2.26}$$

with $a_U, \sigma_U \in \mathbb{R}^+, b_U, c_U \in \mathbb{R}$. In this case the coefficient functions $a(t), b(t), \sigma^2(t)$, for $t \geq 0$, from (2.13) and (2.26), are such that

$$a(t) \equiv -a_U, \quad b(t) \equiv b_U \quad \text{and} \quad \sigma^2(t) \equiv \sigma_U^2. \tag{2.27}$$

Moreover, from (2.10), for $0 \leq \tau < t$

$$\begin{aligned} E_U(t|y,\tau) &= E[U(t)|U(\tau)=y] = \frac{b_U}{a_U} + \left(y - \frac{b_U}{a_U}\right) e^{-a_U(t-\tau)} \\ D_U^2(t|\tau) &= D^2[U(t)|U(\tau)] = \frac{\sigma_U^2}{2a_U}\left[1 - e^{-2a_U(t-\tau)}\right]. \end{aligned} \tag{2.28}$$

The previous ones are examples of time-homogeneous processes. Time-inhomogeneous processes, here called also Generalized Ornstein-Uhlenbeck processes, belong also to the GM class. In the context of applications these processes play a key role in the modeling of phenomena subject to external time-dependent forces.

- A **time-inhomogeneous Ornstein-Uhlenbeck process** $\{V(t), t \geq 0\}$ has the infinitesimal moments for $t \geq 0$

$$A_{1_V}(x,t) = -a_V x + b_V(t), \qquad A_{2_V}(t) = \sigma_V^2, \tag{2.29}$$

and the following mean and covariance factors

$$\begin{aligned} m_V(t) &= [c_V + B_V(t)]\, e^{-a_V t}, \text{ with } B_V(t) = \int_0^t b_V(\tau) e^{a_V \tau} d\tau, \\ h_{1_V}(t) &= \frac{\sigma_V}{2a_V}(e^{a_V t} - e^{-a_V t}), \quad h_{2_V}(t) = \sigma_V e^{-a_V t}, \end{aligned} \tag{2.30}$$

with $a_V, \sigma_V \in \mathbb{R}^+, c_V \in \mathbb{R}$, and $b_V(t)$ a time continuous function. Note that $h_{1_V}(t) = h_{1_U}(t)$ and $h_{2_V}(t) = h_{2_U}(t)$ for $a_V = a_U$ and $\sigma_V = \sigma_U$. Now, the coefficient functions $a(t), b(t), \sigma^2(t)$, for $t \geq 0$, from (2.13) and (2.30), are such that

$$a(t) \equiv -a_V, \quad b(t) = b_V(t) \quad \text{and} \quad \sigma^2(t) \equiv \sigma_V^2. \tag{2.31}$$

Finally, from (2.10) and (2.30), for $0 \leq \tau < t$

$$\begin{aligned} E_V(t|y,\tau) &= E[V(t)|V(\tau)=y] = m_V(t) + e^{-a_V(t-\tau)}\,[y - m_V(\tau)] \\ D_V^2(t|\tau) &= D^2[V(t)|V(\tau)] = \frac{\sigma_V^2}{2a_V}\left[1 - e^{-2a_V(t-\tau)}\right]. \end{aligned} \tag{2.32}$$

An analogous of the transformation (2.15) for the OU and generalized OU processes can be proved (see [25], [54]).
In the case of the OU process, $r(t) = \dfrac{e^{2a_U t} - 1}{2a_U}$ and so

$$U(t) = m_U(t) + \sigma_U e^{-a_U t} W\left(\frac{e^{2a_U t} - 1}{2a_U}\right). \tag{2.33}$$

Whereas the process $V(t)$, having the mean $m_V(t)$ and the same covariance factors of $U(t)$, can be written as follows

$$V(t) = m_V(t) + \sigma_V e^{-a_V t} W\left(\frac{e^{2a_V t} - 1}{2a_V}\right) \tag{2.34}$$

and, since $a_U = a_V$ and $\sigma_U = \sigma_V$, from (2.33)

$$V(t) = m_V(t) + [U(t) - m_U(t)]\,. \tag{2.35}$$

2.2 First Passage Time

The First Passage Time (FPT) is one of the most studied and challanging problems in the framework of stochastic processes ([20], [66] and [69]). The literature devoted to the FPT problem is wide, even if few improvements have been made in the last decades. The FPT problem consists in the determination of the distribution of the first time the process describing the modelled system dynamics enters a particular region or reaches a boundary or threshold. The problem is of fundamental relevance being representative of the evolution of processes in a wide range of applications like in neuroscience ([13], [18], [19], [45], [79]), molecular biology ([10],[11]), population dynamics ([61], [62]), queueing theory ([22], [36]) and finance ([4]).

2.2.1 One boundary: integral equation approach

Let the GD process $X(t)$ evolve in the presence of a boundary $S(t)$, that when specified will be considered constant. The first passage time $\mathcal{T}$ of the process $X(t)$ through $S(t)$ is defined as:

$$\mathcal{T} := \inf_{t \geq t_0} \{t : X(t) \geq S(t)\} \quad \text{with} \quad X(t_0) = x_0 < S(t_0)$$

and with the probability density function (pdf)

$$g(S(t), t|x_0, t_0) := \frac{d\mathbb{P}(\mathcal{T} \leq t)}{dt}.$$

Using the Doob-representation formula (2.15) it is possible to construct the FPT pdf of the GM process $X(t)$ in terms of the FPT pdf $g_W(S(t), t|x_0, t_0)$ of the standard Wiener process:

$$g(S(t), t|x_0, t_0) = \frac{dr(t)}{dt} g_W\{S^*[r(t)], r(t)|x_0^*, r(t_0)\}, \tag{2.36}$$

where the process $W(\vartheta)$ evolves from x_0^* at time ϑ_0 in presence of the continuous boundary $S^*(\vartheta)$ with

$$x_0^* = \frac{x_0 - m[r^{-1}(\vartheta_0)]}{h_2[r^{-1}(\vartheta_0)]}, \qquad S^*(\vartheta) = \frac{S[r^{-1}(\vartheta)] - m[r^{-1}(\vartheta)]}{h_2[r^{-1}(\vartheta)]}. \tag{2.37}$$

Hence results on the FPT pdf for the standard Wiener process can thus be used to obtain the FPT pdf of any continuous GM process. Unfortunately results in closed form in the case of GM processes are available only in few cases and even in those cases exponentially large times are involved for instance when transforming the Ornstein-Uhlenbeck process to the Wiener process and this implies an unacceptable computational time dilation and loss of accuracy in the numerical results.

An alternative approach can be followed. Since the sample paths of $X(t)$ are continuous functions, any sample path that starts at time τ from $y < S(\tau)$ and reaches a state $x > S(t)$ must cross the threshold for the first time at some instant θ between τ and t. This sentence can be translated in the following way:

$$f(x,t|y,\tau) = \int_\tau^t g[S(\theta),\theta|y,\tau] f[x,t|S(\theta),\theta] d\theta \tag{2.38}$$

for $x \geq S(t)$ and $y < S(\tau)$. Equation (2.38) is a first-kind Volterra integral equation in the unknown $g[S(t),t|y,\tau]$. The kernel $f[x,t|S(\theta),\theta]$ exhibits a singularity of the type $\frac{1}{\sqrt{t-\theta}}$ as $\theta \to t$, so the numerical resolution of (2.38) is quite complicated.

An important contribution to the solution of these critical issues is due to Durbin ([28], [29]) who gave an explicit formula for the FPT pdf of a continuous Gaussian process to a general boundary. He suggested also approximations formula, but with no bounds on the errors. In [30] the case of Brownian motion crossing a curved boundary is considered and the formula of [29] is expanded as a series whose terms are multiple integrals of increasing dimensionality. Unfortunately the algorithms proposed were too expensive to run and necessitated of large computation facilities.

In [8] is presented a direct and efficient computational method to obtain evaluation of the FPT pdf for diffusion processes based on the idea of removing the singularity of the kernel in the equation (2.38). It is done modifying the equation itself, or, to put it better, observing that if $S(t) \in \mathcal{C}^1(T)$ the FPT pdf $g(S(t),t|x_0,t_0)$ can be obtained as solution of the following second-

kind Volterra integral equation

$$g(S(t),t|x_0,t_0) = -\Psi[S(t),t|x_0,t_0] + \int_{t_0}^{t} \Psi[S(t),t|S(\tau),\tau] g(S(\tau),\tau|x_0,t_0) d\tau \tag{2.39}$$

with

$$\begin{aligned} \Psi(S(t),t|y,\tau) &= \left\{ S^{'}(t) - A_1[S(t)] + \frac{1}{2} A_2^{'}[S(t)] + k(t) \right\} f(S(t),t|y,\tau) \\ &+ \frac{1}{2} A_2[S(t)] \frac{\partial}{\partial x} f(x,t|y,\tau)\Big|_{x=S(t)} \end{aligned} \tag{2.40}$$

where $k(t)$ is an arbitrary continuous function. Even if equation (2.39) may seem more cumbersome than equation (2.38), it presents a degree of freedom: the specification of $k(t)$. In fact the singularity of the kernel can be removed. Following [8] we have that if $S(t) \in \mathcal{C}^2(T)$ then

$$\lim_{\tau \to t} \Psi[S_1(t),t|S_1(\tau),\tau] = 0 \tag{2.41}$$

if and only if

$$k(t) = \frac{1}{2} \left\{ A_1[S(t)] - \frac{1}{4} A_2^{'}[S(t)] - S^{'}(t) \right\}. \tag{2.42}$$

Hence using the $k(t)$ as in (2.42), the kernel in (2.38) becomes non singular and a simple numerical procedure can be applied.
We observe that the function Ψ in (2.40) can be also written in the following way ([7])

$$\begin{aligned} &\Psi(S(t),t|y,\tau) = f[S(t),t|y,\tau] \\ &\times \left\{ S^{'}(t) - A_1[S(t),t] - A_2(t) \frac{S(t) - E[X(t)|X(\tau)=y]}{2D^2[X(t)|X(\tau)=y]} + k(t) \right\} \end{aligned} \tag{2.43}$$

again imposing

$$\lim_{\tau \to t} \Psi[S(t),t|S(\tau),\tau] = 0. \tag{2.44}$$

In [23] these techniques are improved and specialized in the case of Gauss-Markov processes. This new computationally simple and accurate method allows to construct the FPT pdf for GM processes through time-dependent boundaries for fixed or random initial states. In [23] is proved that if

$$S(t_0) > x_0 \text{ and } S(t), m(t), h_1(t), h_2(t) \in \mathcal{C}^1(T) \tag{2.45}$$

then $g(S(t),t|x_0,t_0)$ can be obtained as solution of a second-kind Volterra integral equation of the form (2.39) with

$$\begin{aligned}\Psi(S(t),t|y,\tau) &= \left\{\frac{S'(t)-m'(t)}{2}-\frac{S(t)-m(t)}{2}\frac{h_1'(t)h_2(\tau)-h_2'(t)h_1(\tau)}{h_1(t)h_2(\tau)-h_2(t)h_1(\tau)}\right. \\ &- \left.\frac{y-m(\tau)}{2}\frac{h_2'(t)h_1(t)-h_2(t)h_1'(t)}{h_1(t)h_2(\tau)-h_2(t)h_1(\tau)}\right\} f[S(t),t|y,\tau]. \quad (2.46)\end{aligned}$$

For a detailed description of the numerical algorithm for the solution of (2.39) with (2.46) we quote [13] and [23], we limit to observe that for its application we need the mean and the covariance of the process $X(t)$, for instance using Theorem 2.1.8. If we know them we can write the normal transition pdf $f[S(t),t|y,\tau]$ and the function $\Psi(S(t),t|y,\tau)$ involved in the Volterra integral equation.

One boundary case: closed form results

As already said, analytical results in closed form for the FPT pdf are available in very few cases. For this reason the numerical approach presented in the previous subsection plays a fundamental role in this context.
Here we present the special conditions that guarantee a closed form expression of the FPT pdf.

If we impose that the kernel of integral equation (2.39) vanishes identically we obtain the following conditions:

Theorem 2.2.1 ([23]). *Under assumptions (2.45) , we have*

$$\Psi[S(t),t|S(\tau),\tau]=0 \quad \forall t,\tau\in T \text{ with } \tau\le t$$

if and only if $\exists\, b_1,b_2\in\mathbb{R}$ *such that*

$$S(t)=m(t)+b_1h_1(t)+b_2h_2(t) \quad \forall t\in T. \tag{2.47}$$

Note that, since $m(t_0)=x_0$, b_2 is not really arbitrary:

$$b_2=\frac{S(t_0)-x_0}{h_2(t_0)}.$$

Using the previous observation and equations (2.20), condition (2.47) can be rewritten as:

$$\exists\, b_1\in\mathbb{R}: S(t)=\left[S(t_0)+\int_{t_0}^{t}b(s)e^{-\int_{t_0}^{s}a(\tau)d\tau}ds\right]e^{\int_{t_0}^{t}a(\tau)d\tau}+b_1h_1(t), \quad \forall t\in T. \tag{2.48}$$

From equation (2.39), if the assumptions of Theorem 2.2.1 hold one obtains

$$g(S(t),t|x_0,t_0) = \frac{S(t_0)-x_0}{r(t)-r(t_0)}\frac{h_2(t)}{h_2(t_0)}\frac{dr(t)}{dt}f[S(t),t|x_0,t_0] \tag{2.49}$$

that is completely determined if one knows the mean and covariance factors of the process $X(t)$.
Furthermore if $t \to +\infty$, then

$$\begin{aligned}\mathbb{P}(\mathcal{T} < +\infty) &= \int_{t_0}^{+\infty} g(S(t),t|x_0,t_0)dt \\ &= \begin{cases} 1, & \text{if } b_1 \leq 0, \\ \exp\left\{-\frac{2b_1[S(t_0)-x_0]}{h_2(t_0)}\right\}, & \text{if } b_1 > 0. \end{cases}\end{aligned} \tag{2.50}$$

Another way to obtain a closed form expression for $g(S(t),t|x_0,t_0)$ is that for which the integral term on the right-hand side of equation (2.39) vanishes ([7]). Using the expression (2.43), we have that

$$\int_{t_0}^{t} \Psi[S(t),t|S(\tau),\tau]g(S(\tau),\tau|x_0,t_0)d\tau = 0 \tag{2.51}$$

if and only if $\exists\, d_1 > 0, d_2 \neq 0$ and d_3 such that $d_1^2 + d_3 > 0$:

$$\begin{aligned} S(t) &= m(t) + d_2h_2(t) - \frac{h_1(t)}{2d_2}\ln[d_1 + \sqrt{\delta(t)}], \text{ and} \\ k(t) &= \frac{A_1[S(t),t] - S'(t)}{2} + \frac{d_1d_2[\sqrt{\delta(t)} - d_1]h_2^2(t_0)}{2h_1(t)[\sqrt{\delta(t)}+d_1]\sqrt{\delta(t)}}, \end{aligned} \tag{2.52}$$

where $\delta(t) = d_1^2 + d_3e^{-4d_2^2\frac{h_2(t)}{h_1(t)}}$. Of course in this case

$$g(S(t),t|x_0,t_0) = -\Psi[S(t),t|x_0,t_0]. \tag{2.53}$$

Anyway this case turns to be not interesting in applications. In the next chapter we will show some examples in which formula (2.49) can be useful for applications.
Another special case in which a closed-form expression of FPT pdf is available is that of the Daniels boundary. We just recall the main result from [23]. Let

$$\begin{aligned} y(t) &= m(t) + d_1h_1(t) + d_2h_2(t) \\ u(t) &= m(t) + d_1^*h_1(t) + d_2^*h_2(t) \\ v(t) &= 2u(t) - y(t) \end{aligned} \tag{2.54}$$

be curves such that $y(t) < u(t) < v(t)$ for all $t \geq t_0$, $t, t_0 \in T$ and t_0 fixed with $d_1, d_2, d_1^*, d_2^* \in \mathbb{R}$.

Theorem 2.2.2 ([23]). *Let*

$$S(t) = u(t) - \frac{h_1(t)h_2(t_0) - h_1(t_0)h_2(t)}{2[u(t_0) - y(t_0)]} \ln\left[\frac{c_1 + \sqrt{\Delta(t;t_0)}}{2}\right]$$

with

$$\Delta(t;t_0) = c_1^2 + 4c_2 \exp\left\{-\frac{4[u(t) - y(t)][u(t_0) - y(t_0)]}{h_1(t)h_2(t_0) - h_1(t_0)h_2(t)}\right\}$$

and

$$c_1 > 0, c_2 \in \mathbb{R}, \lim_{t \to \sup T} \Delta(t;t_0) > 0.$$

Then

$$\begin{aligned} g[S(t),t|y(t_0),t_0] &= \frac{u(t_0) - y(t_0)}{r(t) - r(t_0)} \frac{h_2(t)}{h_2(t_0)} \frac{dr(t)}{dt} \frac{2\sqrt{\Delta(t;t_0)}}{c_1 + \sqrt{\Delta(t;t_0)}} \\ &\times f[S(t),t|y(t_0),t_0] \quad (y(t_0) < u(t_0)). \end{aligned}$$

2.2.2 One boundary: analytical approach

An alternative approach, called analytical in [62], consists in the determination of the Laplace Transform (LT) of the FPT pdf and the calculation of the FPT moments.
Let us limit to the case of time-homogeneous diffusion processes and constant boundary, i.e. $S(t) \equiv S$. In this case equation (2.38) becomes

$$f(x,t|y,0) = \int_0^t g(S,\theta|y,0) f(x,t-\theta|S) d\theta \quad \text{for } x \leq S, y > S. \tag{2.55}$$

An analytical method to solve equation (2.55) is based on the LT. Let $\lambda \in \mathbb{R}$ and let

$$g_\lambda(S|y) = \int_0^\infty e^{-\lambda t} g(S,t|y) dt \qquad f_\lambda(S|y) = \int_0^\infty e^{-\lambda t} f(x,t|z) dt \tag{2.56}$$

be the LT of the functions g and f, respectively. Observing that equation (2.55) is a convolution and recalling that the LT of a convolution of two functions is equal to the product of the LT of the two functions, from (2.55) we have

$$g_\lambda(S|y) = \frac{f_\lambda(x|y)}{f_\lambda(x|S)}. \tag{2.57}$$

It means that if we know the transition pdf of $X(t)$ and we can calculate its LT, then the LT of g follows and g can be obtained as the inverse LT if it is

possible.
For example in [65] the inverse LT of g_λ is calculated in the case of an OU process $X(t)$ with drift $-x/\theta$ and infinitesimal variance μ, for $S = 0$ giving the well-known closed-form solution

$$g(t, 0|x_0) = \frac{2|x_0|}{\sqrt{2\pi}}[e^{2t} - 1]^{-\frac{3}{2}} e^{2t} \exp\left\{-\frac{x_0^2}{2(e^{2t} - 1)}\right\}. \tag{2.58}$$

Even though the inverse LT of g_λ cannot be calculated, it can anyway provide useful information on the FPT. In particular the probability of the first passage time

$$\mathbb{P}(S|y) = \int_0^\infty g(S, t|y)dt \tag{2.59}$$

and the moments

$$t_n(S|y) = \int_0^\infty t^n g(S, t|y)dt \quad (n = 1, 2, \ldots) \tag{2.60}$$

can be evaluated from g_λ, that coincides with the characteristic function of the random variable FPT, as follows:

$$\mathbb{P}(S|y) = g_\lambda(S|y)\Big|_{\lambda=0}, \quad t_n(S|y) = (-1)^n \frac{d^n g_\lambda(S|y)}{d\lambda^n}\bigg|_{\lambda=0} \quad (n = 1, 2, \ldots). \tag{2.61}$$

Starting from equation (2.61), in [65] the authors present the analytical expression of the generic n-th moment, although it is only a formal expression, since it is rather complicated and hard to handle.

The Ricciardi-Sato FPT moments

The case of time-dependent boundaries for Gaussian processes is treated extensively in [63] and [64]. The authors presented the approximate evaluation of the FPT pdf through time varying smooth boundaries for a stationary one-dimensional Gaussian process (see Definition 2.1.1) with differentiable sample paths, in terms of a series expansion.

For all n and $t_1 < t_2 < \ldots < t_n$ let $W_n(t_1, \ldots, t_n|x_0)dt_1 \ldots dt_n$ denote the joint probability that a Gaussian process $X(t)$ crosses $S(t)$ from below in the intervals $(t_1, t_1 + dt_1), \ldots, (t_n, t_n + dt_n)$ given that $X(0) = x_0$. With this notation $g(t, S(t)|x_0)$ can be expressed as the following convergent series ([63]):

$$\begin{aligned} g(t, S(t)|x_0) &= W_1(t|x_0) \\ &+ \sum_{i=1}^{\infty}(-1)^i \int_0^t dt_1 \int_{t_1}^t dt_2 \ldots \int_{t_{i-1}}^t dt_i W_{i+1}(t_1, \ldots, t_i, t|x_0). \end{aligned}$$

Successive even-order partial sums of the above expansion provide progressively improving lower bounds to $g(t, S(t)|x_0)$, while successive odd-order partial sums provide improving upper bounds.

The functions W_n can be explicitly written:

$$\begin{aligned} W_n(t_1, t_2, \cdots, t_n|x_0) &= \int_{\dot{S}(t_1)}^{\infty} d\xi_1 \int_{\dot{S}(t_2)}^{\infty} d\xi_2 \cdots \int_{\dot{S}(t_n)}^{\infty} d\xi_n \prod_{i=1}^{n} \left[\xi_i - \dot{S}(t_i)\right] \\ &\times \; p_{2n}[S(t_1), S(t_2), \ldots, S(t_n); \xi_1, \ldots, \xi_n|x_0], \end{aligned} \quad (2.62)$$

where $\dot{S}(t_i)$ indicates the time derivative of $S(t_i)$ and
$p_{2n}[S(t_1), S(t_2), \ldots, S(t_n); \xi_1, \ldots, \xi_n|x_0]$ is the joint pdf of $X(t_1) = x_1$, ..., $X(t_n) = x_n$, $\xi_1 = \dot{X}_1(t_1)$, ..., $\xi_n = \dot{X}_1(t_n)$ conditional upon $X(0) = x_0$.

The terms of the series expansion cannot be analitically calculated since they do not admit a simplified form and so the multiple integrals should be estimated numerically. Only the first-order term admits a closed form, although very cumbersome, that in [39] is presented in the form

$$\begin{aligned} W_1(t|x_0) = \frac{\Lambda_3(t)^{1/2}}{2\pi[1-\rho^2(t)]} \exp\left\{-\frac{[S(t) - x_0\rho(t)]^2}{2[1-\rho^2(t)]}\right\} \\ \times \left[\exp\left\{-\frac{\sigma^2(t|x_0)}{2}\right\} - \sqrt{\frac{\pi}{2}}\sigma(t|x_0) Erfc\left(\frac{\sigma(t|x_0)}{\sqrt{2}}\right)\right] \end{aligned} \quad (2.63)$$

where

$$|\Lambda_3(t)| = -\ddot{\rho}(0)[1-\rho^2(t)] - [\dot{\rho}(t)]^2,$$

$$\sigma(t|x_0) = \left(\frac{1-\rho^2(t)}{|\Lambda_3(t)|}\right)^{1/2} \left\{\dot{S}(t) + \frac{\dot{\rho}(t)[\rho(t)S(t) - x_0]}{1-\rho^2(t)}\right\}$$

$$Erfc(z) = \frac{2}{\sqrt{\pi}} \int_z^{+\infty} e^{-y^2} dy, \quad z \in \mathbb{R}$$

and $\rho(t)$ is the correlation function of the process $X(t)$,

$$\rho(t) = \frac{c(s,t)}{\sqrt{D_X^2(s) D_X^2(t)}}$$

such that $\rho(0) = 1$, $\dot{\rho}(0) = 0$ and $\ddot{\rho}(0) < 0$. $D_X^2(t)$ indicates the variance of the process $X(t)$ and $c(s,t)$ its covariance.
W_1 is an upper bound to $g(t, S(t)|x_0)$ and constitutes a good approximation for the FPT pdf only for small values of t. Higher order terms should be numerically estimated even if multiple integrals lead to a fast loss of accuracy. Studies on the second-order term and on the asymptotic behaviour of higher order terms are presented in [39], [63] and [64].

A much more concise expression of the FPT pdf for a class of GM and diffusion processes can be obtained studying the asymptotic behavior of the variable FPT both for asymptotically constant and asymptotically periodic thresholds.

2.2.3 One boundary: asymptotic approximations

In the asymptotic regime it is possible to provide an exponential approximation for the FPT pdf that is very useful from an application point of view.

Let us consider a GM process $X(t)$ for which the limit

$$\mathcal{W}(x) := \lim_{t\to+\infty} f(x,t|x_0,t_0) \tag{2.64}$$

exists. We say that $X(t)$ admits the *steady-state pdf* $\mathcal{W}(x)$. For example, the OU process belongs to this class of processes, while the Wiener process does not.

In [53] the asymptotic behaviour of the FPT pdf through a constant boundary for an OU process is investigated, while in [38] asymptotic results for the FPT pdf through special time-varying boundaries are obtained for the whole class of one-dimensional diffusion processes with steady-state pdf. In [56] GM processes with steady-state pdf are considered. In particular for the GM processes the authors use the results on OU processes, in fact from equations (2.15) and (2.33) the following proposition holds.

Proposition 2.2.3 ([56]). *Let $U(t)$ be a non-stationary OU process, i.e. a OU process with zero-mean and covariance*

$$\mathbb{E}[U(s)U(t)] = \sigma^2(e^{\beta s} - e^{-\beta s})e^{-\beta t}/(2\beta)$$

with $\beta > 0$, $\sigma > 0$, $s,t \in T$ and $s < t$. Then any GM process $X(t)$ can be represented in terms of $U(t)$ as follows:

$$X(t) = m(t) + k(t)U[\varphi(t)], \quad t \in T \tag{2.65}$$

where $m(t)$ is the mean function of $X(t)$ and

$$k(t) = h_2(t)\sqrt{1 + \frac{2\beta}{\sigma^2}r(t)}, \quad \varphi(t) = \frac{1}{2\beta}\ln\left(1 + \frac{2\beta}{\sigma^2}r(t)\right). \tag{2.66}$$

with $r(t)$ as in (2.9).

The previous result allows the extension of the results concerning the OU process to the entire class of GM processes that admit steady-state pdf.

In the following we recall the main results on the asymptotic behaviour of the FPT pdf through asymptotically constant and asymptotically periodic thresholds in the form presented in [13], in which the results of [38] for the diffusion processes, and those of [56] specialized for the GM processes are properly specified.

Whenever the transformed threshold $S(t)$ approaches a constant function as the time t diverges, i.e. has an horizontal asymptote, the following approximation holds.

Theorem 2.2.4. *Let $X(t)$ be a GM (or diffusion) process with steady-state pdf and let $S(t)$ be an asymptotically constant threshold:*

$$\lim_{t\to+\infty} S(t) = S.$$

Setting

$$h_X := -\vartheta \lim_{t\to+\infty} \Psi(S(t), t|y, \tau) \tag{2.67}$$

for t and S "big enough" one has

$$g(S(t), t|x_0, t_0) \simeq \frac{h_X}{\vartheta} e^{-\frac{h_X t}{\vartheta}}. \tag{2.68}$$

The parameter $\vartheta = -1/a(t) \equiv -1/a$ of SDE (2.18), the function $\Psi(S(t), t|y, \tau)$ is defined in (2.46), instead the exact meaning of "big enough" will be clarified in the next chapters when an extensive use of these theorems will lead to estimations of the density functions under consideration.

Definition (2.67) and Equation (2.46) make clear why we consider processes with steady-state pdf. In fact we need to take the limit of the function $\Psi(x, t|y, \tau)$ and, as consequence, of the transition pdf $f(x, t|x_0, t_0)$.

For certain periodic boundaries, not very far from the initial value of the process, the FPT pdf of one-dimensional diffusion processes with steady-state density soon exhibits damped oscillations having the same period of the boundary ([38]). If the threshold is asymptotically periodic, we have that $g(S(t), t|x_0, t_0)$ has an asymptotic non-homogeneous exponential form.

Theorem 2.2.5. *Let $X(t)$ be a GM (or diffusion) process with steady-state pdf and let $S(t)$ be an asymptotically P-periodic threshold:*

$$\lim_{n\to+\infty} S(nP + t) = s(t)$$

with

$$s(nP + t) = s(t), \qquad n = 0, 1, \ldots$$

Then, setting

$$h_X(t) := -\vartheta \lim_{n \to +\infty} \Psi[S(t + nP), t + nP | y, \tau] \tag{2.69}$$

for t and S "big enough" one has

$$g(S(t), t|x_0, t_0) \simeq \frac{h_X(t)}{\vartheta} e^{-\int_0^t h_X(\tau) d\tau / \vartheta} \tag{2.70}$$

where $\vartheta = -1/a$.

As we have seen the solutions in closed-form are known only for suitable families of thresholds; in all other cases it is possible to solve equation (2.39) by means of some numerical quadrature procedures obtaining numerical approximations of $g(S(t), t|x_0, t_0)$ with high degree of precision. This procedure is a fast and accurate computational method, mainly centered on the repeated Simpson rule in the case of GM processes and on the Trapezoidal rule in the case of diffusion processes. The noteworth feature of this algorithm is its being implementable after simply specifying the functions $m(t)$, $h_1(t)$, $h_2(t)$ that characterize the process, the threshold $S(t)$ and the discretization step p. Furthermore, it does not involve any heavy computation, neither it requires use of any library subroutines, Monte Carlo methods or other special software packages to calculate high dimension multiple integral (for further details see [23]).

Chapter 3

Neuronal Models: renewal and non-renewal processes

3.1 An overview on neuronal models

The phenomenology of the electrical activity of single neurons and the understanding of the ultimate mechanisms responsible for it have been the object of numerous investigations by neurophysiologists, physicists and mathematicians during the last decades.

Neurons are cells of the nervous system that transmit information through electrical and chemical signals. These signals are generated across the membrane of the neuron and transmitted through synapses.
Neurons can be of different types depending on their position and task, but all have the same main structure: the dendrites that receive the signal from other neurons, the soma that is the processing center of the signals, the axon and the synapses. The signal is generated across the membrane and transmitted along the axon till the axon terminals. Then through the synapses the signal attains the post-synaptic neuron. In absence of input there is a non-zero electrical potential across the membrane due to different concentration of ions inside and outside the membrane. This voltage, called resting potential, is maintained constant by means of metabolically driven ion pumps. When the neuron receives an impulse the sodium channels open and sodium ions enter in the neuron cell generating a positive charge that rejects potassium ions. The potential is inverted and the depolarization or action potential occurs. Then the sodium-potassium pomp returns the potential to the resting value.

In a modeling context the neuron is viewed as a point-size particle, whose membrane voltage fluctuates in response to synaptic inputs and internal

noise. The neuron accumulates inputs and as soon as the threshold voltage is exceeded, the neuron generates an action potential ([18],[79]). Therefore, the generation of an action potential by a neuron involves the first passage of the fluctuating membrane voltage through a threshold (see Fig. 3.1 for a schematic representation of the evolution of the membrane potential). More

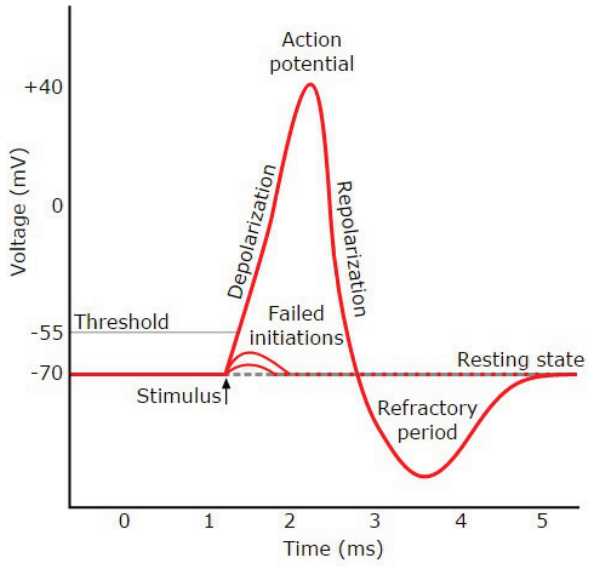

Figure 3.1: The schematic generation of an action potential. Image released by Free Software Foundation.

in detail the membrane potential oscillates across its resting state until stimula arrive. If the inputs are strong enough, the firing threshold is attained and a spike occurs depolarizing the membrane. After that the potential quickly decreases and just after the spike the neuron cannot accumulate inputs for a certain amount of time, called refractory period. Then the dynamics starts anew.
This dynamics of spikes generation underlies neural coding: neurons communicate information through their electrical spiking and the functional relation between the information being encoded and the spikes is called a "neural code".

The first model was proposed by Lapicque in 1907; in this model the membrane potential is studied in terms of an electric circuit consisting of a resistor and a capacitor in parallel. The capacitor is charged (integrate) until it reaches a threshold at which the neuron spikes (fire) and after that immediately the potential is reset to the initial state. For this reason the model is

called integrate-and-fire. Despite the simplicity of the model, Lapicque was able to estimate the spiking-rate of a neuron subject to a constant stimulating input.
Several years later (1952) Hodgkin and Huxley explained the ionic mechanisms underlying the initiation and propagation of action potentials in the squid giant axon. The reason why they studied these kind of animals is the length of their axons that facilitates experiments. They described the behavior of the membrane potential in terms of the evolution of the ion channels located in neurons membrane. Unfortunately this deterministic model is characterized by a large number of equations and parameters. Most of the times the model cannot be analyzed analytically but only with computer simulations.

The above deterministic models cannot describe some features exhibit by neurons in vivo. In the famous paper of Gerstein and Mandelbrot [35] the integrate-and-fire model for the first time incorporate the randomness of the synaptic inputs arrival. This marks the beginning of the history of neuronal models based on diffusion processes. The model is based on the assumption that the random incoming potentials are viewed in the model as random walks, and so the stochastic Wiener process is involved. The authors were also able to show that experimentally recorded interspike intervals, i.e. the time elapsed between two consecutive spikes, could be fitted well using the FPT pdf of a Wiener process. In the case of constant threshold S the FPT pdf $g(S,t|y)$ of the Wiener process with drift μ and infinitesimal variance σ^2 can be analytically written

$$g(S,t|y) = \frac{|S-y|}{\sigma\sqrt{2\pi t^3}} \exp\left[-\frac{(S-y-\mu t)^2}{2\sigma^2 t}\right], \quad S \neq y \tag{3.1}$$

that is an Inverse Gaussian type pdf, obtained for the first time by Bachelier in 1900 ([4]). Also the FPT moments can be evaluated in this case (see [62]), and in particular mean and variance of the neuronal firing are

$$t_1(S|y) = \frac{S-y}{\mu}, \qquad Var(S|y) = \frac{\sigma^2(S-y)}{\mu^3}$$

for $\mu > 0$, $S \neq y$.
Despite the good agreement with experimental data, this model does not include the observed spontaneous decay of the neuron's membrane potential.

The Stein's model [73] goes in this direction introducing a resistor (the leakage) in the electrical circuit representing the electrical evolution of the membrane. The diffusion process used by Stein is a stochastic counterpart

of the phenomenological leaky-integrate-and-fire (LIF) deterministic model. The stochastic LIF is based on an SDE of the form

$$dX(t) = \left(-\frac{X(t)}{\vartheta} + \mu \right) dt + \sigma dW(t), \quad X(t_0) = x_0 \tag{3.2}$$

whose solution is an OU process. In absence of inputs to the neuron, in any interval (t_0, t) the membrane potential $X(t)$ spontaneously decays with exponential law to the resting potential

$$x(t) = x_0 \exp\left\{ -\frac{t - t_0}{\vartheta} \right\}$$

where ϑ is the decay time of the neuron's membrane towards the resting potential. Moreover he modelled the inputs by mean of Poisson processes, distinguishing from excitatory and inhibitory inputs.

Although the OU process depicts more realistically the neurophisiological reality, it is not possible to obtain closed form expressions for the firing pdf in abitrary conditions.

An extensive discussion and a rigorous analysis on the use of diffusion processes and their FPTs in the stochastic LIF model can be found in [20] and [61]. In particular Capocelli and Ricciardi proposed a model in which the effect of the noise decreases when the membrane potential is close to the firing threshold, problem with application in particular biological situations. The above OU process based models exhibit a non realistic feature: the state space in which the stochastic process evolves is the entire real axis. This means that arbitrarily large hyperpolarization values for the membrane potential are possibile, and of course this is not physically reasonable. For this reason Tuckwell [79] assumed the existence of a "reversal potential". He suggested that the state of the depolarization of a nerve cell is state dependent implying that the oscillations of the membrane potential are restricted to a certain region ([16]).

The LIF model is used both in artificial neural networks and description of biological systems, but a wide range of approaches to the modeling of single neurons have been proposed in literature. For instance in [48] the temporal patters of action potentials is investigated by a compartimental model. The model takes into account the distinction between dendritic and axonal potentials, preserving the tractability of the one point model.
Papers devoted to the comparison with experimental data are instead pretty rare for the complexity of the mathematical problems and the lack of analytical results. For this reason the verification of any model has to start with an estimation of its parameters (see [43], [46] and [47]). In [47] is derived a

method for the parameters estimation in the OU model, distinguishing between intrinsic parameters and input parameters. The former parameters are characteristics of the neuron and can be measured directly, the latter have to be estimated from experimental data [45].

Even if some concerns about the LIF model have arisen, it appears a good compromise between the tractability and realism of the model and it is by far the most used. The stochastic LIF model is based on a SDE of the following type ([18]):

$$dV(t) = [-\alpha(V(t) - V_{rest}) + I(t)]\, dt + \sigma dW(t), \quad V(t_0) = v_0 < S. \tag{3.3}$$

In (3.3) $V(t)$ is the stochastic process representing the membrane potential, the parameter $1/\alpha(> 0)$ is the characteristic decay time of the membrane potential, V_{rest} is the resting potential, v_0 is the initial value, $\sigma(> 0)$ represents a constant intensity of the noise and $W(t)$ the Wiener process. Furthermore, $I(t)$ stands for a time-dependent input signal that could play the role of an injected input current or a synaptic current originated from the surrounding neuronal activity. After each spike the membrane depolarization and the input signal $I(t)$ are immediately reset to the initial value and the dynamics starts anew.

This resetting mechanism ensures that the interspike intervals (ISIs) are independent and identically distributed (i.i.d.) random variables: they form a renewal process. The ISI is a random variable defined as the random time elapsed between the reset and the first spike after it. The importance of the ISIs follows as a consequence of the generally accepted hypothesis that the information transferred within the nervous system is encoded by the timing of the action potentials [47], [61] and [62]. In the case of the renewal process, since the ISI are i.i.d, one can consider the first interval that coincides with the random variable FPT. Moreover one can analyze the ISIs separately and build the complete spike train generated by the neuron by concatenation of intervals.

For this reason the determination of the FPT pdf is of key importance in this context. In the next subsection we review some special cases in which the closed form solution for the FPT pdf of Gauss-Diffusion processes describing the neuron's membrane potential evolution exists.

3.1.1 Closed form solutions

Let us apply the results of Section 2.2.1 in some special cases in the context of neuronal models [7].

[(i)] Let $I_{\rm syn}, I_{\rm inj}, v_0, S \in \mathbb{R}$ and $\sigma_{\rm syn} \in \mathbb{R}^+$; the IF model is based on the following stochastic differential equation

$$dV(t) = Idt + \sigma_{\rm syn} dW(t) \quad (t > t_0), \text{ and } V(t_0) = v_0 < S, \tag{3.4}$$

with $I := I_{\rm syn} + I_{\rm inj}$ where $I_{\rm syn}$ is a deterministic constant current describing the effect of synaptic inputs to the neuron, $I_{\rm inj}$ is a constant current eventually injected into the neuron for instance by an intracellular electrode and $\sigma_{\rm syn} > 0$ is the intensity of synaptic noise. The solution of equation (3.4) is the Wiener process $\{W(t), t \geq t_0\}$ with

$$b_W := I \quad \text{and} \quad \sigma_W^2 := \sigma_{\rm syn}^2.$$

Hence, for all constant firing thresholds S the condition (2.48) holds with $b_1 = -I/\sigma_{\rm syn}$ and by means of Eqs. (2.11), (2.24) and (2.49) one has:

$$g[S, t|v_0, t_0] = \frac{S - v_0}{t - t_0} \frac{1}{\sqrt{2\pi D_W^2(t|t_0)}} e^{-\frac{[S - E_W(t|v_0, t_0)]^2}{2D_W^2(t|t_0)}} \quad (t \geq t_0). \tag{3.5}$$

Remark 1. Due to the simple reset mechanism the sequence of interspike intervals is composed of independent and identically distributed random variables; therefore the FPT pdf directly provides the ISI pdf. ◁

The pdf in Eq. (3.5) is of inverse Gaussian type as seen in [35]. The mean of the interspike interval is then $(S - v_0)/(I_{\rm syn} + I_{\rm inj})$ and the variance is $\sigma_{\rm syn}^2(S - v_0)/(I_{\rm syn} + I_{\rm inj})^3$, giving a coefficient of variation equal to

$$\sigma_{\rm syn}/\sqrt{(S - v_0)(I_{\rm syn} + I_{\rm inj})}.$$

Admitting, as proposed by various authors, the eventuality of a time dependent firing threshold $S \equiv S(t)$ then, by means of Eq. (2.48), the function for which exists a closed-form solution is of linear type:

$$S(t) = S(t_0) + (b_W + b_1\sigma)(t - t_0) \quad (t \geq t_0). \tag{3.6}$$

Remark 2. In the reset mechanism, to have a renewal process, since S(t) is time-varying, it is necessary to add the repositioning of the firing threshold value $S(t_0)$. In this way the FPT pdf still directly provides the ISI pdf. ◁

[(ii)] Let $I_{\rm syn}, I_{\rm inj}, v_0, V_{\rm rest}, S \in \mathbb{R}$ and $\theta, \sigma_{\rm syn} \in \mathbb{R}^+$; the LIF model is based on the following stochastic differential equation

$$\begin{aligned} &dV(t) = \left[-\frac{V(t) - V_{\rm rest}}{\theta} + I_{\rm syn} + I_{\rm inj}\right] dt + \sigma_{\rm syn} dW(t) \quad (t > t_0), \text{ and} \\ &V(t_0) = v_0 < S, \end{aligned} \tag{3.7}$$

where $V_{\rm rest}$ is the resting potential and θ is the decay time of the membrane potential; the meaning of the other parameters as in item (i). Eq. (3.7) is that of the time-homogeneous OU process $\{U(t), t \geq t_0\}$ with

$$a_U := \frac{1}{\theta}, \quad b_U := I_{\rm syn} + I_{\rm inj} + \frac{V_{\rm rest}}{\theta} \quad \text{and} \quad \sigma_U^2 := \sigma_{\rm syn}^2.$$

The condition (2.48) only holds with $b_1 = 0$ for $\bar{S} := a_U/b_U$ and by means of Eqs. (2.11), (2.28) and (2.49) one has:

$$g[\bar{S}, t|v_0, t_0] = \sigma \frac{\bar{S} - v_0}{h_{1_U}(t)} \frac{1}{\sqrt{2\pi D_U^2(t|t_0)}} e^{-\dfrac{[\bar{S} - E_U(t|v_0,t_0)]^2}{2D_U^2(t|t_0)}} \ (t \geq t_0). \tag{3.8}$$

We stress that Remark 1 holds.

Note that $\bar{S}$ coincides with the asymptotic mean of the membrane potential: in such a case the neuron may fire even in the absence of synaptic noise (*suprathreshold regime*).

When the membrane potential, instead, evolves in the *subthreshold regime*, i.e.

$$\frac{S - a_U/b_U}{\sqrt{\sigma_{\rm syn}^2/(2a_U)}} \gg 1, \tag{3.9}$$

it is possible to obtain the following asymptotic expression (see Section 2.2.3 and the cited results of [38]):

$$g(S, t|v_0, t_0) \sim a_U h_U e^{-a_U h_U (t - t_0)} \quad \left(t \gg t_0 + \frac{1}{a_U}\right). \tag{3.10}$$

In Eq. (3.10), a_U has dimension $[\text{time}]^{-1}$, whereas h_U is the dimensionless quantity

$$h_U := -\frac{1}{a_U} \lim_{t \to +\infty} \Psi_U[S, t|v_0, t_0] = \frac{S - a_U/b_U}{\sqrt{\pi \sigma_U^2/a_U}} \, e^{-\dfrac{(S - a_U/b_U)^2}{\sigma_U^2/a_U}},$$

and $(h_U a_U)^{-1}$ can be interpreted as an estimate of the firing mean time. To obtain the ISI pdf in the transient phase it is possible to use a numerical quadrature, with a time step much smaller than $1/a_U$, operating on the nonsingular integral equation (2.39); in the following we refer to it simply as the *numerical scheme*.

In the case of $S \equiv S(t)$, from Eq. (2.48) the function for which there exists the closed form solution is of hyperbolic type

$$\begin{aligned} S(t) = S(t_0)e^{-a_U(t-t_0)} + \frac{b_U}{a_U} - \left(\frac{b_U}{a_U} - b_1 \frac{\sigma_U}{2a_U} \right) e^{-a_U(t-t_0)} \\ + b_1 \frac{\sigma_U}{2a_U} e^{a_U(t-t_0)} \quad (t \geq t_0), \end{aligned} \tag{3.11}$$

and

$$\begin{aligned} g[S(t), t|v_0, t_0] = \sigma \frac{S(t_0) - v_0}{h_{1_U}(t)} \frac{1}{\sqrt{2\pi D_U^2(t|t_0)}} \times \\ \times e^{-\frac{[S(t) - E_U(t|v_0, t_0)]^2}{2D_U^2(t|t_0)}} \quad (t \geq t_0). \end{aligned} \tag{3.12}$$

We stress that here Remark 2 holds. If $b_1 = 0$ and $V_{\rm th}(t_0) > \mu/\alpha$ the neuron is in the suprathreshold regime, then the firing threshold

$$S(t) = \frac{b_U}{a_U} + \left[S(t_0) - \frac{b_U}{a_U} \right] e^{-a_U(t-t_0)} \quad (t \geq t_0), \tag{3.13}$$

exponentially decreases to the asymptotic mean of potential membrane (b_U/a_U) and it returns to the case of constant threshold equal to $\bar{S}$ for large time.

[(iii)] Within the framework of item (ii), the LIF model with time dependent synaptic current is based on the following SDE

$$\begin{aligned} &dV(t) = \left[-\frac{V(t) - V_{\rm rest}}{\theta} + I_{\rm syn}(t) + I_{\rm inj} \right] dt + \sigma_{\rm syn} dW(t) \quad (t > t_0), \text{ and} \\ &V(t_0) = v_0 < S. \end{aligned} \tag{3.14}$$

Equation (3.14) is that of the time-inhomogeneous Ornstein-Uhlenbeck process $\{V(t), t \geq t_0\}$ with

$$a_V := \frac{1}{\theta}, \quad b_V(t) := I_{\rm syn}(t) + I_{\rm inj} + \frac{V_{\rm rest}}{\theta} \quad \text{and} \quad \sigma_V^2 := \sigma_{\rm syn}^2.$$

If $m_V(t)$ satisfies the condition (2.47), it is possible to write the form of the function $b_V(t)$ that ensures a closed form solution for the FPT pdf. Using (2.13) and (2.47) we have

$$b_V(t) = S'(t) + a_V S(t) - b_1 \sigma_V e^{a_V(t-t_0)} \tag{3.15}$$

and so in this case:

$$b_V(t) = a_V S - b_1 \sigma_V e^{a_V(t-t_0)} \quad (t \geq t_0). \tag{3.16}$$

From equation (3.16) the following constraints for the deterministic currents follow:

$$I_{\text{inj}} = \alpha(S - V_{\text{rest}}) \quad \text{and} \quad I_{\text{syn}}(t) = -b_1 \sigma e^{a_V(t-t_0)} \quad (t \geq t_0). \tag{3.17}$$

Then, by means of Eqs. (2.11), (2.32) and (2.49) one has:

$$\begin{aligned} g[S,t|v_0,t_0] = \sigma_V \frac{S-v_0}{h_{1_V}(t)} \frac{1}{\sqrt{2\pi D_V^2(t|t_0)}} \times \\ \times e^{-\frac{[S-E_V(t|v_0,t_0)]^2}{2D_V^2(t|t_0)}} \quad (t \geq t_0). \end{aligned} \tag{3.18}$$

3.1.2 Time-dependent input signals

Despite the availability of some mathematical interesting models based on various assumptions on the type of input to which the neuron is subject and on possible generation mechanisms of the corresponding output, a universal model to which refer in general instances is still lacking. In addition, the existing mathematical tools appear to be hardly effective due to the high degree of nonlinearity exhibited by the neuron in the spike-reset behavior. Hence, to focus on the description of neuronal behaviors the choice of the input classes and parameters depends on which aspects one wants to highlight.

We note that in item (iii) of the previous subsection it is possible to change the role of I_{syn} with that of I_{inj}; in general ve have $I := I_{\text{syn}} + I_{\text{inj}}$. LIF models with time-varying input signals are described by inhomogeneous OU processes [19].

With regard to the time dependent input $I(t)$ the case of a periodic type deterministic current is particularly interesting and widely considered in the specialist literature ([12], [16] and [45]). It describes the event of external periodic stimulation of sensory neurons which are in direct contact with the external world and also central neurons for which the stimulation is reflected by synchronized postsynaptic activations.

In [12], for $I, \omega \in \mathbb{R}^+$ and $\phi \in (0, 2\pi)$, is considered the prototype periodic function:

$$I(t) := I \cos(\omega t + \phi) \tag{3.19}$$

and the problem is studied using the Fokker-Planck formulation. In particular the problem with a periodic input and constant threshold is mapped

in a problem with constant input and periodic threshold, showing a spike syncronization to the phase of the driving force. Moreover an asymptotic approximation for the FPT pdf has been obtained. In the case of neurons operating in the subthreshold regime, i.e. using the notation of equations (3.3) and (3.19)

$$\frac{S-(V_{\text{rest}}+I/\alpha)}{\sqrt{\sigma^2/(2\alpha)}} \gg 1, \tag{3.20}$$

they found:

$$g(S,t|v_0,t_0) \sim \alpha h_V(t) e^{-\alpha \int_{t_0}^{t} h_V(s)\,ds} \quad \left(t \gg t_0 + \frac{1}{\alpha}\right). \tag{3.21}$$

It is a result of the Theorem 2.2.5 where $V(t)$ is the time-inhomogeneous OU process solution of (3.3) and $h_V(t)$ is the dimensionless periodic function

$$h_V(t) := -\frac{1}{\alpha} \lim_{n\to+\infty} \Psi_V[S, t+nQ|v_0,t_0],$$

where $Q = 2\pi/\omega$.

The asymptotic expression (3.21) exhibits two important features: it holds for any values of the frequency ω and it is not affected from any additional phase shift with respect to the current $I(t)$.

Further improvements of the stochastic LIF model have been introduced in order to better fit the phenomenological evidences. In [14] the LIF model with time-dependent decay time of the membrane and time-dependet resting potential is considered. It is based on the following SDE:

$$\begin{aligned} &dV(t) = \left[-\frac{V(t)-V_{\text{rest}}(t)}{\theta(t)} + I(t)\right] dt + \sigma dW(t) \quad (t > t_0), \text{ and} \\ &V(t_0) = v_0 < S. \end{aligned} \tag{3.22}$$

Thanks to this generalization the behavior of the driving force is enriched and this permits to consider a wider range of cases. On the other side, of course, the number of parameters increases.

In [16] the authors consider an Ornstein-Uhlenbeck process describing a dynamics occurring in a restricted state-space, while in [15] the presence of a lower reflecting boundary affects the evolution of generic Gauss-Markov processes in order to include a reversal hyper-polarization potential.

The model (3.3) can be modified with the aim to take in account also the phenomenon of the spike-frequency adaptation that some pyramidal cells in

vivo exhibit (see [43]). Roughly speaking neurons show a reduction in the firing frequency of their spike response following an initial activity. In [43] the problem is addressed incorporating an adaptive threshold in the LIF model. In [17] the authors consider separately the role of the potassium ion channels and expresses the relative conductance dependent on the calcium concentration, $[Ca^{2+}](t)$. Such a concentration decays exponentially with its characteristic time τ_{Ca} and each spike generates a calcium influx α.

In these models the adaptation causes the correlation between successive ISIs; in the next section we will show what this correlation implies.

3.1.3 Non-renewal processes

In [71] the authors presented evidences that the model based on the OU process does not fit firing statistics in the case of prefrontal cortex neurons. In fact neurons in vitro under a constant current injection generate regular spike sequences, while cortical neuron in vivo generates irregular spike sequences. A standard LIF model can reproduce the spiking irregularity only if the inhibition is balanced with the excitation. Since the input signals can operate on a single neuron in a complicated non-linear fashion, in [72] is stated that the LIF model can reproduce biological spiking statistics if appropriately choosing the statistical nature of the incoming inputs. The main statistical coefficient that has to be introduced is the correlation, implying that the hypothesis of independence between ISIs is not reasonable.

In addition to adaptation, also other cell-intrinsic properties like neural refractoriness, bursting and short-term plasticity of the synapses cause temporally correlated spike trains [68]. In this case the identification between FPT and ISIs is no more valid and no standard method exists to solve the associated first-passage-time problem.

For instance in case (iii) it is not possible to include $I_{syn}(t)$ in the reset mechanism, being this current exclusively dependent on synaptic activity. Hence, in order to obtain $f_{ISI}(t)$ we need $f_{syn}(i)$, namely the pdf of the value i of the synaptic current at the beginning of the generic ISI; therefore from [7]:

$$\begin{aligned} f_{ISI}(t) :&= \mathbb{E}_{f_{syn}}\left\{g_V[V_{th}, t|v_0, t_0; i]\right\} \\ &= \int_{\mathbb{R}} g_V[V_{th}, t|v_0, t_0; i] f_{syn}(i)\, di \quad (t \geq t_0). \end{aligned} \tag{3.23}$$

Unfortunately the determination of $f_{syn}(i)$ is a really difficult task and in general it depends on the type of function $I_{syn}(t)$.

Instead in the case of the periodic input function (3.19), in [7] the ISI pdf is obtained by averaging the FPT pdf with respect to its normalized hazard

rate function:

$$f_{\mathrm{ISI}}(t) = \frac{\displaystyle\int_{t_0}^{t_0+Q} g_V(V_{\mathrm{th}}, t|v_0, s)h_V(s)\,ds}{\displaystyle\int_{t_0}^{t_0+Q} h_V(s)\,ds}.$$

where $h_V(s)$ is defined in Subsection (3.1.2).

In general time-dependent stimulation complicates the FPT problem, as a different stimulus is presented during each ISI [59]. In [45] Lánský uses the terms *endogenous* stimulation when the input is reset after the spike, and *exogenous* stimulation when the input keeps evolving even if the process has been reset. The complete loss of memory in the reset mechanism has been criticized and appear unbiological, since it would mean that the neuron control completely the input it receives. For this reason it is important to consider non-renewal processes describing the membrane potential activity ([26], [75] and [68]).

3.2 The Recurring Passage Time Problem

The firing activity of stimulated neurons is affected by temporal structure of the injected current. If the input injected is made of random current pulses of varying amplitudes applied to the constant current input we talk about "frozen noise". When a cortical neuron is repeatedly injected with the same frozen noise, the timing of the spikes is highly precise from trial to trial and spike patterns appear [78]. In [32] this phenomenon is explained saying that the prestimulus history of a neuron may influence the precise timing of the spikes, and this, once again, means that the ISIs are correlated.

In this context Taillefumier and Magnasco ([74], [75]) focus on the following sLIF model for a single neuron:

$$dV(t) = -\alpha V(t)dt + dC(t) + \sigma dW(t), \quad \alpha > 0, \quad V(t_0) = r < l, \quad t \geq t_0 \tag{3.24}$$

in the presence of a constant threshold l and a Hölder-continuous load function $C(t)$ such that $dC(t) = I(t)dt$. $I(t)$ is a frozen noise conveying random current pulses of varying amplitudes and a constant current input, injected through synapses or a stimulating electrode.
When $V(t)$ first reaches a threshold value l, an action potential is generated and the voltage $V(t)$ is reset to $r < l$, while $I(t)$ keeps evolving. We note that in this case the time-varying input that is not reset after the spike introduces correlation within the interspike intervals.

The load function $C(t)$ is supposed to be Hölder-continuous of exponent $H \in (0,1)$ i.e. such that

$$H = \inf_t H_t < \infty$$

where

$$H_t = \lim_{\delta \to 0+} \sup_{|t-s| \leq \delta} \frac{|C(t) - C(s)|}{|t-s|^h}$$

is the local Hölder exponent. H is a measure of the degree of singularity of I and in [74] and [75] is considered as the key mathematical property that determine the regime of firing of the single neuron under study.

It is possible to map the dynamics of a neuron with an input, internal noise and a constant threshold voltage, into a neuron with internal noise and a fluctuating threshold voltage. Let assume that t_i and t_{i+1} are instants in which a spike occurs. Following [75], since the non-linearity of the sLIF model lies in the generation of the action potential and the successive reset, between the spikes t_i and t_{i+1} we integrate separately the effect of the input and the noise writing

$$V = U_i + l_i \tag{3.25}$$

as the sum of a stochastic component

$$U_i(t) = re^{-\alpha(t-t_i)} + \int_{t_i}^{t} e^{-\alpha(t-s)} dW(s) \tag{3.26}$$

and a deterministic one

$$l_i(t) = \int_{t_i}^{t} e^{-\alpha(t-s)} dC(s) \tag{3.27}$$

with reset condition $V(t_i^+) = r$. Note that (3.27) is the solution of the ordinary differential equation

$$\frac{dl_i(t)}{dt} = -\alpha l_i + I(t).$$

In this framework the next spike, i.e. the first spike after t_i, is seen as the FPT τ_{i+1} of the stochastic process U_i through the effective barrier $L_i(t)$

$$\tau_{i+1} = \inf \left\{ t > t_i | U_i(t) > L_i(t), U_i(t_i^+) = r \right\}, \tag{3.28}$$

where

$$L_i(t) := l - l_i(t). \tag{3.29}$$

Therefore, a train of spikes $t_0 < t_1 < \ldots < t_n$ can be determined by solving many times the first-passage problems (3.28) for independent processes U_i.

This definition, however, exhibits the undesidered property that the effective barrier $L_i(t)$ depends on the specific value of t_i.

In [75] it has been proved that another FPT problem, related to the previous one, can be considered:

$$\tau'_{i+1} = \inf\left\{t > \tau_i | U_i^{'}(t) > L(t), U_i^{'}(t_i^+) = L(\tau_i) - (l - r)\right\} \tag{3.30}$$

where $L(t) := l - l^0$. We observe that the threshold now does not depend on t_i, while the stochasticity of the problem is transferred to the reset condition. Intuitively in problem (3.28) the OU process U_i evolves in presence of noise and the integrated input l_i is substracted from the threshold l, while in problem (3.30), called the effective barrier representation, the threshold becomes continuous as a convolution of the injected current and the OU process is reset in random points.

The train of spikes results from a succession of FPTs to the effective barrier and the determination of FPT densities of these successive spikes with the reset condition $U_i(t_i^+) = L(\tau_i) - (l - r)$ is called "recurring-passage problem".

As mentioned before, in [74] the Hölder exponent H of the input plays an important role in the determination of the regime of firing of the neuron and evidences of a phase transition of the probability of observing a first passage time of a Gauss-Markov process through a rough boundary of exponent H are shown. If the injected frozen noise is less singular than the internal neuronal noise ($H > 1/2$), the firing activity admits a continuous probability density of spiking times, whereas the probability density becomes singular, almost everywhere either zero or infinity, if the frozen noise is more singular than the internal noise ($H < 1/2$).

The reliability of a spiking event is measured by the fraction of time that the event occurs, while the precision of an individual spiking event is quantified by the variance of its timing conditionally to belonging to a specific pattern [32]. If we can identify narrow phase regions that carry most of the spiking phase statistics, we say that the stochastic LIF neuron spikes reliably. For the above model the larger the Hölder exponent is, the higher is the spike reliability. For small Hölder exponents, we have poor spike reliability but high temporal precision [75].

In Fig. 3.2, for instance, we realized a raster plot in the case of very singular input ($H = 0.26$). We see that the patterns of the spiking activity can be easily detected. We also note that the points of high firing activity, very likely correspond to minima of the boundary. In fact the singularity of the input is transferred into a loss of smoothness of the boundary that exhibits picks of minimum in which, easily, the membrane potential crosses

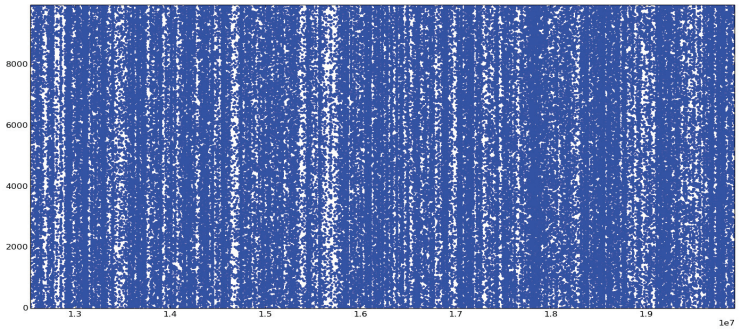

Figure 3.2: Raster plot of the simulated spikes for $H = 0.26$ over 10000 repetitions of the stimulus. The simulated neuron exhibits high temporal precision in the spike activity.

the firing threshold.

3.2.1 Sample statistics and simulations

Paths of the process $U_i(t)$ in presence of the effective boundary $L(t)$ have been simulated for all Hölder exponents H in the range $(0.25 - 0.99)$ in increments of 0.01 using a fast algorithm specialized for the first-passage times of Gauss-Markov processes with Hölder continuous boundaries [76]. For each one of the 75 Hölder exponents, 62000 repetitions of the 10s stimulus were performed accumulating 100 million first passages per Hölder exponent.

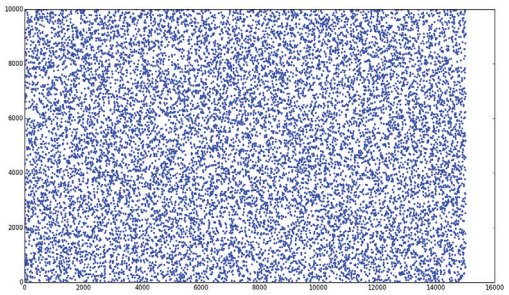

Figure 3.3: Raster plot of a small portion (one million) of the simulated spikes for $H = 0.88$.

In Fig. 3.3 the raster plot in the case of $H = 0.88$ is reported. The rows of the raster indicate the repetitions of the stimulus, while the dots indicate

the occurrence of spike. In order to make the plot readable a mask made of one million dots has been extracted from the original plot.

The times in which $U_i(t)$ crosses $L(t)$ are histogrammed in the peristimulus time histogram (PSTH). The PSTH has on the x axis the temporal bins and on the y axis the number of spikes occured in that temporal bin across the repetitions, so it represents the instantaneous probability distribution of first passage times.

Starting from the PSTH, we plot the histogram of the firing rate (see Fig. 3.4) i.e. on the x axis are reported the number of spikes and on the y axis we report the number of bins that have that number of spikes in the PSTH.

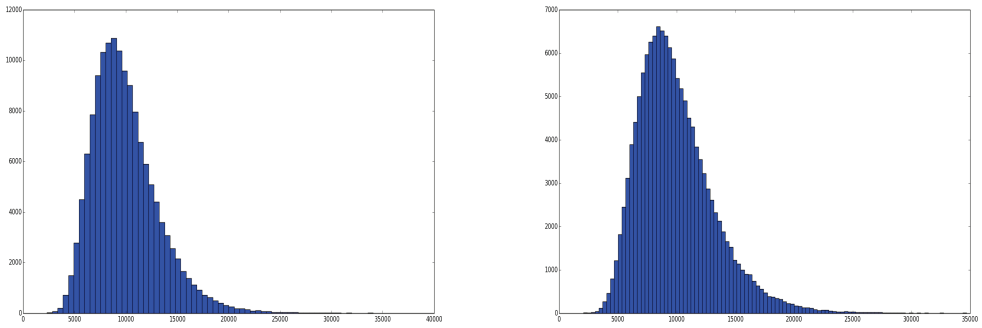

Figure 3.4: Histograms of the firing rate for two particular choices of the exponent H: on the left $H = 0.26(< 0.5)$, on the right $H = 0.88(> 0.5)$.

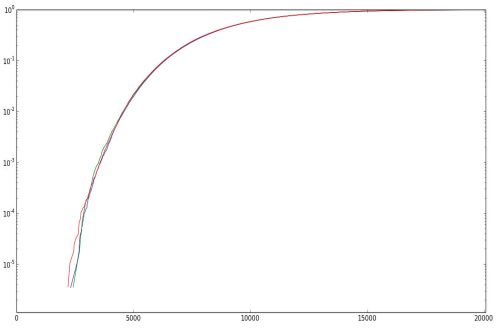

Figure 3.5: Plot of the cumulative distributions obtained integrating the probability density given by the histograms for $H = 0.26$ (in blue), $H = 0.5$ (in red) and $H = 0.97$ (in green).

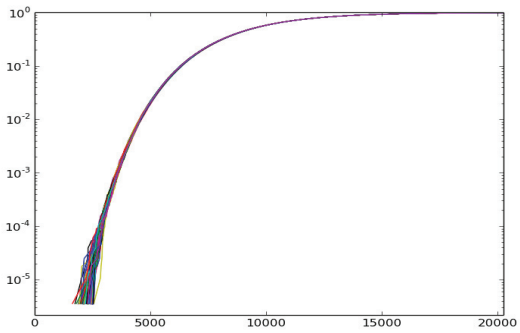

Figure 3.6: Plot of the cumulative distributions obtained integrating the probability density given by the histograms for 75 different exponents H.

Computing the cumulative distribution functions from the histograms of the type of Fig. 3.4, for all considered exponents H, it turned out that the cumulative functions coincide even accross the phase transition $H = 0.5$. In Fig. 3.5 we plot the cumulative distributions in three special cases: one is $H = 0.26$ below the critical value of the phase transition, one above the critical value ($H = 0.97$) and one exactly $H = 0.5$. We see no appreciable differences except at the beginning. It is a strong indication that it is a universal kinematic property of this recurring problem that does not depend on the shape of the boundary (see Fig. 3.6).

Chapter 4

Neuronal Models: successive spike times

In order to address the model presented by Taillefumier and Magnasco in [74] and [75], we propose in [26] and [27] a stochastic model for the prediction of successive spikes by means of FPTs of a sequence of Gauss-Markov processes each of which is identified by a particular mean function dependent on the FPT of the previous process. In [74] the authors mainly focused on the rate codes, i.e. the average number of spikes per unit of time, but of great interest are also the temporal codes, in which the timing of action potentials is related to the information transmission. The temporal codes are very important in the case of time-varying input signals but only poor results have been obtained in this direction.
Recently, in [80], Urdapilleta derived the FPT statistics of a Brownian motion driven by an exponential time-dependent drift through an absorbing threshold. Using the backward Fokker-Planck formulation he writes the FPT density function as a series of terms that are solutions of an inifinite set of recurrence equations.

Concerning the OU process Thomas provided a lower bound for the FPT density in the case of suprathreshold regime, i.e. the case in which the initial state and the asymptotic mean of the process are on opposide sides of the threshold values. This implies that the probability of crossing of the threshold in finite time is one, and can represent the situation in which the neuron is driven by a strong current much greater than the fluctuations due to the presence of noise [77]. In particular Thomas gives a lower bound for the FPT density through a constant threshold S of an Ornstein-Uhlenbeck process $X(t)$ obeying to the SDE $dX = -aXdt + \sigma dW$. In this case there

exist positive constants k, p and u such that

$$g(S,t|x_0,t_0) > k \exp\left\{-pe^{6at}\right\},$$

provided that $t > u$. In particular:

$$\begin{aligned} k &= \frac{1024}{9\pi} a \left(\frac{x_0}{S} - 1\right) \\ p &= 1 + \frac{a}{32}\left(\frac{S}{\sigma}\right)^2 \\ u &= \frac{1}{2a} \ln\left[1 + \max\left\{8, \left(1 + \frac{x_0^2}{S^2}\right), \left(\frac{8\sigma^2}{aS^2}\right)\right\}\right]. \end{aligned} \tag{4.1}$$

Anyway general results on OU processes are missing or fragmentary in the literature. Stimulated by these arguments and other very interesting papers ([21], [40], [49], [59] and [68]), in the next section we show how the GM processes theory can provide approximations of the firing distributions and, in particular, to contribute to the modeling of successive spike times.

4.1 Modeling of successive spike times

We take into account a stochastic LIF model with reset after the spike for the potential $V(t)$, but not for the time-varying input $I(t)$. For this reason the model is based on the time-inhomogeneous diffusion process $\{V(t), t \geq t_0\}$ (with $t_0 \in [0, +\infty)$) solution of the following SDE:

$$dV = [-\alpha(V - V_{rest}) + I(t)]\, dt + \sigma dW, \quad V(t_0) = v_0 < S. \tag{4.2}$$

The involved parameters have the same interpretation of those in SDE (3.3). Assuming $T_0 = t_0$, let T_1 be the FPT through the firing threshold S of the solution process $V(t)$ with reset to v_0, i.e. $V(T_1^+) = v_0$. T_1 stands for the first spike (firing) time; for $t \geq T_1$, the second passage time T_2 occurs and it stands for the second spike time of the train, and so on. It is possible to obtain random samples $T_0, T_1, \ldots, T_n$ of successive spike times simulating random paths of $V(t)$ by applying the well-known Euler discretization method to its SDE and recording the successive crossing times of S . The process is discretized as follows:

$$V(t_{k+1}) = V(t_k) + [-\alpha(V(t_k) - V_{rest}) + I(t_k)]\, \Delta t + \sigma\sqrt{\Delta t}\xi_{k+1}$$

where $V(t_0) = v_0$, $(t_0, \ldots, t_k, t_{k+1}, \ldots)$ is the time vector with $t_{k+1} = t_k + \Delta t$, $k = 1, 2, \ldots$; and ξ_k is a generated standard gaussian number.

In [26] we propose a stochastic model for the prediction of these successive spikes that constitute the train by means of FPTs of a sequence of Gauss-Markov processes each of which is identified by a particular mean function dependent on the FPT of the previous process. In particular we will see in detail the case of the first two spikes and then we will generalize the idea.

4.1.1 Concerning the first firing time T_1

Let us start by considering the process $V_1(t)$ solution of

$$dV_1 = [-\alpha(V_1 - V_{rest}) + I(t)]dt + \sigma dW, \quad V_1(t_0) = v_0 \quad t \in [t_0, +\infty). \quad (4.3)$$

In particular, the parameter $1/\alpha(> 0)$ is the characteristic decay time of the membrane potential, V_{rest} is the resting potential, v_0 is the initial value, $\sigma(> 0)$ represents a constant intensity of the noise and W the standard Brownian motion. Furthermore, $I(t)$ stands for a time-dependent input signal never reset. It can be generated by an injected input current or a synaptic current originated from the surrounding neuronal activity.
According to [3] and [57], under hypotheses of regularity on the function $I(t)$, and due to the form of its infinitesimal moments:

$$A_1^{(1)}(v,t) = -\alpha\,(v - V_{rest}) + I(t), \quad A_2^{(1)}(t) \equiv \sigma^2,$$

the process $V_1(t)$ is a Gauss-Diffusion process. It is also a GM process, i.e. a Gaussian process identified by the mean and by a special covariance of the form (2.8) (see, for details, [23]). Using the results of [13] we are able to write its mean and covariance.
In fact denoting, for $\tau \le t$,

$$\mathcal{M}_1(t|\tau) = V_{rest}\left(1 - e^{-\alpha(t-\tau)}\right) + e^{-\alpha t}\int_\tau^t I(\xi)e^{\alpha\xi}d\xi, \quad (4.4)$$

$V_1(t)$ is characterized by the mean and covariance functions

$$m_{V_1}(t|v_0,t_0) = v_0 e^{-\alpha(t-t_0)} + \mathcal{M}_1(t|t_0), \quad (4.5)$$

$$c_{V_1}(s,t|t_0) = \frac{\sigma^2}{2\alpha}e^{-\alpha(t-t_0)}\left[e^{\alpha(s-t_0)} - e^{-\alpha(s-t_0)}\right] \quad (t_0 \le s \le t) \quad (4.6)$$

with the following transition pdf, for $\tau \le t$,

$$f_{V_1}[x,t|y,\tau] = \frac{\sqrt{\alpha}}{\sqrt{\pi\sigma^2(1 - e^{-2\alpha(t-\tau)})}}\exp\left\{-\alpha\frac{\left[x - ye^{-\alpha(t-\tau)} - \mathcal{M}_1(t|\tau)\right]^2}{\sigma^2\left(1 - e^{-2\alpha(t-\tau)}\right)}\right\}. \quad (4.7)$$

Note that the above pdf is a normal-type transition function with the conditional mean and variance

$$\begin{aligned} \mathbb{E}[V_1(t)|V_1(\tau)=y] &= m_{V_1}(t|y,\tau), \quad (4.8)\\ Var(t|\tau) &= c_{V_1}(t,t|\tau). \quad (4.9) \end{aligned}$$

The FPT $\mathcal{T}_1$ of the process $V_1(t)$ through a constant threshold S is defined as:

$$\mathcal{T}_1 := \inf_{t\geq t_0}\{t : V_1(t) \geq S\} \quad \text{with} \quad V_1(t_0) = v_0 < S$$

and with the pdf

$$g_1(S,t|v_0,t_0) = \frac{d\mathbb{P}(\mathcal{T}_1 \leq t)}{dt}.$$

For input signals $I(t)$ such that the integral $\int_{t_0}^{t} I(\xi)e^{\alpha\xi}d\xi$ exists for any $t \geq t_0$, in [26] we provide a numerical approximation of the pdf $g_1(S,t|v_0,t_0)$ solving, by a numerical procedure, the non-singular second kind Volterra integral equation (2.39) where the function $\Psi[S,t|y,\tau]$ in this case takes the following expression:

$$\begin{aligned} &\Psi_1[S,t|y,\tau] = \\ &= \left\{ -\frac{S\alpha(1+e^{-2\alpha(t-\tau)})}{1-e^{-2\alpha(t-\tau)}} + \frac{2\alpha y e^{-\alpha(t-\tau)}}{1-e^{-2\alpha(t-\tau)}} - [\alpha V_{rest} + I(t)] + \frac{2\alpha\mathcal{M}_1(t|\tau)}{1-e^{-2\alpha(t-\tau)}} \right\} \\ &\times \quad f_{V_1}[S,t|y,\tau]. \quad (4.10) \end{aligned}$$

Using the already mentioned numerical quadrature specialized for the case of time-varying input signal $I(t)$ we can provide evaluations of $g_1(S,t|v_0,t_0)$. Then, from it also $\mathbb{P}(\mathcal{T}_1 \leq t)$ can be evaluated.

In Fig. 4.1 we compare our numerical approximation $\widehat{g}_1(t)$ of $g_1(S,t|v_0,t_0)$ with the histograms of simulated FPTs for different threshold values and starting points v_0. The firing density is represented by histograms of a sample of FPTs $\mathcal{T}_1$, through a constant threshold, of simulated random paths obtained from equation (4.3), discretized by means of the Euler method.

Hence, identifying the first spike time T_1 with the FPT $\mathcal{T}_1$, we obtain, for $t \geq t_0$,

$$\mathbb{P}(T_1 \leq t) \equiv \mathbb{P}(\mathcal{T}_1 \leq t) = G_1(S,t|v_0,t_0) = \int_{t_0}^{t} g_1(S,\xi|v_0,t_0)d\xi. \quad (4.11)$$

Finally, from (4.11), we provide $\widehat{G}_1(t)$ as an approximation of $\mathbb{P}(T_1 \leq t)$ by means of a numerical quadrature applied to $\displaystyle\int_{t_0}^{t} \widehat{g}_1(\xi)d\xi$.

Now, we want to model the successive spike time T_2.

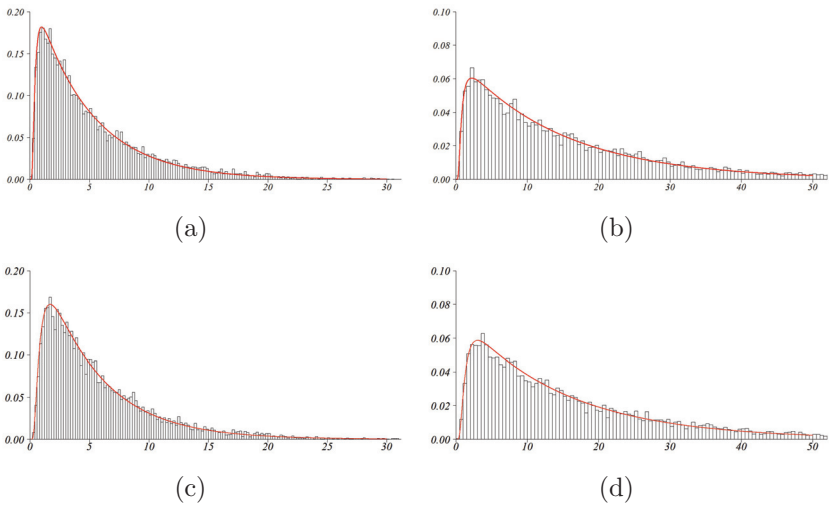

Figure 4.1: Histograms of 10^4 FPTs $\mathcal{T}_1$ of simulated random paths of $V_1(t)$ by discretization of (4.3) and numerical $\widehat{g}_1(t)$ for $S = 1.5$ ((a),(c)) and $S = 2$ ((b),(d)). $I(t) \equiv \mu = 0.25$, $\alpha = 1$, $V_{rest} = 0.2$, $\sigma = 1$, $t_0 = 0$,$v_0 = 0$ in (a),(b) and $v_0 = -0.5$ in (c),(d). The discretization step for simulations and for the numerical procedure is 10^{-3}.

4.1.2 Concerning the second firing time T_2

We now focus our attention on another stochastic process that is useful for the description of the evolution of the neuronal membrane potential in the presence of the threshold S before the spike time T_2. We consider a process $V_2(t)$, that in mean behaves like the process $V_1(t)$ but taking into account that every past instant could have been a realization of $\mathcal{T}_1$, starting from the reset value v_0. So $V_2(t)$ is the GM process with covariance (4.6) and the following mean function

$$m_{V_2}(t|v_0, t_0) = v_0 e^{-\alpha(t-t_0)} + \mathcal{M}_2(t|t_0) \tag{4.12}$$

where we define

$$\mathcal{M}_2(t|t_0) = \mathbb{E}\left\{\mathbb{E}\left[\mathcal{M}_1(t|t_1)|T_1 = t_1\right]\right\} = \int_{t_0}^{t} \mathcal{M}_1(t|t_1) g_1(S, t_1|v_0, t_0) dt_1. \tag{4.13}$$

The probability that each time instant t_1 before t could have been an instant of first spike is translated in the presence of $g_1(S, t_1|v_0, t_0)$ in the formula (4.13). This specific mathematical condition is motivated by the assumption that the average behavior of the neuronal membrane after a spike time (and reset) is almost the same of the ones before the spike, although

in any time t it keeps the memory of the occurrence of a previous spike and at the same time it is subject to the input signal which in the meanwhile has never been reset. With these reasons in mind, we construct the *ad hoc* process $V_2(t)$ as a transformed $V_1(t)$ by (4.13). Proposition 1 of [26], tells us which SDE the process $V_2(t)$ satisfies.

Proposition 4.1.1 ([26]). *The process $V_2(t)$, obtained from the process $V_1(t)$ by* (4.13)*, having mean defined by* (4.12) *and covariance as in* (4.6)*, is a GM process and is solution of the following SDE, for $t \geq t_0$,*

$$dV_2 = \left\{ -\alpha V_2 + \alpha \left[V_{rest} + \frac{I(t)}{\alpha} \right] \mathbb{P}(T_1 \leq t) \right\} dt + \sigma dW, \quad V_2(t_0) = v_0. \tag{4.14}$$

Proof. From (4.4), (4.12) and (4.13), the mean function (4.12) of $V_2(t)$ becomes

$$\begin{aligned} m_{V_2}(t|v_0, t_0) &= v_0 e^{-\alpha(t-t_0)} \\ &+ e^{-\alpha t} \left[\alpha V_{rest} \int_{t_0}^{t} \mathbb{P}(T_1 \leq \xi) e^{\alpha\xi} d\xi + \int_{t_0}^{t} I(\xi) \mathbb{P}(T_1 \leq \xi) e^{\alpha\xi} d\xi \right]. \end{aligned} \tag{4.15}$$

Due to the linearity of relations (4.12) and (4.13), or equivalently from (4.15), and due to the form of covariance (4.6), the process $V_2(t)$ is a GM process. Moreover, we note that the specified process $V_2(t)$ is characterized by the normal transition pdf

$$f_{V_2}[x, t|y, \tau] = \frac{\sqrt{\alpha}}{\sqrt{\pi\sigma^2(1 - e^{-2\alpha(t-\tau)})}} \exp\left\{ -\alpha \frac{\left[x - ye^{-\alpha(t-\tau)} - \mathcal{M}_2(t|\tau) \right]^2}{\sigma^2 \left(1 - e^{-2\alpha(t-\tau)}\right)} \right\}, \tag{4.16}$$

having the same variance of $V_1(t)$ and the following conditional mean

$$\mathbb{E}[V_2(t)|V_2(\tau) = y] = ye^{-\alpha(t-\tau)} + \mathcal{M}_2(t|\tau) \tag{4.17}$$

where

$$\mathcal{M}_2(t|\tau) = e^{-\alpha t} \left[\alpha V_{rest} \int_{\tau}^{t} \mathbb{P}(T_1 \leq \xi) e^{\alpha\xi} d\xi + \int_{\tau}^{t} I(\xi) \mathbb{P}(T_1 \leq \xi) e^{\alpha\xi} d\xi \right], \tag{4.18}$$

and, in particular, from (4.15),

$$\mathcal{M}_2(t|\tau) = m_{V_2}(t|v_0, t_0) - e^{-\alpha(t-\tau)} m_{V_2}(\tau|v_0, t_0). \tag{4.19}$$

Finally, by using the differentiable mean function (4.15), recalling (4.18) and (4.19), along the lines of [23], the infinitesimal drift of $V_2(t)$ is evaluable

in the following way

$$\begin{aligned} A_1^{(2)}(v,t) &= \lim_{\Delta t\to 0}\frac{\mathbb{E}[V_2(t+\Delta t)-V_2(t)|V_2(t)=v]}{\Delta t} \\ &= m'_{V_2}(t|v_0,t_0)-\alpha\left[v-m_{V_2}(t|v_0,t_0)\right] \\ &= \mathcal{M}'_2(t|\tau)-\alpha\left[v-\mathcal{M}_2(t|\tau)\right] \\ &= -\alpha v+\alpha\left[V_{rest}+\frac{I(t)}{\alpha}\right]\mathbb{P}(T_1\le t). \end{aligned}$$

The infinitesimal variance is also evaluable giving $A_2^{(2)}(t)\equiv\sigma^2$. Hence, under hypotheses of regularity on the functions involved in the infinitesimal drift, $V_2(t)$ is also a diffusion process and solves the SDE (4.14). □

Using notation analogous to that for $V_1(t)$, we now consider the FPT of $V_2(t)$, i.e.

$$\mathcal{T}_2 := \inf_{t\ge t_0}\{t : V_2(t)\ge S\} \quad \text{with} \quad V_2(t_0)=v_0<S. \tag{4.20}$$

Let $g_2(S,t|v_0,t_0)$ be the pdf of $\mathcal{T}_2$, i.e. $g_2(S,t|v_0,t_0)=\dfrac{d\mathbb{P}(\mathcal{T}_2\le t)}{dt}$.
It is solution of

$$g_2(S,t|v_0,t_0) = -\Psi_2[S,t|v_0,t_0]+\int_{t_0}^{t}\Psi_2[S,t|S,\tau]g_2(S,\tau|v_0,t_0)d\tau \tag{4.21}$$

with

$$\begin{aligned} &\Psi_2[S,t|y,\tau]= \\ &\left\{-\frac{S\alpha(1+e^{-2\alpha(t-\tau)})}{1-e^{-2\alpha(t-\tau)}}+\frac{2\alpha y e^{-\alpha(t-\tau)}}{1-e^{-2\alpha(t-\tau)}}-[\alpha V_{rest}+I(t)]\,\mathbb{P}(T_1\le t)+\frac{2\alpha\mathcal{M}_2(t|\tau)}{1-e^{-2\alpha(t-\tau)}}\right\} \\ &\quad\times\quad f_{V_2}[S,t|y,\tau] \end{aligned} \tag{4.22}$$

where $f_{V_2}[S,t|y,\tau]$ and $\mathcal{M}_2(t|\tau)$ are as in (4.16) and (4.18), respectively.

As done for the FPT T_1 it is possible to provide numerical estimations $\widehat{g}_2(t)$ of the pdf $g_2(S,t|v_0,t_0)$ solving numerically (4.21) and compare these estimations with results of simulations of equation (4.14). It is possible to obtain also $\widehat{G}_2(t)$ by means of a numerical quadrature of $\widehat{g}_2(t)$. In this case, however, our numerical procedure to solve (4.21), that involves the function (4.22), requires to evaluate $g_1(S,t|v_0,t_0)$ and $\mathbb{P}(T_1\le t)$ before starting. Hence, an iterative numerical strategy has been adequately carried out in [26] to evaluate $\widehat{g}_2(t)$. Similarly, the simulation algorithm applied to (4.14) is based on the previous evaluation of $\mathbb{P}(T_1\le t)$ from (4.3). In Fig. 4.2 the satisfactory agreement between simulations of $V_2(t)$ by discretization of (4.14)

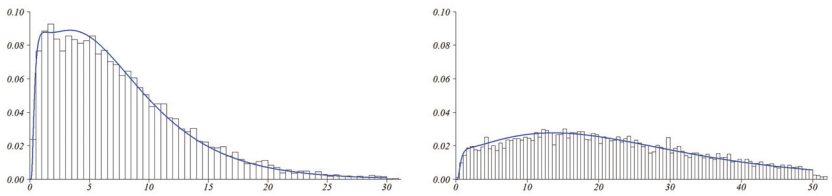

Figure 4.2: Histograms of 10^4 simulated $\mathcal{T}_2$ and numerical $\widehat{g}_2(t)$ for $S = 1.5$ (on the left) and $S = 2$ (on the right). $I(t) \equiv \mu = 0.25$, $\alpha = 1$, $V_{rest} = 0.2$, $v_0 = 0$, $\sigma = 1$. The discretization step for the simulation is 10^{-3} and for the numerical procedure is 10^{-2}.

and our numerical approximations $\widehat{g}_2(t)$ highlights the accuracy of our numerical results.

Let us suppose, for the moment, that the input is constant and $I(t) \equiv \mu$. In Fig. 4.3 are shown the behaviors of $\widehat{g}_1(t)$ and $\widehat{g}_2(t)$, whereas in Fig. 4.4 that of m_{V_1} and m_{V_2} both for $S = 1.5$ and $S = 2$. From the plots the mean function $m_{V_2}(t|v_0, t_0)$ seems to be always smaller than $m_{V_2}(t|v_0, t_0)$ and it looks also valid for the distribution functions $\widehat{G}_1(t)$ and $\widehat{G}_2(t)$ (see Fig. 4.5).

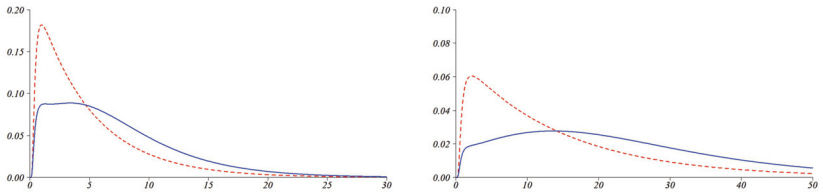

Figure 4.3: Plot of $\widehat{g}_1(t)$ (red dashed) and $\widehat{g}_2(t)$ (blue solid) for $I(t) \equiv \mu = 0.25$, $\alpha = 1$, $V_{rest} = 0.2$, $\sigma = 1$, $t_0 = 0$,$v_0 = 0$, $S = 1.5$ (on the left), $S = 2$ (on the right).

These intuitions motivated the following proposition proved in [26].

It is useful for the following Proposition to recall from [70] the following definition:

Definition 4.1.2. The random variable X is *smaller* than the random variable Y in the usual *stochastic order* (denoted by $X \leq_{st} Y$) if and only if

$$\mathbb{P}(X \geq u) \leq \mathbb{P}(Y \geq u) \quad \forall u \in (-\infty, \infty).$$

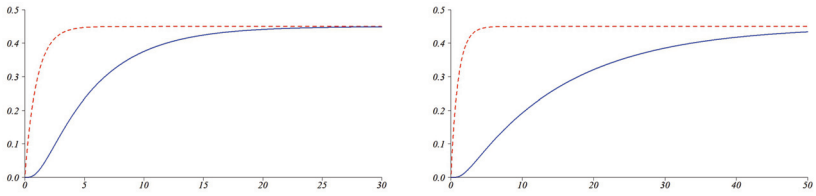

Figure 4.4: Plots of the $m_{V_1}(t|v_0, t_0)$ (red dashed) and $m_{V_2}(t|v_0, t_0)$ (blue solid) for $S = 1.5$ (on the left) and $S = 2$ (on the right). The other parameters are as in Fig. 4.3.

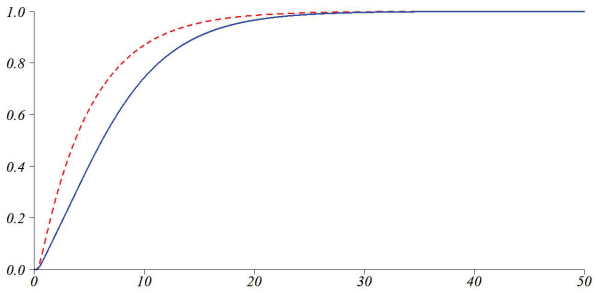

Figure 4.5: Plots of the $\widehat{G}_1(t)$ (red dashed) and $\widehat{G}_2(t)$ (blue solid) for $S = 1.5$, with constant $I(t) \equiv \mu = 0.25$, obtained by numerical quadratures of the corresponding $\widehat{g}_\cdot(t)$. The other parameters are as in Fig. 4.3.

Proposition 4.1.3 ([26]). *The FPT $\mathcal{T}_1$ of $V_1(t)$ and the FPT $\mathcal{T}_2$ of $V_2(t)$ are stochastically ordered as follows*

$$\mathcal{T}_1 \leq_{st} \mathcal{T}_2.$$

Proof. We note that on the basis of (4.13), from (4.18), recalling (4.4),

$$\mathcal{M}_2(t|\tau) \leq \mathcal{M}_1(t|\tau)\mathbb{P}(T_1 \leq t), \quad \forall t > \tau \geq t_0 \tag{4.23}$$

and from (4.12) and (4.4), we have

$$m_{V_2}(t|v_0, t_0) \leq m_{V_1}(t|v_0, t_0), \quad \forall t \geq t_0,\ v_0 < S. \tag{4.24}$$

(As expected from the considerations on Fig. 4.4.) Recalling that $V_1(t)$ and $V_2(t)$ are GM processes, it is known ([13],[23]) that both are transformed process of the Brownian motion $W(\cdot)$ as follows

$$V_1(t) = m_{V_1}(t|v_0, t_0) + \sigma e^{-\alpha(t-t_0)} W\left(\frac{e^{2\alpha(t-t_0)} - 1}{\alpha}\right), \forall t \geq t_0 \tag{4.25}$$

and

$$V_2(t) = m_{V_2}(t|v_0, t_0) + \sigma e^{-\alpha(t-t_0)} W\left(\frac{e^{2\alpha(t-t_0)} - 1}{\alpha}\right), \forall t \geq t_0. \tag{4.26}$$

Hence, taking into account (4.24), (4.25) and (4.26), we can write

$$\mathbb{P}(\mathcal{T}_1 \leq t) = \mathbb{P}\left(\max_{t_0 \leq \tau \leq t} V_1(\tau) \geq S\right) \geq \mathbb{P}\left(\max_{t_0 \leq \tau \leq t} V_2(\tau) \geq S\right) = \mathbb{P}(\mathcal{T}_2 \leq t),$$

$\forall t \geq t_0$. Hence,

$$\mathbb{P}(\mathcal{T}_1 \geq t) \leq \mathbb{P}(\mathcal{T}_2 \geq t), \quad \forall t \geq t_0$$

i.e. $\mathcal{T}_1 \leq_{st} \mathcal{T}_2$. □

Again from [70], $\mathcal{T}_1 \leq_{st} \mathcal{T}_2$ implies that $\mathbb{E}(\mathcal{T}_1) \leq \mathbb{E}(\mathcal{T}_2)$.

See Fig. 4.6 as further intuitive confirmation in the case of an exponential input signal $I(t) = \mu + \lambda e^{-\beta t}$.

4.1.3 Two cases of study: exponential and constant input signals

Now let us see how the previous results can be applied when the expression of the input signal $I(t)$ is specified.
We consider the following exponential form to represent an input signal:

$$I(t) = \mu + \lambda e^{-\beta t} \quad \text{with } \beta > 0, \mu, \lambda \in \mathbb{R}, \quad t \geq t_0 = 0. \tag{4.27}$$

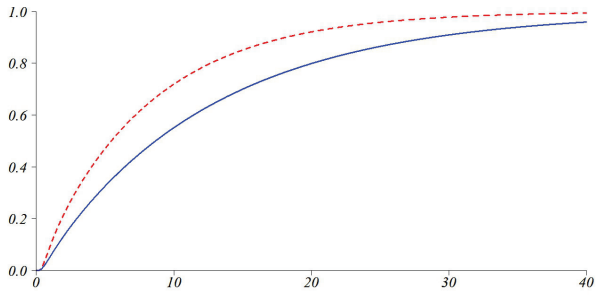

Figure 4.6: Plots of the $\widehat{G}_1(t)$ (red dashed) and $\widehat{G}_2(t)$ (blue solid) for $S = 1.5$, with an exponential input $I(t) = \mu + \lambda e^{-\beta t}$ $(\mu = 0, \lambda = 0.25, \beta = 1.5)$, obtained by numerical quadratures of the corresponding $\widehat{g}_\cdot(t)$. The other parameters are as in Fig. 4.3.

In this way, we can describe an inhibitory current with $\mu \leq 0, \lambda \leq 0$ and an excitatory current for $\mu \geq 0, \lambda \geq 0$ and also currents that change their nature in time when $\mu\lambda < 0$. Moreover, we can also tune the parameter β in (4.27) to different decay times of the current to the constant level μ.
Note that the case of the constant input signal can be derived as a particular case of the exponential input signal (4.27) with $\lambda = 0$.

Now, the SDE for $V_1(t)$ is the following one:

$$dV_1 = [-\alpha(V_1 - V_{rest}) + \mu + \lambda e^{-\beta t}]dt + \sigma dW, \quad V_1(t_0) = v_0 \quad t \geq t_0. \tag{4.28}$$

In this case, we find

$$\mathcal{M}_1(t|\tau) = \left(V_{rest} + \frac{\mu}{\alpha}\right)\left(1 - e^{-\alpha(t-\tau)}\right) + \frac{\lambda}{\alpha - \beta}\left(e^{-\beta t} - e^{-\alpha(t-\tau)-\beta\tau}\right) \tag{4.29}$$

by which in [26] the mean, the covariance, the conditional moments and the transition pdf of the process $V_1(t)$ have been specified. In particular, for evaluating $g_1(S, t|v_0, t_0)$, in the corresponding integral equation, following again [26], we can specify $\Psi_1[S, t|y, \tau]$ in this case with $\mathcal{M}_1(t|\tau)$ as in (4.29):

$$\begin{aligned}\Psi_1[S, t|y, \tau] \;=\; & \left\{ -\frac{S\alpha}{2}\frac{1 + e^{-2\alpha(t-\tau)}}{1 - e^{-2\alpha(t-\tau)}} + \frac{\alpha y e^{-\alpha(t-\tau)}}{1 - e^{-2\alpha(t-\tau)}} \right. \\ & \left. -\frac{\alpha}{2}\left[V_{rest} + \frac{\mu}{\alpha} + \frac{\lambda}{\alpha}e^{-\beta t}\right] + \frac{\alpha\mathcal{M}_1(t|\tau)}{1 - e^{-2\alpha(t-\tau)}} \right\} \times f_{V_1}[S, t|y, \tau].\end{aligned}$$

Furthermore, from Proposition 4.1.1, the process $V_2(t)$, for the input sig-

nal (4.27), satisfies the following SDE:

$$dV_2 = \left[-\alpha V_2 + \alpha\left(V_{rest} + \frac{\mu + \lambda e^{-\beta t}}{\alpha}\right)\mathbb{P}(T_1 \leq t)\right]dt + \sigma dW, \quad V_2(t_0) = v_0,\ t \geq t_0 \tag{4.30}$$

and it is characterized by the following mean

$$\mathcal{M}_2(t|\tau) = e^{-\alpha t}\left[(\alpha V_{rest} + \mu)\int_\tau^t \mathbb{P}(T_1 \leq \xi)e^{\alpha\xi}d\xi + \lambda\int_\tau^t e^{(\alpha-\beta)\xi}\mathbb{P}(T_1 \leq \xi)d\xi\right]. \tag{4.31}$$

Finally, for evaluating $g_2(S, t|v_0, t_0)$, from (4.21) we can specify $\Psi_2[S, t|y, \tau]$ of (4.22) with $I(t)$ as in (4.27), $\mathcal{M}_2(t|\tau)$ as in (4.31) and $\mathbb{P}(T_1 \leq t)$ as the numerical evaluation $\widehat{\mathbb{P}}(\mathcal{T}_1 \leq t)$, having already obtained $\widehat{g}_1(t)$ for $g_1(S, t|v_0, t_0)$. See in Fig. 4.7 (left) the comparison between histograms of $\mathcal{T}_1$ by simulations of (4.28) and numerical approximations $\widehat{g}_1(t)$. See in Fig. 4.7 (right) the comparison between histograms of $\mathcal{T}_2$ by simulations of (4.30) and numerical approximations $\widehat{g}_2(t)$. Fig. 4.8, instead, shows how a threshold that is far from x_0 influences the pdfs $g_1(S, t|v_0, t_0)$ and $g_2(S, t|v_0, t_0)$.

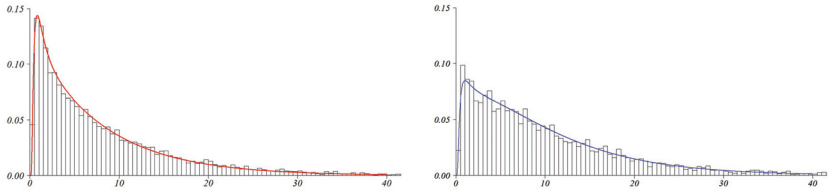

Figure 4.7: Left: histograms of 10^4 simulated $\mathcal{T}_1$ and numerical $\widehat{g}_1(t)$. Right: histograms of 10^4 simulated $\mathcal{T}_2$ and numerical $\widehat{g}_2(t)$ for exponential input signal with $\lambda = 0.25$, $\beta = 1.5 (> \alpha)$, $\mu = 0$, $\alpha = 1$, $V_{rest} = 0.2$, $v_0 = 0$, $\sigma = 1$ and $S = 1.5$. The discretization step for the simulation is 10^{-3} and for the numerical procedure is 10^{-3} on the left and is 10^{-2} on the right.

Note that Fig. 4.9 refers to the case $\beta < \alpha$. In this way, it is possible to take into account the cases in which the characteristic times α of the membrane potential and β of the input signal are different; in particular, the case $\beta < \alpha$ corresponds to the case in which the time-varying effect of the input signal persists beyond the time of decay to the resting level of the potential, whereas the case $\beta > \alpha$ corresponds to the case in which the time-varying effect of the signal is short and vanishes before than the potential attains the resting level. Indeed, the firing densities of Fig. 4.9 show higher

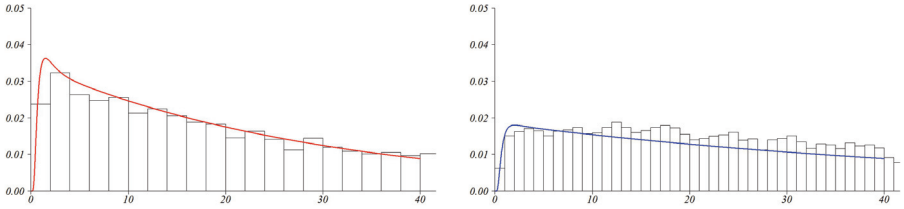

Figure 4.8: The same of Fig. 4.7 for $S = 2$.

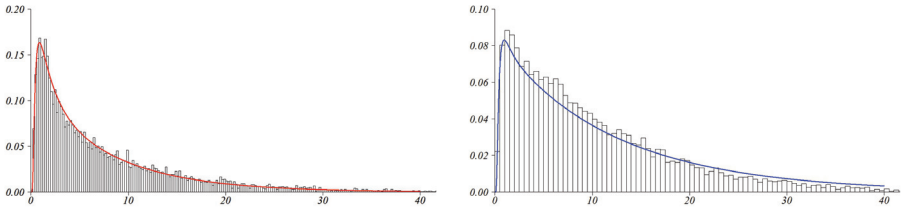

Figure 4.9: The same of Fig. 4.7 for $\beta = 0.5 (< \alpha)$.

values than those of Fig. 4.7, being more persistent the excitatory input effect.

Finally, also the case $\alpha = \beta$ can be considered. In this case, from (4.29) for $\beta \to \alpha$, we have

$$\mathcal{M}_1(t|\tau) = \left[V_{rest} + \frac{\mu}{\alpha}\right]\left(1 - e^{-\alpha(t-\tau)}\right) + \lambda e^{-\alpha t}(t-\tau)$$

and, from (4.31) for $\beta \to \alpha$, we have

$$\mathcal{M}_2(t|\tau) = e^{-\alpha t}\left[(\alpha V_{rest} + \mu)\int_\tau^t P(T_1 \le \xi)e^{\alpha\xi}d\xi + \lambda\int_\tau^t P(T_1 \le \xi)d\xi\right].$$

Coming back to the original task, i.e. the approximation of the successive spike times of the train $T_0, T_1, \ldots, T_n$, we generalize the idea used for the first two spikes ([26]). We model the behavior of the neuronal membrane potential by diffusion processes $\{V_1(t), V_2(t), \ldots, V_n(t)\}$ such that $\{V_k(t), t \ge t_0\}$ (for $k = 1, \ldots, n$) is solution of the SDE

$$dV_k = \left\{-\alpha V_k + \alpha\left[V_{rest} + \frac{I(t)}{\alpha}\right]\mathbb{P}(T_{k-1} \le t)\right\}dt + \sigma dW, \quad V_k(t_0) = v_0 < S, \tag{4.32}$$

with $t_0 \ge 0$, $\mathbb{P}(T_0 = t_0) = 1$. Here, the $\mathbb{P}(T_{k-1} \le t)$ is the probability that the previous spike time T_{k-1} has already occurred, with reference to

time t. We point out that we suitably inserted the factor $\mathbb{P}(T_{k-1} \leq t)$ in order to take into account in some sense the occurrence of the previous spike time T_{k-1}. Then we consider the FPT $\mathcal{T}_k$ of the stochastic process $V_k(t)$ (for $k = 1, \ldots, n$) through a constant threshold S, and use it for the description of the k-th spike time.

4.1.4 Interspike Intervals

Performing simulations of the SDE (4.32) we obtain spike times $T_1, \ldots, T_n$ and this enables us to build also histograms of the ISIs $T_k - T_{k-1}$ for $k = 1, 2, \ldots, n$. Moreover having the approximations $\widehat{g}_1(t)$ and $\widehat{g}_2(t)$ one can give estimations of the distribution of the ISI $T_2 - T_1$. This idea has been presented in [27].

For modeling the general ISIs $T_k - T_{k-1}$, for $k = 1, 2, \ldots, n$, we now consider the following SDEs

$$dY_k(t) = \left\{ -\alpha Y_k(t) + \alpha \left[V_{rest} + \frac{I(t)}{\alpha} \right] \mathbb{P}(\mathcal{T}_k > t) \right\} dt + \sigma dW(t), Y_k(0) = v_0, \tag{4.33}$$

for $t > 0$, where the process $Y_k(t)$ obeys to a similar dynamics of the process $V_k(t)$ except for the probability term $\mathbb{P}(\cdot)$ in (4.33). In particular, $Y_k(t)$ is linked to the process $V_k(t)$, because the dynamics (4.33) of $Y_k(t)$ depends on the probability distribution function of the FPT $\mathcal{T}_k$ of $V_k(t)$. We use the process $Y_k(t)$ to mimic the behavior of the membrane potential before the occurrence of $\mathcal{T}_k$, taking into account that $\mathcal{T}_{k-1}$ is already occurred. Then, we model the ISIs by using the FPTs of $Y_k(t)$, i.e.

$$\mathcal{T}_k^y := \inf_{t \geq 0} \{ t : Y_k(t) \geq S \}, \quad Y_k(0) = v_0 < S,$$

with the pdf

$$g_{Y_k}(S, t | v_0, 0) := \frac{d\mathbb{P}(\mathcal{T}_k^y \leq t)}{dt}.$$

Let us consider again the input current $I(t)$ of the form (4.27).
According to [13], and for the specified $I(t)$, we set for $k = 1, 2, \ldots, n$ and for $0 \leq \tau \leq t$

$$\mathcal{M}_{Y_k}(t|\tau) = [\alpha V_{rest} + \mu] \, e^{-\alpha t} \int_\tau^t \mathbb{P}(\mathcal{T}_k > \xi) e^{\alpha \xi} d\xi + \lambda e^{-\alpha t} \int_\tau^t \mathbb{P}(\mathcal{T}_k > \xi) e^{(\alpha - \beta)\xi} d\xi. \tag{4.34}$$

In analogy with the previous notation, the Gauss-Markov (GM) process $Y_k(t)$, for $k = 1, 2, \ldots, n$, has the following mean function, for $t \geq 0$,

$$m_{Y_k}(t|v_0, 0) = v_0 e^{-\alpha t} + \mathcal{M}_{Y_k}(t|0), \tag{4.35}$$

and covariance function (for $k = 1, 2, \ldots, n$)

$$c_{Y_k}(s,t) = \frac{\sigma^2}{2\alpha} e^{-\alpha t} \left[e^{\alpha s} - e^{-\alpha s} \right] \qquad (0 \le s \le t). \tag{4.36}$$

Furthermore, the normal transition pdf $f_{Y_k}(x,t|y,\tau)$, for $k = 1, 2, \ldots, n$, of $Y_k(t)$ is

$$f_{Y_k}[x,t|y,\tau] = \frac{\sqrt{\alpha}}{\sqrt{\pi\sigma^2(1-e^{-2\alpha(t-\tau)})}} \exp\left\{ -\alpha \frac{\left[x - ye^{-\alpha(t-\tau)} - \mathcal{M}_k(t|\tau)\right]^2}{\sigma^2\left(1-e^{-2\alpha(t-\tau)}\right)} \right\}. \tag{4.37}$$

In [27] a numerical approximation of the FPT pdf $g_{Y_k}(S,t|v_0,0)$ is provided solving, by a numerical procedure, the following non singular second kind Volterra integral equation:

$$g_{Y_k}(S,t|v_0,0) = -\Psi_{Y_k}[S,t|v_0,0] + \int_0^t \Psi_{Y_k}[S,t|S,\tau] g_{Y_k}(S,\tau|v_0,0) d\tau \tag{4.38}$$

for $k = 1, 2, \ldots, n$, with

$$\begin{aligned} \Psi_{Y_k}[S,t|y,\tau] = f_{Y_k}[S,t|y,\tau] \quad & \left\{ -S\alpha \frac{1+e^{-2\alpha(t-\tau)}}{1-e^{-2\alpha(t-\tau)}} + \frac{2\alpha y e^{-\alpha(t-\tau)}}{1-e^{-2\alpha(t-\tau)}} \right. \\ & \left. -\alpha \left[V_{rest} + \frac{\mu + \lambda e^{-\beta t}}{\alpha} \right] \mathbb{P}(\mathcal{T}_k > t) + \frac{2\alpha \mathcal{M}_{Y_k}(t|\tau)}{1-e^{-2\alpha(t-\tau)}} \right\}. \end{aligned} \tag{4.39}$$

In this case, for solving the integral equation (4.38) for $g_{Y_k}(S,t|v_0,0)$ it is required to obtain first $g_{V_k}(S,t|v_0,0)$, because the function $\Psi_{Y_k}[S,t|y,\tau]$ is defined by means of $\mathbb{P}_k(t) = \mathbb{P}(\mathcal{T}_k > t) = 1 - \mathbb{P}(\mathcal{T}_k \le t)$.

Taking into account that $T_0 = 0$ and $\mathcal{T}_1^y \equiv T_1$, in [27] the FPT $\mathcal{T}_2^y$ is presented as a good approximation of the second interspike interval $T_2 - T_1$.

To lighten the procedure, under certain hypoteses, it is possible to make use of the asymptotic approximations of the FPT pdf $g_{V_1}(S,t|v_0,0)$. In the next section we recall the mathematical framework and we show how it can lead to the estimation of the ISI's pdf in particular in the case $T_2 - T_1$.

4.1.5 An asymptotic approximation

At first, we specify an asymptotic approximation valid for the pdf $g_1(S,t|v_0,t_0)$ in the case of asymptotically constant input signals such that

$$I = \lim_{t \to +\infty} I(t).$$

From (4.4), (4.5) and (4.6) we have

$$\lim_{t\to\infty} m_{V_1}(t|v_0,t_0) = V_{rest} + \frac{I}{\alpha}, \tag{4.40}$$

$$\lim_{t\to\infty} Var(t|\tau) = \lim_{t\to\infty} \frac{\sigma^2}{2\alpha}\left(1-e^{-2\alpha(t-\tau)}\right) = \frac{\sigma^2}{2\alpha}. \tag{4.41}$$

Hence, we obtain the stationary transition density function $\mathcal{W}_1(x)$, i.e.

$$\mathcal{W}_1(x) = \lim_{t\to\infty} f_{V_1}[x,t|y,\tau] = \sqrt{\frac{\alpha}{\pi\sigma^2}}\exp\left\{-\frac{\alpha}{\sigma^2}\left[x-\left(V_{rest}+\frac{I}{\alpha}\right)\right]^2\right\}. \tag{4.42}$$

From (4.10) and (4.42), we also obtain that

$$h_{V_1} = -\lim_{t\to\infty}\Psi_1(S,t|y,\tau) = \left\{\alpha\left[S-\left(V_{rest}+\frac{I}{\alpha}\right)\right]\right\}\mathcal{W}_1(S) =$$

$$= \alpha\sqrt{\frac{\alpha}{\pi\sigma^2}}\left[S-\left(V_{rest}+\frac{I}{\alpha}\right)\right]\exp\left\{-\frac{\alpha}{\sigma^2}\left[S-\left(V_{rest}+\frac{I}{\alpha}\right)\right]^2\right\}. \tag{4.43}$$

Along the lines of [13], for $t-t_0 > 1/\alpha$ and

$$S-\left(V_{rest}+\frac{\max\limits_{t_0\le t} I(t)}{\alpha}\right) > \sqrt{\sigma^2\alpha}, \tag{4.44}$$

then the following exponential approximation for $g_1(S,t|v_0,t_0)$ holds:

$$g_1[S,t|v_0,t_0] \approx \widetilde{g}_1(t) = h_{V_1}e^{-h_{V_1}(t-t_0)}. \tag{4.45}$$

Condition (4.44), better explains the words "big enough" used in Theorem 2.2.3.

Finally, as approximation of $\mathbb{P}(T_1 \le t)$, we can have $\widetilde{G}_1(t)$ from a numerical quadrature of (4.11) when in place of $g_1(S,t|v_0,t_0)$ we use $\widetilde{g}_1(t)$ obtaining

$$\mathbb{P}(T_1 \le t) \approx \widetilde{\mathbb{P}}(\mathcal{T}_1 \le t) = 1 - e^{-h_{V_1}(t-t_0)} \tag{4.46}$$

$\forall t \ge t_0$. Then, we adopt the closed form expression of $\widetilde{\mathbb{P}}(\mathcal{T}_1 \le t)$ in (4.15) in place of $\mathbb{P}(T_1 \le t)$ and we finally obtain

$$\widetilde{m}_{V_2}(t|v_0,t_0) = v_0 e^{-\alpha(t-t_0)} + \widetilde{\mathcal{M}}_2(t|t_0) \tag{4.47}$$

with

$$\widetilde{\mathcal{M}}_2(t|t_0) = V_{rest}\left(1-e^{-\alpha(t-t_0)}\right)\left[1+\frac{\alpha e^{-h_{V_1}(t-t_0)}}{h_{V_1}-\alpha}\right]$$

$$+ e^{-\alpha t}\int_{t_0}^{t} I(\xi)e^{\alpha\xi}d\xi - e^{-\alpha t}\int_{t_0}^{t} I(\xi)e^{-(h_{V_1}-\alpha)(\xi-t_0)}d\xi. \tag{4.48}$$

We point out that now our numerical quadrature for evaluating the pdf $g_2(S,t|v_0,t_0)$, can be directly applied without any previous numerical evaluations of $g_1(S,t|v_0,t_0)$ and $\mathbb{P}(T_1 \leq t)$, but using the closed form expressions $\widetilde{g}_1(t)$ and $\widetilde{\mathbb{P}}(\mathcal{T}_1 \leq t)$ of (4.45) and (4.46), respectively.

Let us see as these mathematical results can be applied in the case of input (4.27). Indeed in this case $I(t)$ is asymptotically constant

$$I \equiv \lim_{t\to+\infty} I(t) = \mu, \quad \lim_{t\to\infty} \mathcal{M}_1(t|y,\tau) = V_{rest} + \frac{\mu}{\alpha}, \tag{4.49}$$

and, from (4.42),

$$\mathcal{W}_1(x) = \sqrt{\frac{\alpha}{\pi\sigma^2}} \exp\left\{-\frac{\alpha}{\sigma^2}\left[x - \left(V_{rest} + \frac{\mu}{\alpha}\right)\right]^2\right\}. \tag{4.50}$$

Therefore, for $t - t_0 > 1/\alpha$ and $S - \left(V_{rest} + \frac{\mu+\lambda}{\alpha}\right) > \sqrt{\sigma^2\alpha}$ the asymptotic approximation (4.46) is valid with h_{V_1}

$$\begin{aligned} h_{V_1} &= -\lim_{t\to+\infty} \Psi_{V_1}(S,t|y,\tau) = \\ &= \alpha\sqrt{\frac{\alpha}{\pi\sigma^2}}\left[S - \left(V_{rest} + \frac{\mu}{\alpha}\right)\right] \exp\left\{-\frac{\alpha}{\sigma^2}\left[S - \left(V_{rest} + \frac{\mu}{\alpha}\right)\right]^2\right\}. \end{aligned} \tag{4.51}$$

In Fig. 4.10 is shown the comparison between the FPT pdf $g_1(t)$ and the asymptotic approximation $\widehat{g}_1(t)$ for $S = 2$.

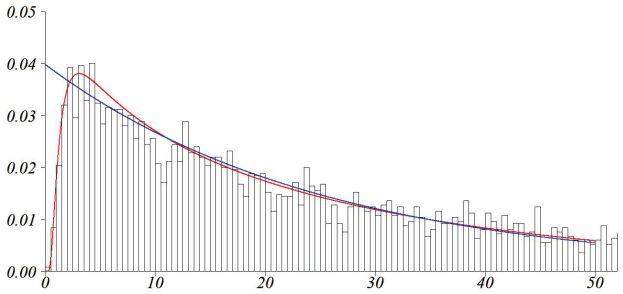

Figure 4.10: Histograms of 10^4 simulated $\mathcal{T}_1$, compared to the numerical $\widehat{g}_1(t)$ (in red) and the asymptotic approximation $\widetilde{g}_1(t)$ (in blue) for an exponential input signal with $\lambda = 0.1$, $\beta = 0.1(< \alpha)$, $\mu = 0.1$, $\alpha = 1$, $V_{rest} = 0.1$, $v_0 = -0.5$, $\sigma = 1$ and $S = 2$. The discretization step for the numerical procedure is 10^{-3}, for simulations is 10^{-4}.

Finally, it is possible to use for the process $V_2(t)$ the approximated mean function $\widetilde{m}_{V_2}(t|v_0,t_0)$ from (4.47), evaluated with the signal $I(t)$ as in (4.27) with

$$\widetilde{\mathcal{M}}_{V_2}(t|0) = \left[V_{rest} + \frac{\mu}{\alpha}\right]\left(1-e^{-\alpha t}\right) + \frac{(\alpha V_{rest}+\mu)}{h_{V_1}-\alpha}\left[e^{-h_{V_1}t} - e^{-\alpha t}\right] + \frac{\lambda}{\alpha-\beta}\left[e^{-\beta t} - e^{-\alpha t}\right] - \frac{\lambda}{\alpha-\beta-h_{V_1}}\left[e^{-h_{V_1}t-\beta t} - e^{-\alpha t}\right] \quad (4.52)$$

Using these results in [27] is presented the good agreement of the numerical evaluations of $g_{V_2}(S,t|v_0,0)$ with histograms of second passage times T_2 of $V(t)$(see Figs. 4.11 and 4.12).

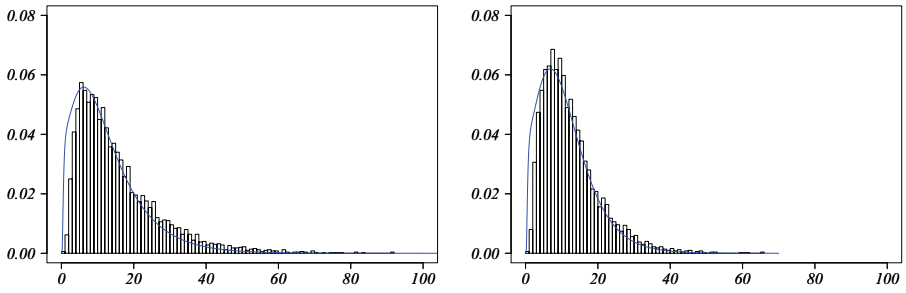

Figure 4.11: Approximations for the pdf of T_2. Numerical evaluations of $g_{V_2}(S,t|v_0,0)$ (blue) and histograms of 10^4 second passage times T_2 of simulated paths of $V(t)$ by (4.32), with time discretization step 10^{-4}, $\lambda = 0.25$, $\mu = 0.25$, $\alpha = 1$, $V_{rest} = 0.2$, $v_0 = 0$, $\sigma = 1$, $S = 1.8$, $\beta = 0.1$ (on the left) and $\beta = 0.01$ (on the right).

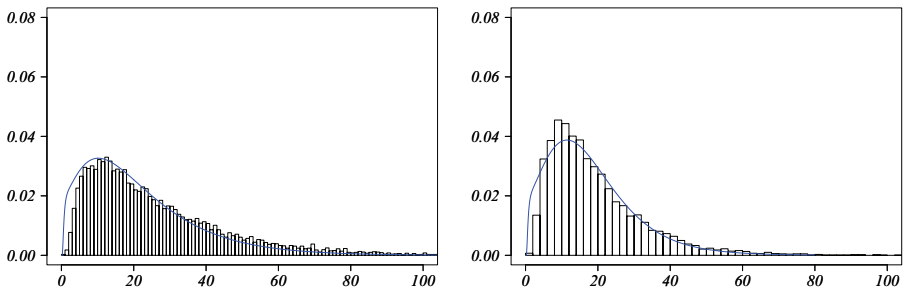

Figure 4.12: Same of Fig.4.11 with $S = 2$

These informations on the FPT pdf $g_{V_2}(S,t|v_0,0)$ can be used to obtain the probability $\mathbb{P}(\mathcal{T}_2 > t) = 1 - \mathbb{P}(\mathcal{T}_2 \leq t)$ necessary to construct the function

$\mathcal{M}_{Y_2}(t|0)$, as in (4.34) for $k = 2$, and also the function $\Psi_{Y_2}[S, t|y, \tau]$ as in (4.39). So a numerical evaluation of the pdf of χ_2 is possible, and in Figs. 4.13 and 4.14 it is compared with the histograms of the second ISI $T_2 - T_1$.

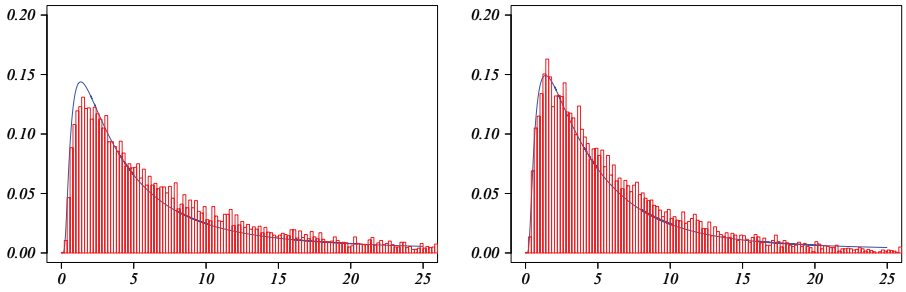

Figure 4.13: Approximations for the ISI pdf of $T_2 - T_1$. Numerical evaluations of $g_{Y_2}(S, t|v_0, 0)$ (blue) and histograms of 10^4 ISI duration $T_2 - T_1$ of $V(t)$ by simulations of (4.32), with time discretization step 10^{-4}. $S = 1.8$ and $\beta = 0.1$ (on the left) and $\beta = 0.01$(on the right), other parameters as in Fig. 4.11.

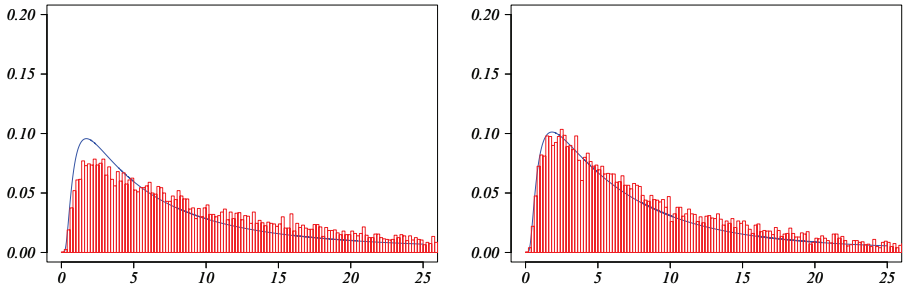

Figure 4.14: Same of Fig.4.13 with $S = 2$.

4.1.6 A modified model: ordered FPTs for successive spike times

Even if the FPT of $V_1(t)$ and the FPT of $V_2(t)$ are stocastically ordered, $\mathcal{T}_2$ can occur before $\mathcal{T}_1$ i.e. $\mathbb{P}(\mathcal{T}_2 < \mathcal{T}_1) \geq 0$. For this reason we assume $\Theta_1 = \mathcal{T}_1$ and consider the random variable $\Theta_2 = \max\{\Theta_1, \mathcal{T}_2\}$ for which $\mathbb{P}(\Theta_2 < \mathcal{T}_1) = 0$, being $\mathbb{P}(\Theta_2 \geq \mathcal{T}_1) = 1$ from its definition, with pdf

$$g_{\Theta_2}(t) = g_1(t)\mathbb{P}(\mathcal{T}_2 \leq t) + g_2(t)\mathbb{P}(\mathcal{T}_1 \leq t) \tag{4.53}$$

where for shortness $g_1(t) = g_1(S, t|v_0, t_0)$ and $g_2(t) = g_2(S, t|v_0, t_0)$.

Following our numerical strategy, evaluations of the functions involved in (4.53) are available, and finally also the evaluation of $\mathbb{P}(\Theta_2 \leq t)$ can be given by means of a quadrature applied to $g_{\Theta_2}(s)$ for $t_0 \leq s \leq t$.

The random variable Θ_2 turns out to be a more suitable tool for modeling the second spike time. Indeed, in all cases of applications, and how it will be shown for specified examples in the following, the numerical evaluation of (4.53) fits the histogram of the simulated T_2 better than the $\widehat{g}_2(t)$ (see Fig.4.15), where T_2 is the second passage time of $V(t)$ through the threshold S.

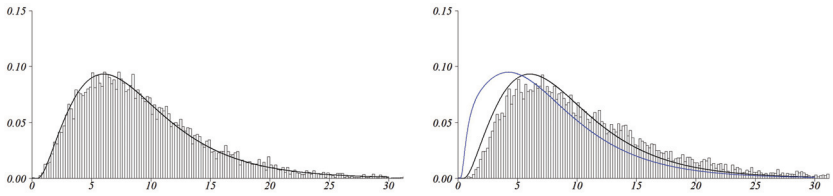

Figure 4.15: Left: histograms of the simulated $\Theta_2 = \max\{\mathcal{T}_1, \mathcal{T}_2\}$ and the numerical evaluation of $g_{\Theta_2}(t)$ (4.53) for an exponential input signal are shown. Right: histograms of 10^4 simulated T_2, the numerical evaluation of $g_{\Theta_2}(t)$ (in black) and $\widehat{g}_2(t)$ (in blue). The values of parameters are: $\lambda = 0.2$, $\beta = 0.01(< \alpha)$, $\mu = 0.1$, $\alpha = 1$, $V_{rest} = 0.2$, $v_0 = -0.5$, $\sigma = 1$ and $S = 1.5$.

Also in Fig. 4.16 can be appreciated how $g_{\Theta_2}(t)$ approximates the pdf of T_2. The satisfactory agreement between the numerical evaluation of (4.53) and the histogram of the maximum of simulated FPTs $\mathcal{T}_1$ and $\mathcal{T}_2$, that is a further support of the consistency of our method, is shown on the left-hand sides of Figs. 4.15 and 4.16 .

Also in this context, under suitable assumptions, an asymptotic approximation can be used. In particular we can write the pdf $g_{\Theta_2}(t)$ using the asymptotic approximation $\widetilde{g}_1(t)$ of $g_1(t)$.
Let $\widehat{g}_2[t; \widetilde{g}_1(t)]$ ($\widehat{\mathbb{P}}[\mathcal{T}_2 \leq t; \widetilde{g}_1(t)]$) be the numerical evaluation of $g_2(t)$ ($\mathbb{P}(\mathcal{T}_2 \leq t)$) obtained by using the asymptotic expression $\widetilde{g}_1(t)$ of $g_1(t)$, we give the following approximation $\gamma_{\Theta_2}(t)$ for $g_{\Theta_2}(t)$:

$$\gamma_{\Theta_2}(t) = h_{V_1} e^{-h_{V_1}(t-t_0)} \widehat{\mathbb{P}}[\mathcal{T}_2 \leq t; \widetilde{g}_1(t)] + \widehat{g}_2[t; \widetilde{g}_1(t)] \left(1 - e^{-h_{V_1}(t-t_0)}\right) . \quad (4.54)$$

In the case of $S = 2$ the hypoteses of asymptotic regime are satisfied, and so the function $g_2[t; \widetilde{g}_1(t)]$ can be evaluated and, as consequence, also $\gamma_{\Theta_2}(t)$ (see Fig. 4.17).

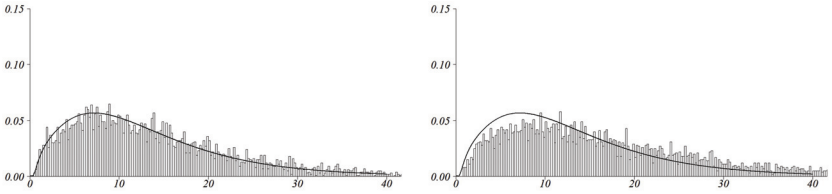

Figure 4.16: Left: histograms of the simulated $\Theta_2 = \max\{\mathcal{T}_1, \mathcal{T}_2\}$ and the numerical evaluation of $g_{\Theta_2}(t)$ (4.53) for an exponential input signal. Right: histograms of 10^4 simulated T_2 and the numerical evaluation of $g_{\Theta_2}(t)$. The values of parameters are the same of Fig. 4.7. The discretization step for the numerical procedure is 10^{-2} and for simulations is 10^{-2} on the left and 10^{-4} on the right.

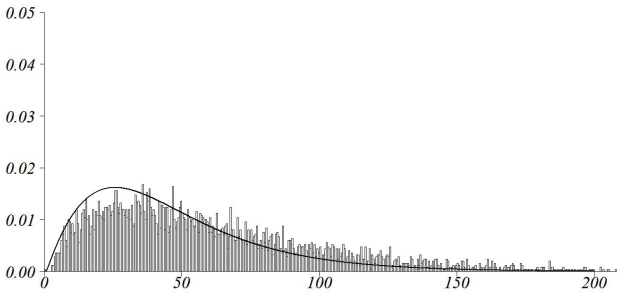

Figure 4.17: Histograms of 10^4 simulated T_2 and the numerical evaluation of $\gamma_{\Theta_2}(t)$ (4.54) for an exponential input signal with $\lambda = 0.1$, $\beta = 0.1 (< \alpha)$, $\mu = 0.1$, $\alpha = 1$, $V_{rest} = 0.1$, $v_0 = -0.5$, $\sigma = 1$ and $S = 2$. The discretization step for the numerical procedure is 10^{-3}, for simulations is 10^{-4}.

Finally, from [26] we give some indications about a quantitative error analysis: the $\mathcal{L}^1$-norm of the difference between two interpolating densities of histograms from two independent samples of T_2 is about 0.08, while the $\mathcal{L}^1$-norm of the difference between one of these densities and the numerical evaluation of $g_{\Theta_2}(t)$ is about 0.54 for the case of Fig. 4.16. The $\mathcal{L}^1$-norm of the difference related to independent histograms of T_2 is about 0.12 for the case of Fig. 4.15 (0.1 for Fig. 4.17), while the $\mathcal{L}^1$-norm of the difference between the histogram of T_2 and the numerical $g_{\Theta_2}(t)$ is about 1.2 for Fig. 4.15 (1.02 for Fig. 4.17). Independent simulations of the second passage times T_2 of the process $V(t)$ have been performed by discretization of (4.2), and the histograms and the interpolating densities have been obtained using the software R.

We also provide a scatter plot to give some indications about the joint distribution of the pairs of the two spike times (see Fig. 4.18). The agreement is satisfactory for small times.

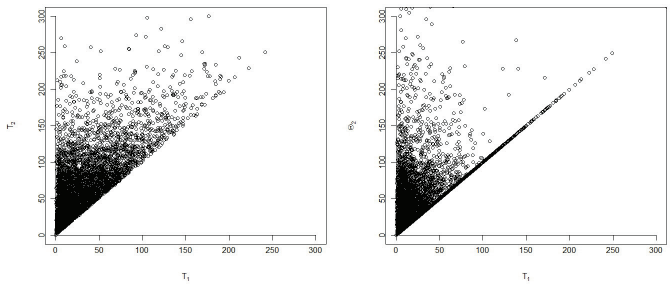

Figure 4.18: Scatter plots of $5 \cdot 10^3$ pairs (T_1, T_2) on the left, and of (T_1, Θ_2) on the right. (T_1, T_2) are simulated first and second passage times of $V(t)$. (T_1, Θ_2) are pairs with simulated FPT $\mathcal{T}_1 (= T_1)$ of $V_1(t)$ and simulated $\Theta_2 = \max\{\mathcal{T}_1, \mathcal{T}_2\}$, with simulated FPTs $\mathcal{T}_2$ of $V_2(t)$. All parameters are specified in the caption of Fig. 4.15.

Finally, for the general *k-th* spike time, the following approximation can be given: $\mathbb{P}(T_k \leq t) \approx \mathbb{P}(\Theta_k \leq t)$ where $\Theta_k = \max\{\Theta_{k-1}, \mathcal{T}_k\}$.

Chapter 5

Two-boundary first exit time of Gauss-Markov processes and biological modeling

The study of the random variable First Exit Time (FET) of Gauss-Markov and Diffusion processes plays a key role in the construction and development of models in a wide variety of fields, as molecular biology, financial markets, population dynamics and in the context of neuronal modeling ([1], [2], [9], [25], [55] and [67]). Here we recall some of the main theoretical results for two-boundary FET densities of some specified GD processes. We will focus on the conditions that guarantee the existence of a closed-form expression or on the methods that provide numerical approximations when these conditions are not satisfied. We will also show how it is possible to use GD processes and the corresponding FET through suitable boundaries for modeling the acto-myosin dynamics responsible of the contraction in the skeletal muscles.

5.1 Two-boundary First Exit Time

Here, we recall definitions and main results of [55]. We now focus our attention on the random variable First Exit Time (FET) $\mathcal{T}_{x_0}^{(1,2)}$ from a strip with absorbing boundaries $S_1(t)$, $S_2(t)$ of a GD process $X(t)$ starting from x_0 at time $t_0 = 0$. Specifically, let $S_1(t)$ and $S_2(t)$ be a $C^1([0, +\infty))$-class functions such that $S_1(t) < S_2(t),\ \forall t,\ S_1(0) < X(0) \equiv x_0 < S_2(0)$. For all $t \geq 0$, we

shall now focus our attention on the random variables:

$$\mathcal{T}_{x_0}^{(1)} = \inf_{t\geq 0}\big\{t : X(t) < S_1(t);\ X(\vartheta) < S_2(\vartheta), \forall \vartheta \in (0,t)\big\} \qquad X(0) = x_0$$

(first-passage time through the lower boundary)

$$\mathcal{T}_{x_0}^{(2)} = \inf_{t\geq 0}\big\{t : X(t) > S_2(t);\ X(\vartheta) > S_1(\vartheta), \forall \vartheta \in (0,t)\big\}, \qquad X(0) = x_0$$

(first-passage time through the upper boundary)

$$\mathcal{T}_{x_0}^{(1,2)} = \inf_{t\geq 0}\big\{t : X(t) \notin \big(S_1(t), S_2(t)\big)\big\}, \qquad X(0) = x_0$$

(first-exit time)

and denote by $g_1(t \mid x_0, 0)$, $g_2(t \mid x_0, 0)$ and $g(t \mid x_0, 0)$, respectively, their pdfs:

$$\begin{aligned} g_1(t \mid x_0, 0) &= \frac{\partial}{\partial t} P\big(\mathcal{T}_{x_0}^{(1)} < t\big), \\ g_2(t \mid x_0, 0) &= \frac{\partial}{\partial t} P\big(\mathcal{T}_{x_0}^{(2)} < t\big), \\ g(t \mid x_0, 0) &= \frac{\partial}{\partial t} P\big(\mathcal{T}_{x_0}^{(1,2)} < t\big) \equiv g_1(t \mid x_0, 0) + g_2(t \mid x_0, 0). \end{aligned} \tag{5.1}$$

Hence, $P(\mathcal{T}_{x_0}^{(1)} < t)$ $[P(\mathcal{T}_{x_0}^{(2)} < t)]$ is the probability that $X(t)$ crosses for the first time $S_1(t)$ $[S_2(t)]$ at some time preceding t before crossing $S_2(t)$ $[S_1(t)]$, whereas $P(\mathcal{T}_{x_0}^{(1,2)} < t)$ is the probability that $X(t)$ crosses for the first time either $S_1(t)$ or $S_2(t)$ before time t.

The functions $g_1(t \mid x_0, 0)$ and $g_2(t \mid x_0, 0)$ satisfy a system of two Volterra integral equations of the first type, each of which analogous to equation (2.38). In [9], as done for the one boundary case, the authors wrote the FPT pdfs as solution of two second-kind Volterra integral equations using two arbitrary functions $k_1(t)$ and $k_2(t)$, whose specification allows to remove the singularities of the kernels.

In [55] the system was adapted to the case of Gauss-Markov processes. In this case we have that if $S_1(t), S_2(t), m(t), h_1(t), h_2(t) \in \mathcal{C}^1(T)$ the FPT pdfs $g_1[t|x_0, 0]$ and $g_2[t|x_0, 0]$ solve the following system of nonsingular second-kind Volterra integral equations:

$$\begin{aligned} g_1(t \mid x_0, 0) &= 2\,\Psi_1(t \mid x_0, 0) \\ &\quad -2\int_0^t \Big\{g_1(\tau \mid x_0, 0)\,\Psi_1[t \mid S_1(\tau), \tau] \ + g_2(\tau \mid x_0, 0)\,\Psi_1[t \mid S_2(\tau), \tau]\Big\}\, d\tau, \end{aligned} \tag{5.2}$$

$$\begin{aligned} g_2(t \mid x_0, 0) &= -2\,\Psi_2(t \mid x_0, 0) \\ &\quad +2\int_0^t \Big\{g_1(\tau \mid x_0, 0)\,\Psi_2[t \mid S_1(\tau), \tau] \ + g_2(\tau \mid x_0, 0)\,\Psi_2[t \mid S_2(\tau), \tau]\Big\}\, d\tau, \end{aligned}$$

where

$$\Psi_j(t \mid y,\tau) = \left\{ \frac{S_j'(t) - m'(t)}{2} - \frac{S_j(t) - m(t)}{2} \, \frac{h_1'(t)\, h_2(\tau) - h_2'(t)\, h_1(\tau)}{h_1(t)\, h_2(\tau) - h_2(t)\, h_1(\tau)} \right.$$
$$\left. - \frac{y - m(\tau)}{2} \, \frac{h_2'(t)\, h_1(t) - h_2(t)\, h_1'(t)}{h_1(t)\, h_2(\tau) - h_2(t)\, h_1(\tau)} \right\} f[S_j(t), t \mid y, \tau] \quad (j = 1, 2) \tag{5.3}$$

and

$$\lim_{\tau \to t} \Psi_i[S_i(t), t | S_j(\tau), \tau] = 0 \quad (i, j = 1, 2). \tag{5.4}$$

5.1.1 Closed form for FET density

Again we recall the hypotheses that guarantee closed form expression for g, g_1, g_2. When these conditions are not satisfied, it is possible to obtain evaluations of FET density by means of numerical quadratures of the integral equations (5.2).

First of all, under suitable assumptions on the boundaries of the GD process, it is possible to prove that the first-exit time pdf $g(t \mid x_0, 0)$ is the solution of a single non-singular Volterra integral equation in place of the system (5.2).

We recall from [55] that, under all above assumptions, if

$$\lim_{t \to +\infty} r(t) = +\infty, \quad P\big\{ S_1(t) \le X(t) < S_2(t) \mid X(0) = x_0 \big\} \neq 1,$$

one has:

$$\int_0^{+\infty} g(t \mid x_0, 0)\, dt = 1. \tag{5.5}$$

Furthermore, if $S_1(t)$ and $S_2(t)$ are such that

$$S_1(t) + S_2(t) = 2\, m(t) + 2\, c\, h_2(t), \qquad (c \in \mathbb{R}), \tag{5.6}$$

for all $t \ge 0$, then

$$g(t \mid x_0, 0) = 2 \Big[\Psi_1(t \mid x_0, 0) - \Psi_2(t \mid x_0, 0) \Big] \tag{5.7}$$
$$-2 \int_0^t g(\tau \mid x_0, 0) \Big\{ \Psi_1[t \mid S_1(\tau), \tau] - \Psi_2[t \mid S_1(\tau), \tau] \Big\}\, d\tau.$$

Finally, if $S_1(t)$ and $S_2(t)$ are such that (5.6) holds for all $t \ge 0$ and if x_0 is such that

$$x_0 = m(0) + c\, h_2(0), \qquad (c \in \mathbb{R}), \tag{5.8}$$

then

$$g_1(t \mid x_0, 0) = g_2(t \mid x_0, 0) \tag{5.9}$$

and as consequence

$$g(t \mid x_0, 0) \equiv 2\, g_1(t \mid x_0, 0) \equiv 2\, g_2(t \mid x_0, 0) \tag{5.10}$$

satisfies the single integral equation (5.7).

Even if there is no reduction to a single integral equation, it is possible to obtain solutions in closed form for the FET pdf. Here, we briefly recall the Theorems 4.1 and 4.2 of [55]. Let $S_1(t)$ and $S_2(t)$ be such that

$$S_1(t) = m(t) + b\, h_1(t) + c_1\, h_2(t), \qquad S_2(t) = m(t) + b\, h_1(t) + c_2\, h_2(t), \tag{5.11}$$

with $S_1(t) < S_2(t)$ for all $t \geq 0$, and let x_0 be such that

$$x_0 = m(0) + b\, h_1(0) + c\, h_2(0), \tag{5.12}$$

with $b, c, c_1, c_2 \in \mathbb{R}$ and $S_1(0) < x_0 < S_2(0)$. Then, the closed form for the following FET density holds:

$$\begin{aligned} g(t \mid x_0, 0) = {} & \frac{h_2(t)}{r(t) - r(0)} \frac{dr(t)}{dt} \sum_{n=-\infty}^{+\infty} \exp\left\{ -\frac{2\, n^2\, (c_2 - c_1)^2}{r(t) - r(0)} \right\} \\ & \times \left\{ \Big[c - c_1 + 2\, n\, (c_2 - c_1) \Big] \exp\left\{ -\frac{2\, n\, (c_2 - c_1)\, (c - c_1)}{r(t) - r(0)} \right\} f[S_1(t), t \mid x_0, 0] \right. \\ & \left. + \Big[c_2 - c - 2\, n\, (c_2 - c_1) \Big] \exp\left\{ \frac{2\, n\, (c_2 - c_1)\, (c_2 - c)}{r(t) - r(0)} \right\} f[S_2(t), t \mid x_0, 0] \right\}. \end{aligned} \tag{5.13}$$

We point out that in [55] is reported also the particular case of two Daniels-type boundaries for which the FET density admits a closed form.

Theorem 5.1.1. *For all $t \geq 0$ we set*

$$u(t) = m(t) + b_1 h_1(t) + c_2 h_2(t)$$

$$v(t) = m(t) + (2b - b_1) h_1(t) + (2c - c_1) h_2(t),$$

with $b, c, b_1, c_1 \in \mathbb{R}$ and $u(t) < v(t)$, and denote

$$\Delta(t) = 1 - 4\alpha_1 \alpha_2 \exp\left\{ -\frac{[v(t) - u(t)][v(0) - u(0)]}{h_1(t) h_2(0) - h_1(0) h_2(t)} \right\}$$

with $\alpha_1 > 0, \alpha_2 > 0$ *and* $\lim_{t \to \sup T} \Delta(t) > 0$. *If* $S_1(t), S_2(t), m(t), h_1(t), h_2(t) \in \mathcal{C}^1([0, +\infty))$ *and the absorbing boundaries and the initial state are of the following forms*

$$\begin{aligned} S_1(t) &= u(t) - \frac{h_1(t)h_2(0) - h_1(0)h_2(t)}{v(0) - u(0)} \ln \left[\frac{1 + \sqrt{\Delta(t)}}{2\alpha_1} \right] \\ S_2(t) &= v(t) + \frac{h_1(t)h_2(0) - h_1(0)h_2(t)}{v(0) - u(0)} \ln \left[\frac{1 + \sqrt{\Delta(t)}}{2\alpha_2} \right] \\ x_0 &= m(0) + b\, h_1(0) + c\, h_2(0), \end{aligned} \tag{5.14}$$

with $S_1(0) < x_0 < S_2(0)$*; then*

$$\begin{aligned} g(t|x_0, 0) &= \frac{v(0) - u(0)}{2[r(t) - r(0)]} \frac{h_2(t)}{h_2(0)} \frac{dr(t)}{dt} \sqrt{\Delta(t)} \\ &\times \{ f[S_1(t), t|x_0, 0] + f[S_2(t), t|x_0, 0] \}. \end{aligned} \tag{5.15}$$

The FET closed form for specific processes

Let us make explicit the (5.13) in specific cases of particular interest for stochastic modeling.

- The Wiener process. We consider the Wiener process $\{W(t), t \geq 0\}$ with $m_W(t)$, $h_{1_W}(t)$ and $h_{2_W}(t)$ as in (2.22). Then, from (5.11) and (5.12), for this kind of process the closed form (5.13) holds for boundaries and initial condition as follows

  $$S_{1_W}(t) = Bt + C_1, \qquad S_{2_W}(t) = Bt + C_2, \qquad x_0 = c_W + C \tag{5.16}$$

  with

  $$B = b_W + b\sigma_W, \quad C_1 = c_W + c_1\sigma_W, \quad C_2 = c_W + c_2\sigma_W, \quad C = c\sigma_W$$

  such that $S_{1_W}(t) < S_{2_W}(t)$ for all t and $S_{1_W}(0) < x_0 < S_{2_W}(0)$. Hence, the closed form of FET (5.13) for the Wiener process is

  $$\begin{aligned} g_W(t \mid x_0, 0) &= \frac{1}{t} \sum_{n=-\infty}^{+\infty} \exp\left\{ -\frac{2n^2L^2}{\sigma_W^2 t} \right\} \\ &\times \left\{ (l_1 + 2nL) \exp\left\{ -\frac{2nl_1L}{\sigma_W^2 t} \right\} f_W[S_{1_W}(t), t \mid x_0, 0] \right. \\ &+ \left. (l_2 - 2nL) \exp\left\{ \frac{2nl_2L}{\sigma_W^2 t} \right\} f_W[S_{2_W}(t), t \mid x_0, 0] \right\} \end{aligned} \tag{5.17}$$

where

$$\begin{aligned} L = S_{2_W}(0) - S_{1_W}(0) &= \sigma_W(c_2 - c_1), \\ l_1 = x_0 - S_{1_W}(0) &= \sigma_W(c - c_1), \\ l_2 = S_{2_W}(0) - x_0 &= \sigma_W(c_2 - c). \end{aligned} \tag{5.18}$$

Note that for $c_1 \to -\infty$ in (5.17), i.e. moving away the lower boundary $S_{1_W}(t)$, only the term with $n = 0$ gives a non-zero contribution, so the FET density (5.17) tends to the well-known Inverse Gaussian type density for the FPT pdf through the linear upper boundary $S_{2_W}(t)$:

$$\lim_{c_1 \to -\infty} g_W(t \mid x_0, 0) = \frac{S_{2_W}(0) - x_0}{\sqrt{2\pi t^3}} \exp\left\{ -\frac{(S_{2_W}(t) - x_0)^2}{2t} \right\}.$$

Furthermore, as particular case, we can put together (5.11) and (5.12) assuming

$$S_{1_W}(t) = Bt + x_0 - \tilde{c}, \qquad S_{2_W}(t) = Bt + x_0 + \tilde{c} \tag{5.19}$$

with the values $B, \tilde{c} \in \mathbb{R}^+$. It can be easily verified that, in this case, one has that $L = 2\tilde{c}$ and $l_1 = l_2 = \tilde{c}$. For $B = b_W, x_0 = c_W, c = 0$ the conditions (5.6) and (5.8) hold and so we can use (5.10) to obtain $g_1(t \mid x_0, 0)$ and $g_2(t \mid x_0, 0)$ with the following expression for FET density provided by (5.17):

$$\begin{aligned} g(t \mid x_0, 0) &= \frac{\tilde{c}}{t}\Big\{ f_W[Bt - \tilde{c}, t \mid 0, 0] + f_W[Bt + \tilde{c}, t \mid 0, 0] \Big\} \\ &+ \frac{2\tilde{c}}{t} \sum_{n=1}^{+\infty} \exp\left\{ -\frac{8n^2\tilde{c}^2}{\sigma_W^2 t} \right\} \\ &\times \left\{ f_W[Bt - \tilde{c}, t \mid 0, 0] \left[\cosh\left(\frac{4n\tilde{c}^2}{\sigma_W^2 t} \right) - 4n \sinh\left(\frac{4n\tilde{c}^2}{\sigma_W^2 t} \right) \right] \right. \\ &+ \left. f_W[Bt + \tilde{c}, t \mid 0, 0] \left[\cosh\left(\frac{4n\tilde{c}^2}{\sigma_W^2 t} \right) - 4n \sinh\left(\frac{4n\tilde{c}^2}{\sigma_W^2 t} \right) \right] \right\}. \end{aligned}$$

- The OU process. For the $U(t)$ process with $m_U(t)$, $h_{1_U}(t)$ and $h_{2_U}(t)$ as in (2.26), from (5.11) and (5.12), the closed form (5.13) holds for the hyperbolic-type boundaries

$$S_{1_U}(t) = A_1 e^{a_U t} + B_1 e^{-a_U t} + C_1, \qquad S_{2_U}(t) = A_1 e^{a_U t} + B_2 e^{-a_U t} + C_1, \tag{5.20}$$

and initial condition $x_0 = c_U + C$ where

$$A_1 = \frac{b\sigma_U}{2a_U}, \quad B_1 = c_U - \frac{b_U}{a_U} - \frac{b\sigma_U}{2a_U} + c_1\sigma_U,$$
$$B_2 = c_U - \frac{b_U}{a_U} - \frac{b\sigma_U}{2a_U} + c_2\sigma_U, \quad C_1 = \frac{b_U}{a_U}, \quad C = c\sigma_U, \qquad (5.21)$$

such that $S_{1_U}(t) < S_{2_U}(t)$ for all $t \geq 0$ and $S_{1_U}(0) < x_0 < S_{2_U}(0)$. Specifically, the closed form FET (5.13) for the OU process is

$$\begin{aligned} g_U(t \mid x_0, 0) &= \frac{2a_U e^{a_U t}}{e^{2a_U t} - 1} \sum_{n=-\infty}^{+\infty} \exp\left\{-\frac{2n^2L^2}{\sigma_U^2(e^{2a_U t} - 1)}\right\} \\ &\times \left\{(l_1 + 2nL)\exp\left\{-\frac{2nl_1L}{\sigma_U^2(e^{2a_U t} - 1)}\right\} f_U[S_{1_U}(t), t \mid x_0, 0]\right. \\ &\left. +(l_2 - 2nL)\exp\left\{\frac{2nl_2L}{\sigma_U^2(e^{2a_U t} - 1)}\right\} f_U[S_{2_U}(t), t \mid x_0, 0]\right\} \end{aligned} \qquad (5.22)$$

where

$$\begin{aligned} L = S_{2_U}(0) - S_{1_U}(0) &= \sigma_U(c_2 - c_1), \\ l_1 = x_0 - S_{1_U}(0) &= \sigma_U(c - c_1), \\ l_2 = S_{2_U}(0) - x_0 &= \sigma_U(c_2 - c). \end{aligned}$$

We note that it is possible to obtain (5.22) from (5.17) by means of the Doob-transformation rule between Wiener and OU process. Indeed applying (2.36) to each one of the pdfs of the FPT through S_{1_U} and S_{2_U}, for $r(t) = (e^{2a_U t} - 1)/(2a_U)$, manipulating properly the functions $f_W[S_{1_W}(t), t \mid x_0, 0]$ and $f_W[S_{2_W}(t), t \mid x_0, 0]$, we obtain the result (5.22).

- The generalized OU process. Let $V(t)$ be the generalized OU process with mean and covariance as in (2.30). From (5.11) and (5.12), the closed form (5.13) holds for boundaries

$$S_{1_V}(t) = A_1 e^{a_V t} + B_1(t)e^{-a_V t},\ S_{2_V}(t) = A_1 e^{a_V t} + B_2(t)e^{-a_V t} \qquad (5.23)$$

and initial condition $x_0 = c_V + C$, where

$$\begin{aligned} A_1 &= \frac{b\sigma_V}{2a_V}, \qquad C = c\sigma_V, \\ B_1(t) &= c_V + c_1\sigma_V - \frac{b\sigma_V}{2a_V} + B_V(t), \\ B_2(t) &= c_V + c_2\sigma_V - \frac{b\sigma_V}{2a_V} + B_V(t), \end{aligned}$$

such that $S_{1_V}(t) < S_{2_V}(t)$ for all $t \geq 0$ and $S_{1_V}(0) < x_0 < S_{2_V}(0)$. We note that now $B_1(t), B_2(t)$ are functions of time, since they depend on $B_V(t)$, specified in (2.30).
From these positions we obtain a closed form FET pdf that is the same of (5.22) with $a_U = a_V$, $\sigma_U = \sigma_V$ and

$$\begin{aligned} L &= S_{2_V}(0) - S_{1_V}(0) = \sigma_V(c_2 - c_1), \\ l_1 &= x_0 - S_{1_V}(0) = \sigma_V(c - c_1), \\ l_2 &= S_{2_V}(0) - x_0 = \sigma_V(c_2 - c), \end{aligned}$$

whereas the transition normal densities $f_U[S_{1_U}(t), t \mid x_0, 0]$ and $f_U[S_{2_U}(t), t \mid x_0, 0]$ are substituted by $f_V[S_{1_V}(t), t \mid x_0, 0]$ and $f_V[S_{2_V}(t), t \mid x_0, 0]$, respectively.

Two-boundary: asymptotic approximation

If closed-form results of the FPT pdf are not available, particularly useful are the asymptotic approximations. Results in this direction hold for time-homogeneous one-dimensional diffusion processes with steady-state pdf in three cases:

i) both boundaries possess horizontal asymptotes,

ii) both boundaries are asymptotically periodic,

iii) one boundary possesses an horizontal asymptote while the other boundary is asymptotically periodic.

From [38] we recall here the main results about the three cases.
Let $\{X(t), t \geq 0\}$ be a time-homogeneous diffusion process defined over the interval $I = (r_1, r_2)$ such that $\mathbb{P}(X(0) = x_0) = 1$ with x_0 in the interior of I.

Concerning Case i) we have the following result:

Theorem 5.1.2. *Let $S_1(t)$ and $S_2(t)$ be asymptotically constant thresholds:*

$$\lim_{t \to +\infty} S_i(t) = S_i \qquad (i = 1, 2).$$

Setting

$$R_i(S_i) := 2(-1)^{i+1} \lim_{t \to +\infty} \Psi_i[S_i(t), t|y, \tau], \quad (i = 1, 2) \tag{5.24}$$

and

$$\mathcal{U}(S_1, S_2) := R_1(S_1) + R_2(S_2). \tag{5.25}$$

Then we have asymptotically that

$$g(t|x_0, 0) \sim \mathcal{U}(S_1, S_2) \exp\{-\mathcal{U}(S_1, S_2)t\}. \tag{5.26}$$

Theorem 5.1.2 is the natural extension to the two-boundary case of Theorem 2.2.4 for the single boundary.

For Case ii) we assume that each $S_i(t)$ is asymptotically periodic of period Q_i, $i = 1, 2$.

Theorem 5.1.3. *Let $S_1(t)$ and $S_2(t)$ be asymptotically periodic and bounded functions:*

$$\lim_{n\to+\infty} S_i(t + nQ_i) = \phi_i(t) \qquad (i = 1, 2),$$

where $\phi_i(t)$'s are periodic functions of periods Q_i. Setting

$$S_i := \frac{1}{Q_i}\int_0^{Q_i} \phi_i(\tau)d\tau \qquad (i = 1, 2), \tag{5.27}$$

$$R_i[\phi_i(t)] := 2(-1)^{i+1} \lim_{n\to+\infty} \Psi_i[S_i(t + nQ_i), t + nQ_i|y, \tau], \quad (i = 1, 2) \tag{5.28}$$

and

$$\mathcal{U}[\phi_1(t), \phi_2(t)] := R_1[\phi_1(t)] + R_2[\phi_2(t)]. \tag{5.29}$$

Then, we have for $S_1 \to r_1$ and $S_2 \to r_2$ the following asymptotic result:

$$g(t|x_0, 0) \sim \mathcal{U}[\phi_1(t), \phi_2(t)] \exp\left\{-\int_0^t \mathcal{U}[\phi_1(\vartheta), \phi_2(\vartheta)]d\vartheta\right\}. \tag{5.30}$$

For Case iii), let us suppose, for instance, that $S_1(t)$ has the horizontal asymptote S_1 and $S_2(t)$ is asymptotically periodic of period Q_2. It is possible to obtain a result analogous to (5.30) defining

$$\mathcal{U}[S_1, \phi_2(t)] := R_1[S_1] + R_2[\phi_2(t)]. \tag{5.31}$$

5.2 The acto-myosin dynamics

In order to show how it is possible to use GD processes and the corresponding FET through suitable boundaries in the context of molecular biology, we recall and specialize a model presented in [11] on the acto-myosin dynamics. In fact putting together theoretical, numerical and simulative results about GD processes it is possible to obtain improvements in the theoretical and applicative apparatus jointly to additional understandings of experimental evidences. In particular, we point out the key role played by the time-inhomogeneous OU process for modeling phenomena subject to additional (external) time-dependent forces.

5.2.1 Physiology and classical models

The sarcomer is the basic unit of a skeletal muscle. It is composed of two kinds of protein filaments: the actin and the myosin. These proteins slide past each other when the muscle contract and relax and for this reason we talk about "sliding mechanism". There are 17 different types of myosins, in the following we will always consider the so-called "Myosin II". The myosin II has a long tail and a head that can bind to actin. While still bound to actin, the myosin flexes pulling the actin filament along with it; this causes the actin filament to slide by the myosin filament. For the presence of ATP the myosin head releases from the actin and unflexes. This frees the myosin head to bind with a different actin site and the process may be repeated. In the myosin head the ATP is idrolized producing the energy supply for the muscles movement. The underlying mechanism producing this energy conversion remains obscure. For detailed and extensive readings on molecular motors see [50], [60], [81] and references therein.
This mechanism suggests a tight coupling between ATP cycles and protein movement that leads to the deterministic *lever-arm* theory: each ATP cycle generates one single power-stroke that causes a sliding of constant length and preassigned direction of the actin filament. This deterministic approach needs however to be improved. A stochastic approach can be used in this context: during the time elapsing between the attachment of myosin head to the actin filament and the final release of the phosphoric anion, the position of the myosin head is determined both by the lever-arm swing and by the action of Brownian motion induced by thermal agitation of the environmental molecules of watery solution in which the involved proteins are embedded (see [11]). The results of the experiments conducted by Yanagida and his group in 1985 [83] supports this criticism on the tight coupling. In fact measurements of the total displacement produced by the myosin head during a complete ATP cycle obtained in their experimental set-up, are in disagreement with the deterministic lever-arm theory:

- the total distance traveled by the myosin head is not constant,
- this displacement is the sum of a random number of steps of amplitude $X_D = 5.5$ nm, i.e. the distance between two successive actin monomers. During the time elapsing between two successive steps, the myosin head randomly jitters around an equilibrium position performing a Brownian motion. Denoting by X_R the displacement induced by the thermal watery solution, by r and d two constants, the total displacement X of the myosin head during one ATP cycle is

$$X = rX_R + dX_D$$

- steps mainly occur in a preferred "forward"direction, although some of them occasionally can take place in the opposite "backward"direction. Hereafter, forward steps will be taken as positive and backward steps as negative. The total displacement is thus the algebraic sum of the number of performed forward and backward steps.

For these reasons the coupling between the ATP cycle and the generation of the power-stroke is weakened and the term "loose-coupling"is used.
The reason why we talk about the myosin head displacement instead of the more intuitive actin displacement is due to the technologies exploited during the experiments. A single myosin head was fixed to the tip of a microneedle and placed near a binding site of an actin filament that had been previously immobilized on a microscopy slide by means of optical tweezers. The deflections of the needle with respect to its resting position were then measured and recorded. This measurements constitutes the myosin displacement.
In a modeling context the myosin moves along the actin filament performing steps, mainly forwards and rarely backwards ([11], [24]). It is assumed that the acto-myosin dynamics is overdamped (disregarding the inertial force) and confined to only one space-period of the periodical morphology of the actin filament. The particle diffuses in a symmetric one-well potential (the binding site) tilted by a time-dependent force driving the particle motion. The myosin steps are represented as escapes from the potential well: the escape happens when the particle crosses over a local maximum of the potential (see Fig. 5.1).

5.2.2 A Gauss-Markov based approach to model the proteins dynamics

In the framework of the loose-coupling theory a new model for the acto-myosin dynamics has been proposed in [11]. It is based on the following assumptions:

- the complex myosin II, ADP and the phosphoric anion (M.ADP.Pi) + energy is viewed as a point-size particle moving along an axis whose positive direction is associated with forward steps of the myosin head;
- the particle is embedded in a fluid; thus it is subject to a dissipative force of drag coefficient β and thermal agitation. These foces are described macroscopically by Gaussian noise of intensity $2\beta\kappa_B\mathrm{T}$, where κ_B is the Boltzmann constant and T is the absolute temperature;
- the global interaction of the particle with the actin filament is synthesized in a conservative unique force deriving from a potential $U(x)$;

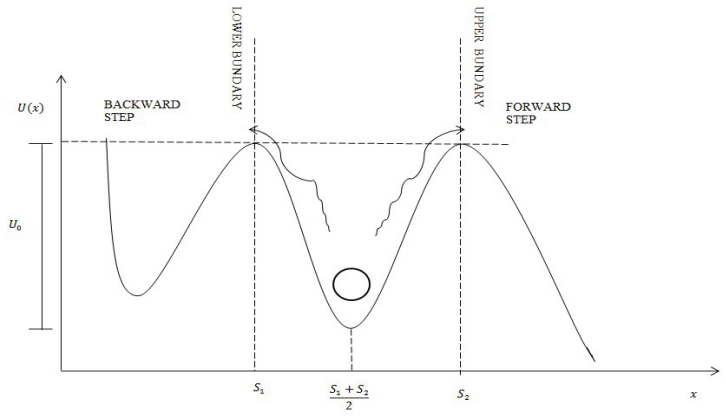

Figure 5.1: A graphical illustration: a scheme of the biological phenomenon. A myosin head (the circle) diffuses around the minimum of the potential well. Two possible evolutions of the myosin potential are drawn to provide an illustration of backward and forward steps. The steps happen when the particle crosses over a local maximum of the potential. These maxima constitute the two boundary confining the dynamics. In particular, note that the position of the myosin is in $x = S_1$ for a backward step, while the position of the myosin is in $x = S_2$ for a forward step.

- the particle's dynamics is described by Newton's equation;
- two forces act on the particle: F_i ed F_e. The internal force F_i is related to the largest force that the myosin head is able to generate endogenously, whereas F_e is an external force likely applied from outside by the experimenter.

The space periodic structure of the actin filament suggests that the function $U(x)$ is periodic of period L i.e. the lenght of an actin monomer:

$$U(x) = U(x + cL), \quad \forall c \in \mathbb{Z}.$$

Moreover, by the above assumptions, the particle is subject to a tilted potential $V(x)$

$$V(x) = U(x) - Fx \tag{5.32}$$

where $F := F_i - F_e$. Different profiles of the potential can be considered (see [11]), here we choose a parabolic profile:

$$U(x) = \frac{U_0}{L^2/4}\left(x - \frac{L}{2}\right)^2 \tag{5.33}$$

where U_0 is the depth of the potential well.
In Fig. 5.1 is represented the dynamics in the periodic parabolic potential, tilted by a driving force. Although the potential $U(x)$ is simmetric, the tilting drives the motion, favoring the forward steps.

We consider the model proposed in [11] including the effect of a time-dependent force $F(t)$ and improving the prediction of the occurence of backward steps of myosin head. The assumption of the presence of a time-dependent internal force is widely accepted, as in [52], [60].

The model is described by an SDE for the real-valued stochastic process $\{X(t), t \geq 0\}$ that represents the evolution in time of the position of the particle:

$$dX = -\left[\frac{U'(X) - F(t)}{\beta}\right] dt + \sqrt{\frac{2\mathrm{K}_B\mathrm{T}}{\beta}} dW, \tag{5.34}$$

with the initial condition $X(0) = x_0$. We use $(\prime)$ to indicate the space derivative, and as usual W is the standard Brownian motion.
We model the diffusive displacement of a myosin head along an actin filament via a Gauss-Markov process confined to a strip (see Fig. 5.1). The new assumption on the particle (myosin head) is that it is subject not only to random fluctuations of the surrounding thermal bath but also to an additional driving force conveying the external load and the internal time-dependent force arising from proteins interaction (see [52]). The dwell time, i.e., the time elapsed in the potential well before escaping from it, is here modeled by the FET of the GD process from the strip. The FET is equal to the FPT through the upper (with respect to initial position of the process) boundary or to FPT through the lower boundary. The attainment of one of the two boundaries is used to represent escape from the well. In particular, if the FET is equal to the FPT through the upper boundary, we say that a forward step occurred; otherwise, if the FET is equal to the FPT through the lower boundary, a backward step occurred. We remark that in our model we consider the not customary presence of a lower boundary in the state space of the GD process in order to include steps of the myosin in the opposite direction of the driving force ([44]). We stress that the potential profile, drawn symmetric in Fig. 5.1, is actually tilted by the driving force, and this implies that the forward steps are more frequent than the backward steps.

In Fig. 5.2 is shown the effect of the force F on the parabolic potential $U(x)$. In particular the tilted potential $V(x)$ is plotted in one space-period for $F = 0$ (symmetric potential), $F > 0$ and $F < 0$. We note that, for the cases that will be considered here for the proteins dynamics ($F > 0$), the potential is tilted favouring the forward steps.
Experimental data confirm that, as it is natural to expect, the frequency

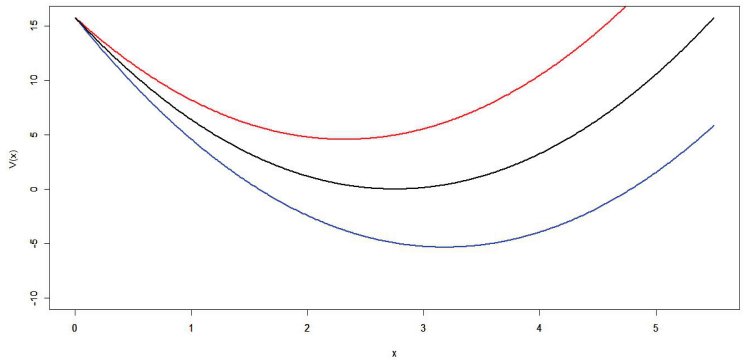

Figure 5.2: Plot of $V(x)$ from equations (5.32) and (5.33), in one period-space for $U_0 = 15.75$ pN nm and $L = 5.5$ nm. The black line represents the symmetric parabolic potential ($F = 0$), the red line is obtained when $F = -1.88$ pN and the blue line is $V(x)$ for $F = 1.88$ pN.

of forward steps decreases as the applied load F_e increases, while the dwell times increase with the load. Moreover as F_i increases the mean time that the particle spends in the strip decreases.

Using the parabolic profile (5.33) in the SDE (5.34), we finally consider the following SDE

$$dX = -\frac{1}{\theta}\left[X - \rho(t)\right] dt + \sigma dW \tag{5.35}$$

where we have posed

$$\theta = \frac{\beta L^2}{8U_0}, \quad \sigma = \sqrt{\frac{2\kappa_B \mathrm{T}}{\beta}}, \quad \rho(t) = \frac{L}{2} + \theta\frac{F(t)}{\beta} := \frac{L}{2} + \mathcal{A}(t). \tag{5.36}$$

We note that (5.35) describes the stochastic evolution of a particle subject to Brownian fluctuations in presence of a time-dependent equilibrium level where the characteristic time θ denotes the time elapsed to reach it and $\mathcal{A}(t)$ represents the time-dependent component of the attractor state ρ.
We set the starting point $x_0 = (S_1 + S_2)/2$ and, in order to model the step of the myosin from a site to the next one and the time required to perform it, we represent the myosin dwell time as the FET random variable

$$T_X = \inf\{t \geq 0 : X(t) \leq S_1 \quad \text{or} \quad X(t) \geq S_2\} \tag{5.37}$$

through the constant boundaries S_1 located at the origin (the lower one) and S_2 located at L (the upper one). The FET pdf is:

$$g_X(t|x_0, 0) = \frac{d}{dt}P\{T_X \leq t\}, \quad \text{with} \quad x_0 = \frac{S_1 + S_2}{2}. \tag{5.38}$$

Under suitable regularity conditions on coefficients, we have seen in Section 2.1 that the process $X(t)$ solution of (5.35) is a diffusion process. We can specify the mean and covariance functions of the Gauss-Markov diffusion process $X(t)$ solution of SDE (5.35) by using the result of Theorem 2.1.8. In the specific case of SDE (5.35), the coefficient functions are

$$a(t) = -\frac{1}{\theta}, \quad b(t) = \frac{L}{2\theta} + \frac{\mathcal{A}(t)}{\theta}, \quad \sigma^2 = \frac{2\mathrm{K}_B\mathrm{T}}{\beta}. \tag{5.39}$$

The assumptions of Theorem 2.1.8 are that the coefficient functions $a(t), b(t), \sigma$ have to be defined in $[0, +\infty[$ and they have to be such that the following functions

$$\begin{aligned} B_1(t) &= \int_0^t a \, d\tau, \quad B_2(t) = \int_0^t b(\tau) e^{-B_1(\tau)} \, d\tau, \\ B_3(t) &= \int_0^t \sigma^2 e^{-2B_1(\tau)} \, d\tau \end{aligned} \tag{5.40}$$

exist in $[0, +\infty[$. For regular enough $F(t)$ the mean and covariance functions of the GD process $X(t)$ are specified as follows

$$m(t) = [x_0 + B_2(t)] \, e^{B_1(t)}, \quad 0 \le t < +\infty \tag{5.41}$$

$$c(\tau, t) = e^{B_1(t)+B_1(\tau)} B_3(\tau), \quad 0 \le \tau \le t < +\infty. \tag{5.42}$$

Since in this case

$$\begin{aligned} B_1(t) &= -\frac{t}{\theta}, \quad B_2(t) = \frac{L}{2}(e^{t/\theta} - 1) + \int_0^t \frac{\mathcal{A}(t)}{\theta} e^{\tau/\theta} d\tau, \\ B_3(t) &= \frac{\sigma^2\theta}{2}(e^{2t/\theta} - 1). \end{aligned} \tag{5.43}$$

it is sufficient to choose a function $\mathcal{A}(t)$ such that $\displaystyle\int_0^t \frac{\mathcal{A}(t)}{\theta} e^{\tau/\theta} d\tau$ exist and we have

$$m(t) = x_0 e^{-t/\theta} + \frac{S_1 + S_2}{2} \left(1 - e^{-t/\theta}\right) + e^{-t/\theta} \int_0^t \frac{A(t)}{\theta} e^{\tau/\theta} d\tau \tag{5.44}$$

and the following covariance function

$$c(\tau, t) = \frac{\sigma^2\theta}{2} \left(e^{\tau/\theta} - e^{-\tau/\theta}\right) e^{-t/\theta} \quad (0 \le \tau \le t). \tag{5.45}$$

In particular, the covariance function (5.45) is the product of two functions

$$h_1(t) = \sigma \frac{\theta}{2} \left(e^{t/\theta} - e^{-t/\theta}\right), \quad h_2(t) = \sigma e^{-t/\theta} \tag{5.46}$$

whose ratio $r(t) = h_1(t)/h_2(t)$ is a monotonically non decreasing function. Finally, the infinitesimal moments of $X(t)$ are

$$A_1(x,t) = -\frac{1}{\theta}\left[x - \rho(t)\right], \quad A_2 = \sigma^2. \tag{5.47}$$

Hence $X(t)$ is the time-inhomogeneous OU process solution of (2.18) with $a(t) = -1/\theta$ and $b(t) = \rho(t)/\theta$. Making explicit the form of $F(t)$ in (5.44), the mean remains determined.

5.2.3 Different forces $F(t)$ to model different cases

It is interesting to specify for which kind of driving force $F(t)$ it is possible to provide a closed-form function for the FET density useful to model the dwell-time of the myosin head in a potential well. It can be made finding relations between threshold values, mean behavior of the protein dynamics and input forces ([25]).

For this purpose we re-consider the theoretical results presented in Section 5.1 specialized for processes that find application in the dynamics of the actin and myosin proteins.

Closed-form results

With this aim let us consider the more general GD process with infinitesimal moments

$$A_1(x,t) = a(t)x + b(t), \qquad A_2(t) = \sigma^2(t). \tag{5.48}$$

Given the boundaries $S_1(t), S_2(t)$, by adding side-by-side the conditions (5.11), we can write the following condition on the mean of the process

$$m(t) = \frac{S_1(t) + S_2(t)}{2} - bh_1(t) - \frac{c_1 + c_2}{2}h_2(t), \tag{5.49}$$

where the parameter b must not be confused with the function $b(t)$. From (2.13) we know that

$$b(t) = m'(t) - a(t)m(t). \tag{5.50}$$

Using (5.49) in (5.50), we obtain

$$b(t) = \frac{S_1'(t) + S_2'(t)}{2} - bh_1'(t) - \left[\frac{S_1(t) + S_2(t)}{2} - bh_1(t)\right]\frac{h_2'(t)}{h_2(t)}. \tag{5.51}$$

For constant boundaries S_1 and S_2, we have

$$b(t) = -bh_1'(t) - \left[\frac{S_1 + S_2}{2} - bh_1(t)\right]\frac{h_2'(t)}{h_2(t)}. \tag{5.52}$$

This expression for $b(t)$ ensures that, for the GD process solution of the SDE

$$dX = [a(t)X + b(t)]dt + \sigma dW \quad \text{with} \quad X(0) = x_0, \quad S_1 < x_0 < S_2$$

in presence of constant boundaries S_1 and S_2, the FET density admits the closed form (5.13) for suitable values of the involved parameters. Specifically, for the generalized OU process $V(t)$ solution of

$$dV = [-a_V V + b_V(t)]dt + \sigma_V dW, \quad S_1 < V(0) = v_0 < S_2 \tag{5.53}$$

the FET density has a closed form of type (5.22) if

$$b_V(t) = -b\sigma_V e^{a_V t} + \left(\frac{S_1 + S_2}{2}\right) a_V \tag{5.54}$$

with $a_U = a_V$, $S_{1_U}(t) = S_1$, $S_{2_U}(t) = S_2$, $\sigma_U = \sigma_V$, $c = 0$ and for $\sigma_V(c_1+c_2) = S_1 + S_2 - 2x_0$.
Furthermore, if $S_2 = S = -S_1$ the condition (5.54) becomes

$$b_V(t) = -b\sigma_V e^{a_V t}.$$

Finally, the FET density admits a closed form if $V(t)$ is solution of

$$dV = [-a_V V - b\sigma_V e^{a_V t}]dt + \sigma_V dW, \quad -S < V(0) = v_0 < S. \tag{5.55}$$

Concerning the application to the proteins dynamics, we have that Eq. (5.53) is the same of Eq. (5.35) when $a_V = 1/\theta$, $b_V(t) = \theta\rho(t) = \dfrac{L}{2\theta} + \dfrac{F(t)}{\beta}$, $\sigma_V = \sigma$, $S_1 = 0$ and $S_2 = L$. So from (5.54) we can say that for an input force of type: $\dfrac{F(t)}{\beta} = -b\sigma e^{\frac{t}{\theta}}$, the corresponding FET pdf from $(0, L)$ admits a closed form. Specifically, the time inhomogeneous OU process $X(t)$ with the following mean and covariance factors:

$$m_X(t) = x_0 e^{-t/\theta} - b\frac{\sigma\theta}{2}\left(e^{t/\theta} - e^{-t/\theta}\right),$$
$$h_{1_X}(t) = \frac{\sigma\theta}{2}(e^{t/\theta} - e^{-t/\theta}), \qquad h_{2_X}(t) = \sigma e^{-t/\theta} \tag{5.56}$$

with $0 < x_0 < L$, admits the following FET closed form in presence of

constant boundaries $(0, L)$:

$$\begin{aligned} g_X(t \mid x_0, 0) &= \frac{2e^{t/\theta}}{\theta(e^{2t/\theta}-1)} \sum_{n=-\infty}^{+\infty} \exp\left\{-\frac{2n^2L^2}{\sigma^2(e^{2t/\theta}-1)}\right\} \\ &\times \left\{(2nL+x_0)\exp\left\{-\frac{2nLx_0}{\sigma^2(e^{2t/\theta}-1)}\right\} f_X[0,t \mid x_0,0]\right. \\ &\left. +[(1-2n)L-x_0]\exp\left\{\frac{2nL(L-x_0)}{\sigma^2(e^{2t/\theta}-1)}\right\} f_X[L,t \mid x_0,0]\right\}. \end{aligned} \tag{5.57}$$

The form (5.57) is obtained from (5.22) with $a_U = 1/\theta$, $\sigma_U = \sigma$, $c = 0$, $L = S_2 - S_1 = \sigma(c_2 - c_1)$, $l_1 = x_0 = -\sigma c_1$ and $l_2 = L - x_0 = \sigma c_2$, whereas the transition normal densities $f_U[S_{1_U}(t), t \mid x_0, 0]$ and $f_U[S_{2_U}(t), t \mid x_0, 0]$ are substituted by $f_X[0, t \mid x_0, 0]$ and $f_X[L, t \mid x_0, 0]$, respectively.

Although the force

$$F(t) = -b\beta\sqrt{\frac{2\mathrm{K}_B\mathrm{T}}{\beta}}e^{\frac{t}{\theta}} \tag{5.58}$$

in SDE (5.35) guarantees a closed form for the FET density for $S_1 = 0$ and $S_2 = L$, most of the times it is of a limited interest from a biological point of view. In fact it has a positive exponential behavior and it can be used in this context only to describe some phenomena in which an increasing (in absolute value) and unbounded force is involved.

Other cases of study

We consider the case of a time-increasing force acting in the dynamics and also the case of a time-decreasing force ([24]). We remark that for different choices of $F(t)$ the covariance function (5.45) does not change, but only the mean functions have to be specified.

Case 1. In (5.35) we consider an increasing exponential force such that

$$\mathcal{A}(t) = k\theta(1 - e^{-t/\vartheta}) \tag{5.59}$$

with k positive real number (nm/ns) to model a force that attract the myosin head to the next actin monomer (i.e., the upper boundary) rising during the interaction between the proteins and that grows when the distance between the two filaments decreases ([33], [51]). Note that the time constant ϑ characterizes the time that the force takes to assume its maximum value $k\beta$. In general, ϑ is different from θ. The

choices $\vartheta > \theta$, $\vartheta = \theta$ or $\vartheta < \theta$ can be used to model different situations.

Case 2. In (5.35) we consider the decreasing exponential force such that

$$\mathcal{A}(t) = k\theta e^{-t/\vartheta} \tag{5.60}$$

with k positive real number (nm/ns) to model a quasi-impulsive force that rapidly decays. This could be the case of an initial strong impact between the myosin head and the actin filament that may cause the so-called conformational change in the myosin neck. Here, ϑ is the decay time of the force.

The simulation strategy and the numerical approach are mandatory because no closed form results hold for the specified cases. Discretizing the considered SDE using the Euler method described in the previous chapters, we simulated particle paths and we recorded the instants of crossing of the boundaries obtaining statistical approximations of FET density. We compare these results with evaluations of FET density obtained by numerical quadrature of the two corresponding integral equations (of type (5.2)) and also with some experimental data. We note that we only need mean and covariance functions of the GD process to apply the numerical procedure; indeed, if we know them we can write the normal transition pdf $f_X[x, t|z, \tau]$ and also the functions $\Psi_i(t|z, \tau)$ $(i = 1, 2)$ involved in the integral equations (5.2).

In [24], using the cited numerical procedure, we provided numerical approximations of the FET pdf in the two cases. In Fig. 5.3 are shown different curves characterized by different decay times of the force for Case 1. Different values of ϑ represent different rates of growth of the force acting on the particle. We have also chosen two internal forces F_i in order to consider different forces that the head of the myosin is able to generate. Numerical approximations of the FET pdfs $g_X(t|x_0, 0)$ for different values of ϑ for Case 2 can be found in Fig. 5.4.

Finally we underly that, for suitable values of parameters, the proposed model can include a wide range of phenomenological evidences. In particular in [24] we fitted experimental data, obtained in the Yanagida laboratory ([11], [44]). In Tables 5.1 and 5.2 we provide accurate estimates of the measured dwell-times for different loads applied to the particle for Case 1 and Case 2. We note that the bigger is the load the longest is the time the particle elapses inside the potential well.

We stress again the importance of all characteristic times involved in the model. In particular in the simulation strategy the choice of a very small

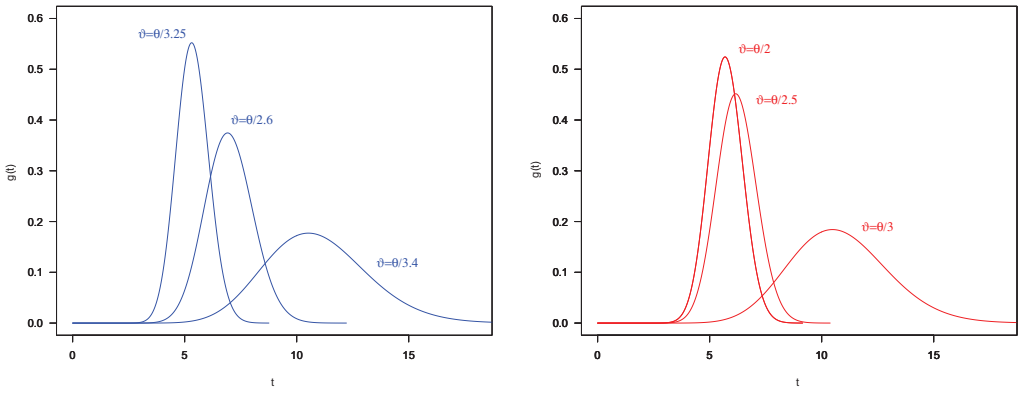

Figure 5.3: Numerical approximations $g(t)$ of FET pdfs $g_X(t|x_0, 0)$ for different values of ϑ for Case 1. The blue curves on the left refer to $F_i/\beta = 1.8$ nm/ns, the red curves on the right refer to $F_i/\beta = 2.5$ nm/ns. In both figures $U_0 = 15.75$ pN nm, $k = 1.8$ nm/ns, $\theta = 21.6$ ns. The values of ϑ are reported in the plots. The time discretization step is 10^{-3}.

size of discretization time step is almost always essential to obtain reliable estimations. This time step is chosen taking into account the characteristic times.

FITTING THE EXPERIMENTAL DATA: CASE 1

F_i/β	F_e	θ/ϑ	Estimated FET mean	Measured Dwell times
1.8	0.046	3.2	5.3	5.3
1.8	0.19	3.2	5.7	5.7
1.8	0.3	2.7	6.2	6.0
1.8	0.47	2.6	6.9	7.1
1.8	0.69	2.0	8.9	8.9
1.8	1.24	3.4	11.0	11.1
2.5	0.19	2.0	5.7	5.7
2.5	0.83	2.5	6.2	6.2
2.5	1.89	3.0	10.9	11.0

Table 5.1: Case 1. Estimations of mean FET of $X(t)$ by using the numerical procedure for different values of ϑ, internal and external forces and comparison with the experimental measurements of the dwell-times ([11],[44]).

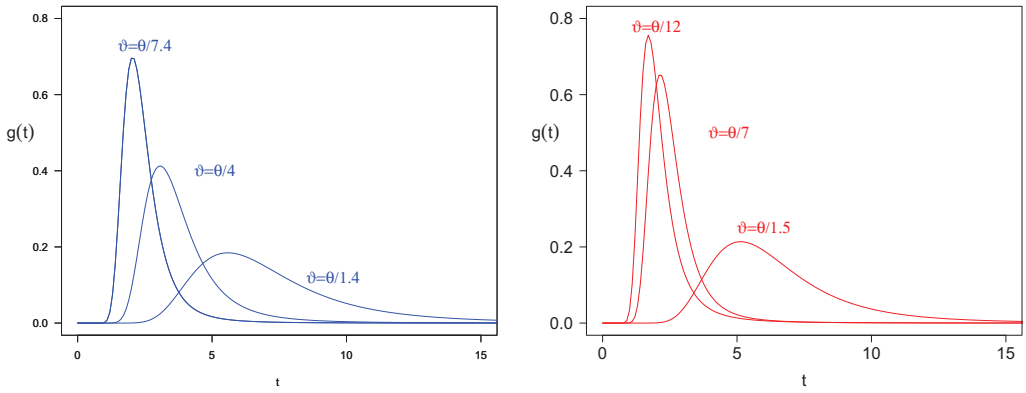

Figure 5.4: Numerical approximations $g(t)$ of FET pdfs $g_X(t|x_0, 0)$ for different values of ϑ for Case 2. The blue curves on the left refer to $F_i/\beta = 1.8$ nm/ns, the red curves on the right refer to $F_i/\beta = 2.5$ nm/ns. In both figures $U_0 = 15.75$ pN nm, $k = 1.8$ nm/ns, $\theta = 21.6$ ns. The values of ϑ are reported in the plots. The time discretization step is 10^{-3}.

FITTING THE EXPERIMENTAL DATA: CASE 2

F_i/β	F_e	θ/ϑ	Estimated FET mean	Measured Dwell times
1.8	0.046	3.2	5.3	5.3
1.8	0.19	3.2	5.7	5.7
1.8	0.3	2.7	6.2	6.0
1.8	0.47	2.6	7.2	7.1
1.8	0.69	2.0	8.9	8.9
1.8	1.24	3.4	11.1	11.1
2.5	0.19	2.0	5.6	5.7
2.5	0.83	2.5	6.2	6.2
2.5	1.89	3.0	11.0	11.0

Table 5.2: Case 2. Estimations of mean FET of $X(t)$ by using the numerical procedure for different values of ϑ, internal and external forces and comparison with the experimental measurements of the dwell-times ([11],[44]).

In [24] we also propose a refining of the model (5.35) in order to describe more realistically the occurence of backward steps. The model proposed is:

$$dX = -\frac{1}{\theta}\left[X - \rho(t)\right] dt + \sigma dW \tag{5.61}$$

with $X(0) = L/2$ and $\rho(t) = L/2 + \mathcal{A}(t)$, where $\mathcal{A}(t)$ is now

$$\mathcal{A}(t) = \theta \frac{F(t) - \delta_2 F_e}{\beta}$$

and

$$k\beta = F_i - \delta_1 F_e \quad \text{with} \quad 0 \leq \delta_1, \delta_2 \leq 1.$$

The main idea of this model is that the external load F_e affects the force $F(t)$ and the equilibrium level $\rho(t)$ with different weights δ_1 and δ_2. From the point of view of the approximation of the experimental data, this allows us to have a new free parameter useful for the description of the percentage of backward steps.

Moreover the presence of a non negligible number of backward steps, affects the form of the FET pdfs. In fact, also in this case, we performed simulations of equation (5.61) and numerical approximations of the FET density (see Fig. 5.5). Due to the presence of backward steps, we observe bimodal densities. In particular for Case 2 (Fig. 5.5 - right), for the considered choices of parameters, we have that almost all the mass is concentrated in the interval $(0, 10)$, since the force is very strong at the beginning. Moreover since the potential is very tilted at the beginning, the occurence of backward steps is unlikely. They occur only after time 20, when the force is reduced and the potential is less tilted.

The last intuition is supported by Fig. 5.6 where we have plotted the pdf of the FPT through the lower boundary, i.e. the density of the backward steps.
Similar considerations can be made for Case 1 (Fig. 5.5 - left). Here it is possible to observe a remarkable probability of backward steps (see Fig. 5.6 - left) for small times, since the force is not strong enough to tilt completely the potential. After time $t = 10$ we observe an high probability only of forward steps.

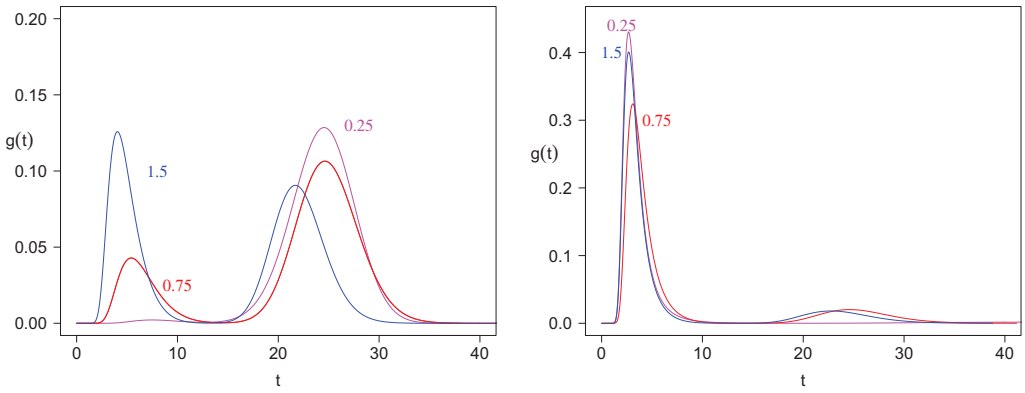

Figure 5.5: Numerical approximations $g(t)$ of FET pdfs for the refined model (5.61) for different values of ϑ for Case 1 (on the left) and Case 2 (on the right). The different values assigned to $F_e/\beta = 0.25, 0.75, 1.5$ nm/ns are reported in the plots, $F_i/\beta = 2.5$ nm/ns, $U_0 = 15.75$ pN nm, $\theta = 21.6$ ns and suitable choices of δ_1 and δ_2.

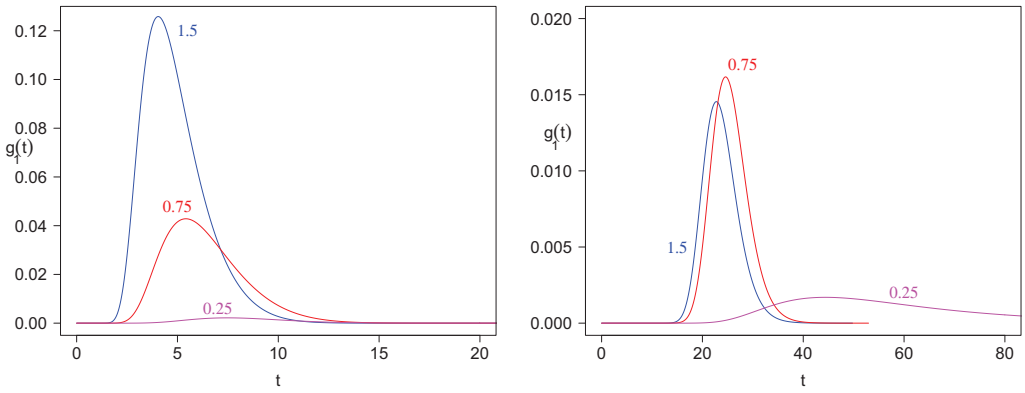

Figure 5.6: Numerical approximations of FPT densities $g_1(t|x_0, 0)$ of $X(t)$ are plotted for the same values of the parameters of Fig. 5.5. Case 1 is considered on the left, Case 2 on the right.

Bibliography

[1] Abundo M., One-dimensional reflected diffusions with two boundaries and an inverse first-hitting problem, *Stochastic Anal. Appl*, **32**, 975–991, 2014.

[2] Abundo M., Macci C. and Stabile G., Asymptotic results for exit probabilities of stochastic processes governed by an integral type rate function, *Prob. Math. Statis.*, **32(1)**, 25–39, 2012.

[3] Arnold L., *Stochastic Differential Equations: Theory and Applications*, Wiley-Interscience, 1974.

[4] Bachelier L., *Théorie de la spéculation*, Gauthier-Villars, 1900.

[5] Baldi P., *Equazioni differenziali stocastiche e applicazioni*, Pitagora Editrice, 2000.

[6] Benedetto,E., Polito F. and Sacerdote L., On Firing Rate Estimation for Dependent Interspike Intervals, *Neural Computation*, **27(3)**, 699–724, 2015.

[7] Buonocore A., Caputo L., D'Onofrio G. and Pirozzi E., Closed-Form Solutions for the First-Passage-Time Problem and Neuronal Modeling, *Ricerche di Matematica*, **64(2)**, 421–439, 2015.

[8] Buonocore A., Nobile A.G. and Ricciardi L.M., A new integral equation for the evaluation of first-passage-time probability densities, *Adv. Appl. Prob.*, **19(4)**, 784–800, 1987.

[9] Buonocore A., Giorno V., Nobile A.G. and Ricciardi L.M., On the Two-Boundary First-Crossing-Time Problem for Diffusion Processes, *Journal of Applied Probability*, **27(1)**, 102–114, 1990.

[10] Buonocore A., Caputo L. and Pirozzi E., On a pulsating Brownian motor and its characterization, *Mathematical Biosciences*, **207**, 387-401, 2007.

[11] Buonocore A., Caputo L., Ishii Y., Pirozzi E., Yanagida T. and Ricciardi L.M., On Myosin II dynamics in the presence of external loads, *BioSystems* **81**, p. 165-177, 2005.

[12] Buonocore A., Caputo L. and Pirozzi E., On the evaluation of firing densities for periodically driven neuron models, *Mathematical Biosciences* **214**, 122–133, 2008.

[13] Buonocore A., Caputo L., Pirozzi E. and Ricciardi L.M., The First Passage Time Problem for Gauss-Diffusion Processes: Algorithmic Approaches and Applications to LIF Neuronal Model, *Methodology and Computing in Applied Probability*, **13**, Springer, 2011.

[14] Buonocore A., Caputo L., Pirozzi E. and Ricciardi L.M., On a Stochastic Leaky Integrate-and-Fire Neuronal Model, *Neural Computation*, **22**, 2558–2585, 2010.

[15] Buonocore A., Caputo L., Nobile A.G. and Pirozzi E., Gauss-Markov processes in the presence of a reflecting boundary and some applications in neuronal models, *Applied Mathematics and Computation*, **232**, 799-809, 2014.

[16] Buonocore A., Caputo L., Nobile A.G. and Pirozzi E., Restricted Ornstein-Uhlenbeck process and applications in neuronal models with periodic input signals, *J. Comput. Appl. Math.*, **285**, 59-71, 2015.

[17] Buonocore A., Caputo L., Pirozzi E. and Carfora M.F., A leaky integrate-and-fire model with adaptation for the generation of a spike train , *Mathematical Biosciences and Engineering*, **13(3)**, 483–493, 2016.

[18] Burkitt A.N., A review of the integrate-and-fire neuron model: I. Homogeneous synaptic input, *Biological Cybernetics*, **95**, 1–19, 2006.

[19] Burkitt A.N., A review of the integrate-and-fire neuron model: II. Inhomogeneous synaptic input and network properties, *Biological Cybernetics*, **95**, 97–112, 2006.

[20] Capocelli R.M. and Ricciardi L.M., Diffusion approximation and first passage time problem for a model neuron, *Kybernetik*, **8(6)**, 214–223, 1971.

[21] Chacron M. J., Pakdaman K. and Longtin A., Interspike interval correlations, memory, adaptation, and refractoriness in a leaky integrate-and-fire neuron with threshold fatigue, *Neural Computation*, **15**, 253–276, 2003.

[22] Di Crescenzo A., Giorno V., and Nobile A.G., On the M/M/1 queue with catastrophes and its continuous approximation, *Queueing Systems*, **43**, 329–347, 2003.

[23] Di Nardo E., Nobile A.G., Pirozzi E. and Ricciardi L.M., A computational approach to first passage-time problems for Gauss-Markov processes, *Adv. Appl. Prob.*, **33**, 453–482, 2001.

[24] D'Onofrio G. and Pirozzi E., Two-boundary first exit time of Gauss-Markov processes for stochastic modeling of acto-myosin dynamics, *submitted*.

[25] D'Onofrio G. and Pirozzi E., On Two-Boundary First Exit Time of Gauss-Diffusion Processes: closed-form results and biological modeling, *Lecture Notes of Seminario Interdisciplinare di Matematica*, **12**, 111–124, 2015.

[26] D'Onofrio G. and Pirozzi E., Successive Spike Times Predicted by a Stochastic Neuronal Model with a Variable Input Signal, *Mathematical Biosciences and Engineering*, **13(3)**, 495–507, 2016.

[27] D'Onofrio G., Pirozzi E. and Magnasco M.O., Towards Stochastic Modeling of Neuronal Interspike Intervals Including a Time-Varying Input Signal, *Lecture Notes in Computer Science*, Springer-Verlag, **9520**, 166–173, 2015.

[28] Durbin J., Boundary-crossing probabilities for the Brownian motion and poisson processes and techniques for computing the power of the Kolmogorov-Smirnov test, *Journal of Applied Probability*, **8(3)**, 431–453, 1971.

[29] Durbin J., The First-Passage Density of a Continuous Gaussian Process to a General Boundary, *Journal of Applied Probability*, **22(1)**, 99–122, 1985.

[30] Durbin J. and Williams D., The First-Passage Density of the Brownian Motion Process to a Curved Boundary, *Journal of Applied Probability*, **29(2)**, 291–304, 1992.

[31] Feller W., Diffusion processes in one dimension, *Trans. Amer. Math. Soc.*, **77**, 1–31, 1954.

[32] Fellous J.M., Tiesinga P.H., Thomas P.J. and Sejnowski T.J., Discovering spike patterns in neuronal responses, *The Journal of Neuroscience*, **24**, 2989–3001, 2004.

[33] Finer J.T., Simmons R.M. and Spudich J.A., Single myosin molecule mechanics: piconewton forces and nanometre steps, *Nature*, **368**, 113–119, 1994.

[34] Gardiner C.W., *Handbook of Stochastic Methods for Physics, Chemistry and Natural Sciences*, Springer, 1985.

[35] Gerstein G.L. and Mandelbrot B., Random walk models for the spike activity of a sigle neuron, *Biophysical Journal* **4**, 1964.

[36] Giorno V., Nobile A.G. and Ricciardi L.M., On some time non homogeneous diffusion approximations to queueing systems, *Advances in Applied Probability* , **19**, 974–994, 1987.

[37] Giorno V., Nobile A., Ricciardi L. and Sato S., On the Evaluation of First-Passage-Time Probability Densities via Non-Singular Integral Equations, *Advances in Applied Probability* **21(1)**, 20-36, 1989.

[38] Giorno V., Nobile A. and Ricciardi L.M., On the asymptotic behaviour of first-passage-time densities for one-dimensional diffusion processes and varying boundaries, *Advances in Applied Probability* **22**, 883–914, 1990.

[39] Giorno V., Nobile A. and Pirozzi E., Upcrossing first passage times for correlated Gaussian Processes, *Computer Aided SystemsTheory - EUROCAST 2005* **3643**, 447–456, 2005.

[40] Giorno V. and Spina S., On the return process with refractoriness for a non-homogeneous Ornstein-Uhlenbeck neuronal model, *Math. Bios. Eng.*, **11**, 285–302, 2014.

[41] Itô K., Stochastic integral, *Proceedings of the Imperial Academy Tokyo*, **20**, 1944.

[42] Karatzas I. and Shreve S. E., *Brownian Motion and Stochastic Calculus*, Second Edition, Springer, 1998.

[43] Kim H. and Shinomoto S., Estimating nonstationary inputs from a single spike train based on a neuron model with adaptation, *Math. Bios.* **11(1)**, 49–62, 2014.

[44] Kitamura K., Tokunaga M., Iwane A.H. and Yanagida T., A single myosin head moves along an actin filament with regular steps of 5.3 nanometres, *Nature* **397**, 129–134, 1999.

[45] Lánský P., Sources of periodical force in noisy integrate-and-fire models of neuronal dynamics, *Graduate text in Mathematics* **113**, Springer, 1991.

[46] Lánský P. and Ditlevsen S., A review of the methods for signal estimation in stochastic diffusion leaky integrate-and-fire neuronal models, *Biol. Cybern.* **99**, 253–262, 2008.

[47] Lánský P. and Ditlevsen S., Estimation of the input parameters in the Ornstein-Uhlenbeck neuronal model, *Physical Review E* **71**, 011907(1–9), 2005.

[48] Lánský P. and Rospars J.P., Ornstein-Uhlenbeck neuronal model revisited, *Biol. Cybern.* **72**, 397–406, 1995.

[49] Lindner B., Interspike interval statistics for neurons driven by colored noise, *Physical Review E*, **69**, 022901 pp 1–4, 2004.

[50] Magnasco M.O. and Stolovitzky G., Feynman's Ratchet and Pawl, *Journal of Statistical Physics*, **93(3-4)**, 615–632, 1998.

[51] Masuda T., Molecular dynamics simulation of a myosin subfragment-1 dockingwith an actin filament, *Biosystems*, **113**, 144-148, 2013.

[52] Masuda T., A possible mechanism for determining the directionality of myosin molecular motors, *Biosystems*, **93(3)**, 172–180, 2008.

[53] Nobile A.G., Ricciardi L.M. and Sacerdote L., Exponential Trends of Ornstein-Uhlenbeck First-Passage-Time Densities. *Journal of Applied Probability*, **22(2)**, 360–369, 1985.

[54] Nobile A.G., Pirozzi E. and Ricciardi L.M., On the estimation of first-passage time densities for a class of Gauss-Markov processes. *LNCS* **4739** Berlin, Springer-Verlag, 146–153, 2007.

[55] Nobile A.G., Pirozzi E. and Ricciardi L.M., On the two-boundary first-passage-time problem for Gauss-Markov processes. *Scientiae Mathematicae Japonicae*, **64(2)**, 421–442, 2006.

[56] Nobile A.G., Pirozzi E. and Ricciardi L.M., Asymptotics and evaluations of FPT densities through varying boundaries for Gauss-Markov processes. *Scientiae Mathematicae Japonicae*, **67(2)**, 241–266, 2008.

[57] Oksendal B., *Stochastic Differential Equations. An Introduction with Applications*, Springer, 2000.

[58] Orsingher E. and Beghin L., *Probabilità e modelli aleatori*, Aracne, 2009.

[59] Plesser H.E. and Geisel T., Stochastic resonance in neuron models: Endogenous stimulation revisited, *Physical Review E* **63(3)**,031916, 2001.

[60] Reimann P., Brownian motors: noisy transport far from equilibrium, *Physics Reports* **361**, p.57-265, 2002.

[61] Ricciardi L.M., Diffusion Processes and Related Topics in Biology, *Lecture Notes in Biomathematics* **14**, 1977.

[62] Ricciardi L.M., Di Crescenzo A., Giorno V. and Nobile A.G. , An outline of theoretical and algorithmic approaches to first passage time problems with applications to biological modeling, *Mathematica Japonica*, **50(2)**, 247–322, 1999.

[63] Ricciardi L.M. and Sato S., A Note on First Passage Time Problems for Gaussian Processes and Varying Boundaries, *IEEE*, **29(3)**, 454–457, 1983.

[64] Ricciardi L.M. and Sato S., On the evaluation of first passage time densities for Gaussian processes, *Signal Processing*, **11(4)**, 339–357, 1986.

[65] Ricciardi L.M. and Sato S., First-Passage-Time Density and Moments of the Ornstein-Uhlenbeck Process, *Journal of Applied Probability*, **25(1)**, 43–57, 1988.

[66] Sacerdote L. and Giraudo M.T., Stochastic Integrate and Fire Models: a Review on Mathematical Methods and their Applications, *In Stochastic Biomathematical Models with Applications to Neuronal Modeling, Lecture Notes in Mathematics*, **2058**, 99–142, 2013.

[67] Sacerdote L., Telve O. and Zucca C., Joint densities of first passage times of a diffusion process through two constant boundaries, *Journal of Advanced Applied Probability*, **4(1)**, 186–202, 2013.

[68] Schwalger T., Droste F. and Lindner B., Statistical structure of neural spiking under non-Poissonian or other non-white stimulation, *Journal of Computational Neuroscience*, **39**, 29–51, 2015.

[69] Siegert A.J.F., On the First Passage Time Probability Problem, *Phys. Rev.* **81(4)**, 617–623, 1951.

[70] Shaked M. and Shanthikumar J.G., *Stochastic Orders and Their Applications*, Academic Press, Boston (USA), 1994.

[71] Shinomoto S., Sakai Y. and Funahashi S., The Ornstein-Uhlenbeck process does not reproduce spiking statistics of cortical neurons, *Neural Computation*, **11**, 935–951, 1997.

[72] Y. Sakai, S. Funahashi and S. Shinomoto, Temporally correlated inputs to leaky integrate-and-fire models can reproduce spiking statistics of cortical neurons, *Neural Netw*, **12**, 1181–1190, 1999.

[73] Stein R.B., A theoretical analysis of neuronal variability, *Biophysical Journal* **5**, 1965.

[74] Taillefumier T. and Magnasco M.O., A phase transition in the first passage of a Brownian process through a fluctuating boundary: Implications for neural coding, *PNAS*, **110**, E1438–E1443, 2013.

[75] Taillefumier T. and Magnasco M.O., A transition to sharp timing in stochastic leaky integrate-and-fire neurons driven by frozen noisy input, *Neural Computation*, **26**, 819–859, 2014.

[76] Taillefumier T. and Magnasco M.O., A fast algorithm for the first-passage times of Gauss-Markov processes with Holder continuous boundaries, *J. Stat. Phys.*, **140**, 1130–1156, 2010.

[77] Thomas P.J., A lower bound for the first passage time density of the suprathreshold Ornstein-Uhlenbeck process, *J Appl Probab* , **48**, 420–434, 2011.

[78] Toups J. V., Fellous J. M., Thomas P. J., Sejnowski T. J. and Tiesinga P. H., Multiple spike time patterns occur at bifurcation points of membrane potential dynamics, *PLoS Comput. Biol.*, **8**, e1002615 1–19, 2012.

[79] Tuckwell H.C., *Stochastic Processes in the Neurosciences*, Society for industrial and applied mathematics, 1989.

[80] Urdapilleta E., Series solution to the first-passage-time problem of a Brownian motion with an exponential time-dependent drift, *J. Stat. Phys.,* **140**, 1130–1156, 2010.

[81] Wang H. and Oster G., Ratchets, power strokes and molecular motors, *Appl. Phys. A*, **75**, 315-323, 2002.

[82] Williams D., *Probability with Martingales*, Cambridge University Press, 1991.

[83] Yanagida T., Arata T. and Oosawa F., Sliding distance of actin filament induced by a myosin crossbridge during one ATP hydrolysis cycle. *Nature*, **316**, 366–369, 1985.